

ENZYMATIC REGULATION OF SKELETAL MUSCLE OXYGEN TRANSPORT:
NOVEL ROLES FOR NEURONAL NITRIC OXIDE SYNTHASE

by

STEVEN WESLEY COPP

M.S., Kansas State University, 2008

AN ABSTRACT OF A DISSERTATION

submitted in partial fulfillment of the requirements for the degree

DOCTOR OF PHILOSOPHY

Department of Anatomy and Physiology
College of Veterinary Medicine

KANSAS STATE UNIVERSITY
Manhattan, Kansas

2013

Abstract

Nitric oxide (NO) is synthesized via distinct NO synthase (NOS) enzymes and constitutes an essential cardiovascular signaling molecule. Whereas important vasomotor contributions of endothelial NOS (eNOS) have been well-described, the specific vasomotor contributions of nNOS-derived NO in healthy subjects during exercise are unknown. The purpose of this dissertation is to test the global hypothesis that nNOS-derived NO is a critical regulator of exercising skeletal muscle vascular control. Specifically, we utilized the selective nNOS inhibitor S-methyl-L-thiocitrulline (SMTC) to investigate the effects of nNOS-derived NO on skeletal muscle vascular function within established rodent models of exercise performance. The first investigation (Chapter 2) identifies that nNOS inhibition with SMTC increases mean arterial pressure (MAP) and reduces rat hindlimb skeletal muscle blood flow at rest whereas there are no effects during low-speed (20 m/min) treadmill running. In Chapter 3 it is reported that nNOS inhibition with SMTC reduces blood flow during high-speed treadmill running (>50 m/min) with the greatest relative effects found in highly glycolytic fast-twitch muscles and muscle parts. Chapter 4 demonstrates that nNOS-derived NO modulates contracting skeletal muscle blood flow (increases), O₂ consumption ($\dot{V}O_2$, increases), and force production (decreases) in the rat spinotrapezius muscle and thus impacts the microvascular O₂ delivery- $\dot{V}O_2$ ratio (which sets the microvascular partial pressure of O₂, PO_{2mv} , and represents the pressure head that drives capillary-myocyte O₂ diffusion). In Chapter 5 we report that systemic administration of the selective nNOS inhibitor SMTC does not impact lumbar sympathetic nerve discharge. This reveals that the SMTC-induced peripheral vascular effects described herein reflect peripheral nNOS-derived NO signaling as opposed to centrally-derived regulation. In conclusion, nNOS-derived NO exerts exercise-intensity and muscle fiber-type selective peripheral vascular effects during whole-body locomotor exercise. In addition, nNOS-derived NO modulates skeletal muscle contractile and metabolic function and, therefore, impacts the skeletal muscle PO_{2mv} . These data identify novel integrated roles for nNOS-derived NO within healthy skeletal muscle and have important implications for populations associated with reduced NO bioavailability and/or impaired nNOS structure and/or function specifically (e.g., muscular dystrophy, chronic heart failure, advanced age, etc.).

ENZYMATIC REGULATION OF SKELETAL MUSCLE OXYGEN TRANSPORT:
NOVEL ROLES FOR NEURONAL NITRIC OXIDE SYNTHASE

by

STEVEN WESLEY COPP

M.S., Kansas State University, 2008

A DISSERTATION

submitted in partial fulfillment of the requirements for the degree

DOCTOR OF PHILOSOPHY

Department of Anatomy and Physiology
College of Veterinary Medicine

KANSAS STATE UNIVERSITY
Manhattan, Kansas

2013

Approved by:

Major Professor
Dr. Timothy I. Musch

Copyright

STEVEN WESLEY COPP

2013

Abstract

Nitric oxide (NO) is synthesized via distinct NO synthase (NOS) enzymes and constitutes an essential cardiovascular signaling molecule. Whereas important vasomotor contributions of endothelial NOS (eNOS) have been well-described, the specific vasomotor contributions of nNOS-derived NO in healthy subjects during exercise are unknown. The purpose of this dissertation is to test the global hypothesis that nNOS-derived NO is a critical regulator of exercising skeletal muscle vascular control. Specifically, we utilized the selective nNOS inhibitor S-methyl-L-thiocitrulline (SMTC) to investigate the effects of nNOS-derived NO on skeletal muscle vascular function within established rodent models of exercise performance. The first investigation (Chapter 2) identifies that nNOS inhibition with SMTC increases mean arterial pressure (MAP) and reduces rat hindlimb skeletal muscle blood flow at rest whereas there are no effects during low-speed (20 m/min) treadmill running. In Chapter 3 it is reported that nNOS inhibition with SMTC reduces blood flow during high-speed treadmill running (>50 m/min) with the greatest relative effects found in highly glycolytic fast-twitch muscles and muscle parts. Chapter 4 demonstrates that nNOS-derived NO modulates contracting skeletal muscle blood flow (increases), $\dot{V}O_2$ (increases), and force production (decreases) in the rat spinotrapezius muscle and thus impacts the microvascular O_2 delivery- $\dot{V}O_2$ ratio (which sets the microvascular partial pressure of O_2 , PO_{2mv} , and represents the pressure head that drives capillary-myocyte O_2 diffusion). In Chapter 5 we report that systemic administration of the selective nNOS inhibitor SMTC does not impact lumbar sympathetic nerve discharge. This reveals that the SMTC-induced peripheral vascular effects described herein reflect peripheral nNOS-derived NO signaling as opposed to centrally-derived regulation. In conclusion, nNOS-derived NO exerts exercise-intensity and muscle fiber-type selective peripheral vascular effects during whole-body locomotor exercise. In addition, nNOS-derived NO modulates skeletal muscle contractile and metabolic function and, therefore, impacts the skeletal muscle PO_{2mv} . These data identify novel integrated roles for nNOS-derived NO within healthy skeletal muscle and have important implications for populations associated with reduced NO bioavailability and/or impaired nNOS structure and/or function specifically (e.g., muscular dystrophy, chronic heart failure, advanced age, etc.).

Table of Contents

List of Figures	viii
List of Tables	ix
Acknowledgements.....	x
Preface.....	xi
Chapter 1 - Introduction.....	1
References.....	7
Chapter 2 - Effects of neuronal nitric oxide synthase inhibition on resting and exercising hindlimb muscle blood flow in the rat	11
Summary.....	12
Introduction.....	13
Methods	15
Results.....	19
Discussion.....	21
References.....	34
Chapter 3 - Muscle fiber-type dependence of neuronal nitric oxide synthase-mediated vascular control in the rat during high-speed treadmill running.....	39
Summary.....	40
Introduction.....	41
Methods	43
Results.....	48
Discussion.....	50
References.....	63
Chapter 4 - Role of neuronal nitric oxide synthase in modulating skeletal muscle microvascular and contractile function	67
Summary.....	68
Introduction.....	69
Methods	71
Results.....	77
Discussion.....	79

References.....	92
Chapter 5 - Neuronal nitric oxide synthase inhibition and regional sympathetic nerve discharge: implications for peripheral vascular control	98
Summary.....	99
Introduction.....	100
Methods	101
Results.....	104
Discussion.....	105
References.....	111
Chapter 6 - Conclusions.....	114
Appendix A - Curriculum Vitae	116

List of Figures

Figure 1.1. Unanswered questions regarding physiological roles of nNOS-derived NO.....	6
Figure 2.1. Effects of nNOS inhibition on resting skeletal muscle blood flow and VC.....	28
Figure 2.2. Relationships between changes in resting blood flow and VC following SMTC and muscle fiber-type composition.....	29
Figure 2.3. Relationships between resting blood flow and VC and the changes in resting blood flow and VC.....	30
Figure 2.4. Effects of nNOS inhibition on exercising skeletal muscle blood flow and VC	31
Figure 2.5. Effects of nNOS inhibition on resting and exercising MAP and HR.....	32
Figure 2.6. Effects of SMTC and L-NAME on the hypotensive response to ACh	33
Figure 3.1. Estimation of critical speed for a representative rat	58
Figure 3.2. Effects of nNOS inhibition on hindlimb skeletal muscle blood flow and VC	59
Figure 3.3. Relative changes in blood flow and VC following nNOS inhibition.....	60
Figure 3.4. Relative changes in blood flow and VC following nNOS inhibition.....	61
Figure 3.5. MAP data demonstrating the efficacy and selectivity of nNOS inhibition	62
Figure 4.1. Effects SMTC and L-NAME on the hypotensive response to ACh.....	86
Figure 4.2. Effects of SMTC infusion on PO_{2mv}	87
Figure 4.3. Effects of nNOS inhibition on contracting muscle PO_{2mv}	88
Figure 4.4. Effects of nNOS inhibition on spinotrapezius muscle blood flow and VC.....	89
Figure 4.5. Effects of nNOS inhibition on spinotrapezius muscle $\dot{V}O_2$	90
Figure 4.6. Effects of nNOS inhibition on spinotrapezius muscle force production.....	91
Figure 5.1. Original tracings of lumbar and renal SND from a representative rat	108
Figure 5.2. Effects of saline and SMTC infusions on lumbar and renal SND.....	109
Figure 5.3. Effects of saline and SMTC infusions on MAP and HR.....	110
Figure 6.1. Summary of results.....	115

List of Tables

Table 2.1. Effects of nNOS inhibition on resting skeletal muscle blood flow and VC	26
Table 2.2. Effects of nNOS inhibition on kidney and splanchnic organ blood flow and VC.....	27
Table 3.1. Effects of nNOS inhibition on MAP and HR	54
Table 3.2. Effects of nNOS inhibition on blood flow and VC	55
Table 3.3. Effects of nNOS inhibition on blood flow and VC	57
Table 4.1. Effects of nNOS inhibition on HR and MAP	84
Table 4.2. Effects of nNOS inhibition on contracting skeletal muscle PO_{2mv} parameters.....	85

Acknowledgements

I am deeply indebted to the many wonderful individuals who have helped make my graduate school experience simultaneously rewarding, challenging, productive, and fun.

First, I am extremely grateful for the outstanding academic mentorship of my major professor, Dr. Timothy Musch, who was willing to take a chance and allow an unknown student to wander into his research laboratory in the fall of 2006. I would like also like to thank Dr. David Poole for his vital role in my professional development and assure him that I will never take anyone at their word but demand to see the scientific evidence for myself. Together, Dr. Musch and Dr. Poole have taught me the importance and value of scientific research while providing constant reminders that academic and professional success is only a worthwhile pursuit if I enjoy what I am doing.

In addition to Dr. Musch and Dr. Poole, I am grateful for the professional and scientific influence, guidance, and critique from my committee members: Dr. Michael Kenney, Dr. Thomas Barstow, Dr. Craig Harms, and Dr. Mark Haub.

I am grateful to the many former and current Musch/Poole students with whom I have shared lab (and LAB) time with including Sue Hageman, Dr. Leonardo Ferreira, Kyle Herspring, Lauren McDaniel, Dr. Robert Davis, Peter Schwagerl, Scott Ferguson, Clark Holdsworth, and Gabi Sims. Special gratitude is reserved for Dr. Daniel Hirai with whom the majority of my graduate studies and LAB time have overlapped.

I would like to thank my parents for always supporting me in my decision to pursue graduate training. Finally, I owe a special thanks to my wife Melissa and daughter Kieryn for always supporting me, encouraging me, and understanding that rats still need to run on Saturdays.

Preface

Chapters 2-5 of this dissertation represent original research articles that have been published or accepted for publication following the peer-review process (citations may be found below). They are reproduced here with permission from the publishers.

Copp SW, Hirai DM, Schwagerl PJ, Musch TI, and Poole DC. Effects of neuronal nitric oxide synthase inhibition on resting and exercising hindlimb muscle blood flow in the rat. *J Physiol* 588, 1321-1331, 2010.

Copp SW, Holdsworth CT, Ferguson SK, Hiari DM, Poole DC and Musch TI. Muscle fibre-type dependence of neuronal nitric oxide synthase-mediated vascular control in the rat during high speed treadmill running. *J Physiol* In press, doi:10.1113/jphysiol.2013.251082.

Copp SW, Hirai DM, Ferguson SK, Musch TI, and Poole DC. Role of neuronal nitric oxide synthase in modulating microvascular and contractile function in rat skeletal muscle. *Microcirculation* 18, 501-511, 2011.

Copp SW, Hirai DM, Sims GE, Musch TI, Poole DC, and Kenney MJ. Neuronal nitric oxide synthase inhibition and regional sympathetic nerve discharge: implications for peripheral vascular control. *Resp Phys Neurobiol* 186: 285-289.

Chapter 1 - Introduction

Elevations in skeletal muscle metabolic demand during exercise are supported by robust increases in skeletal muscle blood flow and, therefore, O₂ delivery. Specifically, skeletal muscle blood flow increases 5-6 liters for every 1 liter increase in muscle O₂ consumption ($\dot{V}O_2$) across the spectrum of muscle fiber-type compositions (2). This tight coupling serves to constrain the fall in skeletal muscle microvascular O₂ pressure (PO_{2mv} , which reflects the skeletal muscle O₂ delivery/ $\dot{V}O_2$ ratio) during contractions preserving the pressure head driving capillary-myocyte O₂ diffusion. The increase in muscle blood flow during exercise is accomplished via complex interactions among neurohumoral activation (to increase cardiac output and facilitate peripheral blood flow redistribution to working skeletal muscle), local mechanical vascular influences (e.g., muscle pump and arteriolar compression-mediated vasodilation), and metabolic and humoral vasodilators (17, 31). However, resolution of the specific spatial and temporal actions of the various vasomotor regulators has proved elusive owing to the highly redundant and synergistic nature of the exercise hyperemic control (17).

Among the numerous putative vasodilator candidates, perhaps none has been so extensively investigated as the biological cardiovascular signaling molecule nitric oxide (NO). This is true despite the relatively recent history of NO-related research. Gruetter *et al.* (9) originally identified the smooth muscle relaxant properties of NO via its application within an organ bath containing pre-contracted strips of bovine coronary arteries. In 1980, a landmark paper by Furchgott and Zawadzki (5) identified that an intact endothelium was required to elicit vasodilation in response to acetylcholine and the term “endothelial-derived relaxing factor” (EDRF) was coined. It was not until 1987 that two groups working independently demonstrated that EDRF was in fact NO (16, 27). Only one year later came the observation that the amino acid L-arginine acted as an obligatory precursor for NO synthesis (26). Shortly thereafter it was identified that a cytosolic calcium-regulated enzyme utilized L-arginine to produce a substance that possessed similar vasoactive properties to EDRF (this molecule was not identified definitely as NO and consistent use of “NO” rather than “EDRF” was not yet commonplace) and acted through soluble guanylate cyclase (21). Although it was not stated as such at the time, this was the first identification of the NO synthase (NOS) enzyme. Subsequently, the first isolation of

NOS was reported in brain tissue (1) although this so called type I NOS or neuronal NOS (nNOS) enzyme was later identified to exist also within skeletal muscles (19), the vascular endothelium, and neurons (8). The initial NOS discovery was followed quickly by isolation of inducible NOS (type II NOS or iNOS) from macrophages (10) and endothelial NOS (type III NOS or eNOS) from endothelial cells of the bovine aorta (28). Since those seminal studies, NO-related research has spanned the fields of cardiovascular, immunological/inflammatory, neurological, and skeletal muscle/metabolic physiology and medicine (23).

A significant advancement in NO-related research came with the demonstration that N^G -monomethyl-L-arginine (L-NMMA) acted as an inhibitor of NO synthesis. This constituted a valuable experimental tool and opened the door to investigations in which acute pharmacological NOS inhibition could be administered to individual preparations/subjects and physiological responses could be measured before and after NOS inhibition. The first report utilizing such a strategy came from Rees *et al.* (29) who observed that L-NMMA administration rapidly and robustly increased blood pressure in anesthetized rabbits. The identification that pressure regulation depended on a tonic vasodilator signal, rather than tonic vasoconstriction, changed our understanding of cardiovascular and arterial blood pressure control (23). Importantly, that early work on NO and blood pressure regulation was completed prior to the discovery of the various NOS isoforms. Thus, the entirety of the NO-mediated blood pressure control signal was ascribed to the only confirmed source of NO production; the endothelium. The subsequent discoveries of the 3 distinct NOS isoforms (which included, of course, eNOS) and the fact that L-NMMA and L-NAME lacked specificity for a given isoform did little to quell the commonly held belief that eNOS-derived NO was the principal, if not exclusive, peripheral NO-mediated basal blood pressure control signal.

The experimental use of non-selective NOS inhibition via L-NMMA or another L-arginine analogue N^G -arginine-methyl-ester (L-NAME) has remained prominent. For example, studies utilizing non-selective NOS inhibition have provided evidence that NO constitutes a key vasoactive molecule which contributes importantly to contracting skeletal muscle hyperemia in both animals (e.g., 13, 18) and humans (e.g., 12, 32) and controls the temporal matching of the contracting muscle PO_{2mv} and changes thereof (3). While the majority of such investigations have failed to identify the specific cardiovascular effects of the distinct NOS isoforms, given the central role of the endothelium in shear-stress related signal transduction and vasodilation during

exercise, NO-mediated peripheral vascular regulation in exercising muscle has been essentially synonymous with endothelial and eNOS-mediated function (39).

There is limited information regarding the potential vasodilatory roles for nNOS-derived NO during exercise in healthy subjects (22). Evidence supporting vasomotor influences of nNOS-derived NO emanates primarily from genetically-altered mouse models in which nNOS expression is reduced or absent and the ability to attenuate sympathetic vasoconstrictor signals within contracting skeletal muscle is impaired (36, 37). The ability to modulate sympathetic vasoconstriction during forearm contractions is similarly impaired in children with Duchenne muscular dystrophy, a disease condition hallmarked by reduced intramuscular nNOS expression and muscle weakness (30). However, the blood flow response to muscle contractions *per se* was preserved in those investigations suggesting no obligatory exercise hyperemic role for nNOS-derived NO specifically. It also must be considered that chronic nNOS absence in disease and disease models is associated with impaired skeletal muscle growth and function which may impact vasomotor signaling pathways (30) and that alternate NOS isoforms may compensate when one isoform is altered chronically (14). Notwithstanding these considerations, given the localization of calcium-regulated nNOS near the sarcolemma of skeletal myocytes and the unrestricted diffusibility of NO across biological membranes, nNOS-derived NO seems a logical paracrine vasodilator candidate responsible for linking skeletal muscle O₂ supply to O₂ demand; an essential feature of exercise hyperemia (17). Exercise intensity and/or muscle-fiber type selective characteristics of nNOS-derived vasomotor regulation are also plausible given that nNOS activity is higher in glycolytic fast-twitch versus oxidative slow-twitch rat muscle (19) and that the attenuation of sympathetic vasoconstriction is present in glycolytic but not oxidative rat muscle during high contraction intensities only (35). In addition, myoglobin concentration is higher in oxidative compared to glycolytic skeletal muscles (11) and it has been demonstrated that myoglobin possesses potent NO scavenging properties (4). Collectively, those observations suggest that an nNOS-derived NO vasomotor signal may exist within glycolytic muscles during high-intensity exercise, however, direct empirical observations regarding requisite characteristics of nNOS-mediated vascular control in healthy subjects are lacking. Specifically, it remains unknown whether nNOS-derived NO vasomotor regulation: 1) contributes importantly to skeletal muscle hyperemia in healthy subjects during whole-body locomotor exercise, 2) varies as a function of exercise intensity and/or muscle fiber-type composition during voluntary

exercise, or 3) occurs concurrent with nNOS-derived NO contractile and metabolic regulation (Figure 1.1).

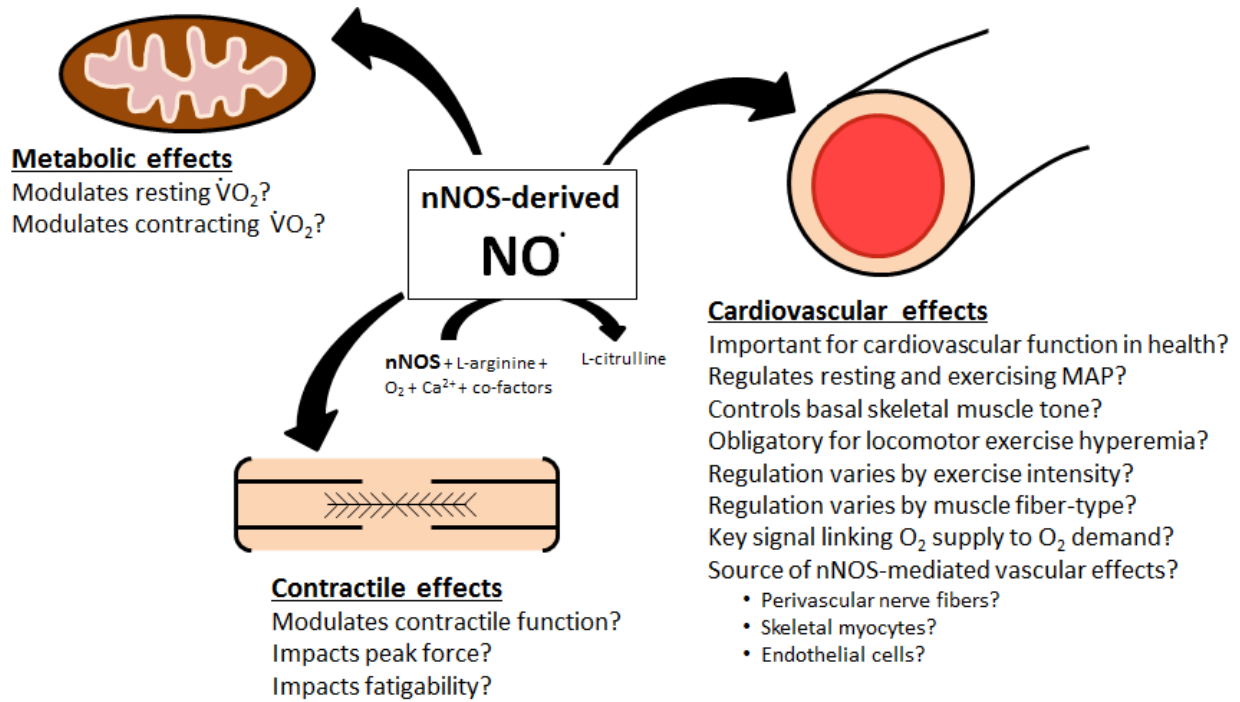
In 1994, development of the pharmacological selective nNOS inhibitor S-methyl-L-thiocitrulline (SMTC; 6, 24) afforded the opportunity to investigate the physiological roles of nNOS-derived specifically. Subsequently, marked pressor effects were observed when SMTC was administered to intact animals *in vivo* (7, 25). Tragically, given the established dogma that eNOS-derived NO controlled basal blood pressure, those pressor effects were often interpreted to represent SMTC-induced effects on eNOS rather than important physiological contributions from nNOS (7, 25, 38). Thus, the use of SMTC as a means to investigate nNOS-mediated function *in vivo* did not gain significant traction initially. In 1998, Ichihara and colleagues (15) examined the role of nNOS inhibition via SMTC on renal arteriolar function. Cognizant of the concerns regarding the selectivity of SMTC for nNOS over eNOS, the investigators examined the vasodilatory response of isolated renal afferent and efferent arterioles to acetylcholine (ACh, an eNOS agonist). The fact that SMTC did not blunt the vasodilatory response to ACh, whereas it was completely inhibited following non-selective NOS administration, supported the selectivity of SMTC for nNOS. Moreover, the precedent for the assessment of the selectivity of SMTC for nNOS via ACh administration was established (15). Komers *et al.* (20) then followed with a study utilizing systemically-administered SMTC in rats and demonstrated that low SMTC doses do not impact the hypotensive response to systemic ACh infusions whereas they are blunted at high SMTC doses (consistent with the loss of selectivity for nNOS at high SMTC doses only). Wakefield *et al.* (38) subsequently completed an SMTC dose-response assessment to various vasoactive agents including ACh, sodium nitroprusside (SNP, an NO donor), salbutamol (a beta-2 receptor agonist the effects of which are L-NAME sensitive), and bradykinin. That investigation has provided the strongest support to date for the selectivity of nNOS inhibition with systemic low-dose SMTC administration *in vivo*. More recently, the selectivity of SMTC for nNOS has been confirmed in humans (33, 34) concurrent with the demonstration that nNOS-derived NO modulates basal brachial (33) and coronary (34) artery blood flow.

There are currently no investigations that have utilized selective nNOS inhibition with SMTC to examine the role of nNOS-derived NO in the regulation of contracting skeletal muscle vascular control. Thus, the overarching purpose of this dissertation is to employ selective nNOS

inhibition with SMTC to test the global hypothesis that nNOS-derived NO is a critical regulator of skeletal muscle vascular control during exercise in healthy subjects. Specifically, acute systemic SMTC administration was utilized to investigate the effects of nNOS-derived NO on rat hindlimb skeletal muscle blood flow and vascular conductance (VC) at rest and during low-speed treadmill running (Chapter 2). Given the potential for exercise intensity and muscle-fiber type dependency of nNOS-mediated vascular control we examined the effects of SMTC administration on skeletal muscle blood flow during high-speed treadmill running above critical speed which evokes marked fast-twitch fiber recruitment (Chapter 3). In anesthetized rats, SMTC was employed to examine the influence of nNOS-derived NO on resting skeletal muscle PO_{2mv} , the dynamic PO_{2mv} response following the onset of contractions, and skeletal muscle metabolic (i.e., $\dot{V}O_2$) and contractile function (Chapter 4). Finally, we investigated the effects of systemically-administered SMTC on lumbar sympathetic nerve discharge to dissect the contributions of central versus peripheral nNOS inhibition in the previous experiments (Chapter 5). Importantly, evidence supporting the efficacy and selectivity of nNOS inhibition is presented and discussed within each investigation.

Chapters 2-5 of this dissertation are self-contained and presented in standard journal article format with introduction, methods, results, discussion and reference sections. The last chapter of this dissertation (Chapter 6) provides an overall summary and conclusion which synthesizes and integrates the primary findings from the individual studies.

Figure 1.1. Unanswered questions regarding physiological roles of nNOS-derived NO



Schematic representation of the unanswered questions regarding the physiological roles of nNOS-derived NO within skeletal muscle and associated vascular beds in healthy subjects.

$\dot{V}O_2$, O_2 consumption; MAP, mean arterial pressure.

References

1. **Bredt DS and Snyder SH.** Isolation of nitric oxide synthetase, a calmodulin-requiring enzyme. *Proc Natl Acad Sci USA* 87: 682-685, 1990.
2. **Ferreira LF, McDonough P, Behnke BJ, Musch TI, and Poole DC.** Blood flow and O₂ extraction as a function of O₂ uptake in muscles composed of different fiber types. *Respir Physiol Neurobiol* 153: 237-49, 2006a.
3. **Ferreira LF, Padilla DJ, Williams J, Hageman KS, Musch TI, and Poole DC.** Effects of altered nitric oxide availability on rat muscle microvascular oxygenation during contractions. *Acta Physiologica* 186: 223-32, 2006b.
4. **Flögel U, Merx MW, Godecke A, Decking UK, Schrader J.** Myoglobin: A scavenger of bioactive NO. *Proc Natl Acad Sci USA* 98: 735-40, 2001
5. **Furchgott RF and Zawadzki JV.** The obligatory role of endothelial cells in the relaxation of arterial smooth muscle by acetylcholine. *Nature* 288: 373-376, 1980.
6. **Furfine ES, Harmon MF, Paith JE, Knowles RG, Salter M, Kiff RJ, Duffy C, Hazelwood R, Oplinger JA, and Garvey EP.** Potent and selective inhibition of human nitric oxide synthases. Selective inhibition of neuronal nitric oxide synthase by S-methyl-L-thiocitrulline and S-ethyl-L-thiocitrulline. *J Biol Chem* 269: 26677-26683, 1994.
7. **Gozal D, Torres JE, Gozal YM, and Littwin SM.** Effect of nitric oxide synthase inhibition on cardiorespiratory responses in the conscious rat. *J Appl Physiol* 81: 2068-2077, 1996.
8. **Griffith OW and Stuehr DJ.** Nitric oxide synthases: properties and catalytic mechanism. *Annu Rev Physiol* 57: 707-36, 1995.
9. **Gruetter CA, Barry BK, McNamara DB, Gruetter DY, Kadowitz PJ, and Ignarro L.** Relaxation of bovine coronary artery and activation of coronary artery guanylate cyclase by nitric oxide, nitroprusside and a carcinogenic nitrosoamine. *J Cyclic Nucleotide Res* 5: 211-224, 1979.
10. **Hevel JM, White KA, and Marletta MA.** Purification of the inducible murine macrophage nitric oxide synthase. *J Biol Chem* 266: 22789-22791, 1991.

11. **Hickson RC.** Skeletal muscle cytochrome c and myoglobin, endurance, and frequency of training. *J Appl Physiol* 51: 746-9, 1981.
12. **Hickner RC, Fisher JS, Ehsani AA, Kohrt WM.** Role of nitric oxide in skeletal muscle blood flow at rest and during dynamic exercise in humans. *Am J Physiol* 273: 405-10, 1997.
13. **Hirai T, Visneski MD, Kearns KJ, Zelis R, and Musch TI.** Effects of NO synthase inhibition on the muscular blood flow response to treadmill exercise in rats. *J Appl Physiol* 77: 1288-93, 1994.
14. **Huang A, Sun D, Shesely EG, Levee EM, Koller A, and Kaley G.** Neuronal NOS-dependent dilation to flow in coronary arteries of male eNOS-KO mice. *Am J Physiol Heart Circ Physiol* 282: H429-436, 2002.
15. **Ichihara A, Inscho EW, Imig JD, and Navar LG.** Neuronal nitric oxide synthase modulates rat renal microvascular function. *Am J Physiol* 274: F516-524, 1998.
16. **Ignarro LJ, Buga GM, Wood KS, Byrns RE, and Chaudhuri G.** Endothelium-derived relaxing factor produced and released from artery and vein is nitric oxide. *Proc Natl Acad Sci USA* 84: 9265-9269, 1987.
17. **Joyner MJ and Wilkins BW.** Exercise hyperaemia: is anything obligatory but the hyperaemia? *J Physiol* 583: 855-60, 2007.
18. **King CE, Melinyshyn MJ, Mewburn JD, Curtis SE, Winn MJ, Cain SM, and Chapler CK.** Canine hindlimb blood flow and O₂ uptake after inhibition of EDRF/NO synthesis. *J Appl Physiol* 76: 1166-71, 1994.
19. **Kobzik L, Reid MB, Bredt DS, and Stamler JS.** Nitric oxide in skeletal muscle. *Nature* 372: 546-548, 1994.
20. **Komers R, Oyama TT, Chapman JG, Allison KM, and Anderson S.** Effects of systemic inhibition of neuronal nitric oxide synthase in diabetic rats. *Hypertension* 35: 655-661, 2000.
21. **Mayer B, Schmidt K, Humbert P, and Bohme E.** Biosynthesis of endothelium-derived relaxing factor: a cytosolic enzyme in porcine aortic endothelial cells Ca²⁺-dependently converts L-arginine into an activator of soluble guanylyl cyclase. *Biochem Biophys Res Commun* 164: 678-685, 1989.

22. **Melikian N, Seddon MD, Casadei B, Chowienczyk PJ, and Shah AM.** Neuronal nitric oxide synthase and human vascular regulation. *Trends Cardiovasc Med* 19: 256-262, 2009.
23. **Moncada S and Higgs EA.** The discovery of nitric oxide and its role in vascular biology. *Br J Pharmacol* 147: 193-201, 2006.
24. **Narayanan K and Griffith OW.** Synthesis of L-thiocitrulline, L-homothiocitrulline, and S-methyl-L-thiocitrulline: a new class of potent nitric oxide synthase inhibitors. *J Medicinal Chem* 37: 885-887, 1994.
25. **Narayanan K, Spack L, McMillan K, Kilbourn RG, Hayward MA, Masters BS, and Griffith OW.** S-alkyl—Lthiocitrullines. Potent and stereoselective inhibitors of nitric oxide synthase with strong pressor activity in vivo. *J Biol Chem* 270(19): 11103-10, 1995.
26. **Palmer RM, Ashton DS, and Moncada S.** Vascular endothelial cells synthesize nitric oxide from L-arginine. *Nature* 333: 664-666, 1988.
27. **Palmer RM, Ferrige AG, and Moncada S.** Nitric oxide release accounts for the biological activity of endothelium-derived relaxing factor. *Nature* 327: 524-526, 1987.
28. **Pollock JS, Fostermann U, Mitchell JA, Warner TD, Schmidt HH, Nakane M, and Murad F.** Purification and characterization of particulate endothelium-derived relaxing factor synthase from cultured and native bovine aortic endothelial cells. *Proc Natl Acad Sci USA* 88: 10480-10484, 1991.
29. **Rees DD, Palmer RM, Moncada S.** Role of endothelium-derived nitric oxide in the regulation of blood pressure. *Proc Natl Acad Sci USA* 86: 3375-8, 1989.
30. **Sander M, Chavoshan B, Harris SA, Iannaccone ST, Stull JT, Thomas GD, and Victor RG.** Functional muscle ischemia in neuronal nitric oxide synthase-deficient skeletal muscle of children with Duchenne muscular dystrophy. *Proc Natl Acad Sci USA* 97: 13818-13823, 2000.
31. **Sarelius I and Pohl U.** Control of muscle blood flow during exercise: local factors and integrative mechanisms. *Acta Physiologica* 199: 349-65, 2010.
32. **Schrage WG, Joyner MJ, and Dinunno FA.** Local inhibition of nitric oxide and prostaglandins independently reduces forearm exercise hyperaemia in humans. *J Physiol* 557: 599-611, 2004.

33. **Seddon MD, Chowienczyk PJ, Brett SE, Casadei B, and Shah AM.** Neuronal nitric oxide synthase regulates basal microvascular tone in humans in vivo. *Circulation* 117: 1991-1996, 2008.
34. **Seddon MD, Melikian N, Dworakowski R, Shabeeh H, Jiang B, Byrne J, Casadei B, Chowienczyk PJ, and Shah AM.** Effects of neuronal nitric oxide synthase on human coronary artery diameter and blood flow in vivo. *Circulation* 119: 2656-2662, 2009.
35. **Thomas GD, Hansen J, and Victor RG.** Inhibition of alpha 2-adrenergic vasoconstriction during contraction of glycolytic, not oxidative, rat hindlimb muscle. *Am J Physiol* 266: H920-929, 1994.
36. **Thomas GD, Sander M, Lau KS, Huang PL, Stull JT, and Victor RG.** Impaired metabolic modulation of alpha-adrenergic vasoconstriction in dystrophin-deficient skeletal muscle. *Proc Natl Acad Sci USA* 95: 15090-15095, 1998.
37. **Thomas GD, Shaul PW, Yuhanna IS, Froehner SC, and Adams ME.** Vasomodulation by skeletal muscle-derived nitric oxide requires alpha-syntrophin-mediated sarcolemmal localization of neuronal Nitric oxide synthase. *Circ Res* 92: 554-560, 2003.
38. **Wakefield ID, March JE, Kemp PA, Valentin JP, Bennett T, and Gardiner SM.** Comparative regional haemodynamic effects of the nitric oxide synthase inhibitors, S-methyl-L-thiocitrulline and L-NAME, in conscious rats. *Br J Pharmacol* 139: 1235-1243, 2003.
39. **Yetik-Anacak G and Catravas JD.** Nitric oxide and the endothelium: History and impact on cardiovascular disease. *Vasc Pharmacol* 45: 268-276, 2006.

Chapter 2 - Effects of neuronal nitric oxide synthase inhibition on resting and exercising hindlimb muscle blood flow in the rat

Summary

Nitric oxide (NO) derived from endothelial NO synthase (eNOS) is an integral mediator of vascular control during muscle contractions. However, it is not known whether neuronal NOS (nNOS) derived NO regulates tissue hyperemia in healthy subjects, particularly during exercise. We tested the hypothesis that selective nNOS inhibition would reduce blood flow and vascular conductance (VC) in rat hindlimb locomotor muscle(s), kidneys, and splanchnic organs at rest and during dynamic treadmill exercise (20 m/min, 10% grade). 19 male Sprague-Dawley rats (555±23 g) were assigned to either rest (n=9) or exercise (n=10) groups. Blood flow and VC were determined via radiolabelled microspheres before and after the intra-arterial administration of the selective nNOS inhibitor *S*-methyl-L-thiocitrulline (SMTC, 2.1±0.1 µmol/kg). Total hindlimb muscle blood flow (control: 20±2, SMTC: 12±2 ml/min/100g, $p<0.05$) and VC (control: 0.16±0.02, SMTC: 0.09±0.01 ml/min/100g/mmHg, $p<0.05$) were reduced substantially at rest. Moreover, the magnitude of the absolute reduction in blood flow and VC correlated ($p<0.05$) with the proportion of oxidative muscle fibers found in the individual muscles or muscle parts of the hindlimb. During exercise, total hindlimb blood flow (control: 108±7, SMTC: 105±8 ml/min/100g) and VC (control: 0.77±0.06; SMTC: 0.70±0.05 ml/min/100g/mmHg) were not different ($p>0.05$) between control and SMTC conditions. SMTC reduced ($p<0.05$) blood flow and VC at rest and during exercise in the kidneys, adrenals, and liver. These results enhance our understanding of the role of NO-mediated circulatory control by demonstrating that nNOS does not appear to subserve an obligatory role in the exercising muscle hyperemic response in the rat.

Introduction

Nitric oxide (NO) is a low molecular-weight, highly diffusible signaling molecule synthesized through the conversion of L-arginine to L-citrulline via the calcium dependent enzyme NO synthase (NOS). In healthy subjects, NO derived from two constitutively expressed NOS isoforms, neuronal NOS (nNOS) and endothelial NOS (eNOS), exerts influences on a vast array of biological functions including, for example, the regulation of vascular control, facilitation of skeletal muscle glucose uptake, modulation of muscle contractile function, and myoblast differentiation (40). Specifically in regards to vascular control, experimental pharmacological non-selective NOS inhibition in human and animal models provides the foundation for a substantial body of evidence that NO plays integral roles in regulating blood flow in skeletal muscle at rest and during exercise (20, 32) the kidney (16) and splanchnic organs (12).

One consequence of non-selective NOS inhibition is the inability to differentiate the specific NOS isoform origin of vasoactive NO within various vascular beds and physiological conditions (i.e., rest or exercise). Given that vascular endothelial dysfunction commonly underlies peripheral circulatory derangements manifested in conditions such as chronic heart failure (CHF; 24), diabetes (19), and advancing age (37), NO-mediated circulatory control has been ascribed principally to eNOS. However, the localization of nNOS near the sarcolemmal membrane (26) makes nNOS-derived NO a viable candidate in the regulation of the peripheral circulation, particularly during exercise. In this regard, emergent theoretical (21) and empirical (15, 26, 38, 39, 42) evidence has identified a more substantial role for nNOS-derived NO in vascular smooth muscle and blood flow regulation than considered previously. For example, nNOS-derived NO modulates vascular responses in isolated mouse hindlimb muscle (10, 27) and modulates basal (i.e., resting) total forearm (39) and coronary artery (38) blood flow in humans.

Strong support for the importance of nNOS-derived NO in blood flow regulation is that sympathetic vascular modulation is impaired in nNOS deficient skeletal muscle from both mice (42, 43) and humans (36). Consequently, skeletal muscle perfusion during exercise is compromised in nNOS deficient mice (26). However, to our knowledge obligatory participation of nNOS-derived NO in the hyperemic response to active locomotor skeletal muscle in healthy

individuals during physiologic exercise has not been investigated. Given that many clinical populations are hallmarked by skeletal muscle blood flow decrements and resultant exercise intolerance, resolution of this issue would constitute a fundamental step in the development of pharmacological and non-pharmacological interventions to mitigate vascular dysfunction in affected individuals.

The aim of the present study was to investigate the effects of nNOS inhibition via the selective nNOS blocker *S*-methyl-L-thiocitrulline (SMTC; 9, 44) on total and inter- and intramuscular hindlimb, kidney, and splanchnic organ blood flow and vascular conductance (VC) at rest and during submaximal dynamic treadmill exercise in healthy rats. Based on the evidence summarized above regarding the role of nNOS in peripheral circulatory control we hypothesized that nNOS inhibition would significantly reduce blood flow and VC to these tissues at rest and during exercise.

Methods

Animal selection and assignment

A total of 19 young adult (age: 4-6 months) male Sprague-Dawley rats (body weight: 555 ± 23 g) were utilized. All animals were purchased from Charles River Laboratories (Wilmington, MA, USA) and, upon arrival at Kansas State University, were housed in approved facilities and maintained on a 12:12 hour light-dark cycle with food and water available *ad libitum*. All experimental procedures described herein were conducted according to the guidelines established by the *Journal of Physiology* (7) and the National Institutes of Health and were approved by Kansas State University's Institutional Animal Care and Use Committee. Initially, rats were assigned randomly to either a rest (n=9) or exercise (n=6) group with 4 additional rats added to the exercise group to increase statistical power. Prior to the initiation of the experimental protocol, the exercise group was familiarized with running on a custom-built motor-driven treadmill over a ~2 week period in which rats ran for ~5 min/day at a speed of 20 m/min up a 10% grade.

Surgical procedure

On the day of data collection, animals were anesthetized with 5% isoflurane. Subsequently, while being maintained on a 2-3% isoflurane-oxygen mixture, one catheter (PE-10 connected to PE-50, Clay Adams Brand, Sparks, MD, USA) was placed in the ascending aorta via the right carotid artery and a second was placed in the caudal (tail) artery, as described previously (31). Both catheters were tunneled subcutaneously to the dorsal aspect of the cervical region, exteriorized through a puncture wound in the skin, and incisions were closed. Anesthesia was then terminated and the animal was given 1-2 hours to recover prior to the initiation of the final experimental protocol (Figure 2.1).

Rest (n=9)

Following recovery, the tail artery catheter was attached to a pressure transducer (Gould Statham P23ID, Valley View, OH, USA) which was connected to a recorder and 10 $\mu\text{g}/\text{kg}$ of acetylcholine (ACh: Sigma Chemical, St. Louis, MO, USA) was injected via the carotid artery

catheter. The subsequent peak hypotensive response to ACh injections was measured and recorded. Following the normalization of mean arterial pressure (MAP), the tail artery catheter was connected to a 1 ml syringe and blood withdrawal was initiated at a rate of 0.25 ml/min via a Harvard infusion/withdrawal pump (model 907, Cambridge, MA, USA). Simultaneously, heart rate (HR) and MAP were measured and recorded via the carotid artery catheter for ~10 s. Immediately after the HR and MAP recording, the carotid artery catheter was disconnected from the pressure transducer and $0.5\text{-}0.6 \times 10^6$ 15 μm diameter microspheres (^{85}Sr or ^{46}Sc in random order: Perkin Elmer Life and Analytical Sciences, Waltham, MA, USA) were injected into the aortic arch to determine regional blood flows.

Following the initial microsphere injection, the animal remained in the resting condition for ~10 minutes after which 2.1 ± 0.1 $\mu\text{mol/kg}$ of SMTC (Sigma, St. Louis, MO, USA), an nNOS inhibitor with a 17-fold selectivity for nNOS over eNOS (9), dissolved in 1.2 ml of saline was infused into the tail artery catheter for 6 min. This dose of SMTC was selected based on previous investigations in which similar doses were used to inhibit nNOS (15, 38, 39, 44) and preliminary studies in our laboratory where we examined the highest possible SMTC dose that could be administered without affecting the hypotensive responses to ACh (Copp, Hirai, Schwagerl, Musch, Poole, unpublished observations). Once the infusion was complete, a second microsphere injection (differently labeled from the first injection) followed by a second ACh injection protocol were performed exactly as described above. Subsequent to the recovery of MAP after the second ACh injection (~5 min), 10 mg/kg of the non-selective NOS inhibitor N^G -nitro-L-arginine-methyl-ester (L-NAME: Sigma Chemical, St. Louis, MO, USA) was administered into the carotid artery catheter and HR and MAP were monitored for 5 minutes. A third injection of 10 $\mu\text{g/kg}$ of ACh was then performed and the hypotensive response was again measured.

Exercise (n=10)

Each rat was placed initially on the treadmill and, after a period of stabilization (~2 hours after instrumentation), 10 $\mu\text{g/kg}$ of ACh was injected into carotid artery catheter. The peak hypotensive response was measured and recorded from the tail artery catheter. After the injection, the tail artery catheter was connected to a 1 ml plastic syringe and the Harvard infusion/withdrawal pump. Exercise was initiated, and the speed of the treadmill increased

progressively over the next 30 s to a speed of 20 m/min (10% grade) which has been demonstrated previously to elicit ~55-65% of peak O₂ uptake ($\dot{V}O_2 peak$; 29). The rat was then exercised steadily and after ~3.5 min of total exercise time, blood withdrawal from the tail artery catheter was initiated at a rate of 0.25 ml/min. HR and MAP were measured simultaneously and recorded via the carotid artery catheter for ~10 s. Immediately afterwards, the carotid artery catheter was disconnected from the pressure transducer and 0.5-0.6x10⁶ microspheres (⁸⁵Sr or ⁴⁶Sc in random order) were injected into the aortic arch. Approximately 15-30 seconds after microsphere injection, exercise was terminated and each rat was allowed a minimum of 30 min to recover.

After recovery from this exercise bout, 2.1±0.1 μmol/kg of SMTC dissolved in 1.2 ml of saline was infused via the tail catheter over a 6 min period. Following the infusion, the tail catheter was re-connected to a syringe and the Harvard pump for blood withdrawal. The second bout of exercise, microsphere injection (differently labeled from the first run), and ACh injection protocols were performed exactly as described above for the control (non-SMTC infusion) condition. Following recovery from the second ACh injection and as described at rest, L-NAME was administered and MAP and HR were monitored for 5 min. Subsequently, a third ACh injection was performed. The hypotensive responses from the rest and exercise groups were combined and the responses were then compared among conditions in order to determine the efficacy of selective (SMTC) and non-selective NOS inhibition (L-NAME).

Determination of blood flow and vascular conductance

Following the final (third) ACh injection, each animal was euthanized by means of pentobarbital overdose administered via the carotid artery catheter. The thorax was opened, and placement of the carotid artery catheter into the aortic arch was confirmed by anatomical dissection. Organs of the splanchnic region, the kidneys, and principal locomotor muscles of both hindlimbs were identified and removed. The tissues were blotted, weighed, and placed immediately into counting vials.

The radioactivity of each tissue was determined on a gamma scintillation counter (Packard Auto Gamma Spectrometer, model 5230, Downers Grove, IL, USA). Accounting for cross-talk between isotopes (⁴⁶Sc and ⁸⁵Sr), blood flows to each tissue were determined using the reference sample method (31) and expressed as milliliters per minute per 100 g of tissue

(ml/min/100g). Adequate mixing of the microspheres was verified for each injection by demonstrating a <15% difference between blood flow to the right and left kidneys and/or to the right and left hindquarter musculature. All blood flow data were normalized to the MAP measured immediately prior to the microsphere injection and expressed as VC (ml/min/100g/mmHg).

Statistical analyses

Resting HR and MAP values as well as the hypotensive responses to ACh from the resting and exercising experimental groups were combined (n=19) and compared among conditions (pre- and post-SMTC and post-L-NAME) via repeated measures one-way ANOVA. Where significant differences were found a Student-Newman-Keuls *post-hoc* test was used to determine where differences existed. In the exercising group, HR and MAP measured during the two exercise bouts were compared via paired Student's *t*-tests. Muscle blood flows and tissue VCs measured either at rest or during exercise before and after SMTC administration were compared using paired two-tailed Student's *t*-tests. Pearson product moment correlations were performed to determine whether the absolute and relative reductions in resting blood flow (Δ blood flow) and VC (Δ VC) in the individual muscles or muscle parts of the hindlimb produced by SMTC administration were correlated with their estimated fiber type composition and/or relative blood flow and VC during the control condition. The fiber type composition of each muscle or muscle part was based on the percentage of type I and IIa fibers in the individual muscles and muscle parts of the rat hindlimb as described by Delp and Duan (4). Results are presented as mean \pm SEM. Significance was accepted at $p<0.05$.

Results

Effects of SMTC on hindlimb muscle(s) blood flow and vascular conductance

Total resting hindlimb muscle blood flow (control: 20 ± 2 , SMTC: 12 ± 2 ml/min/100g, $p < 0.05$) and VC (control: 0.16 ± 0.02 , SMTC: 0.09 ± 0.01 ml/min/100g/mmHg, $p < 0.05$) were reduced following SMTC administration (Figure 2.1). Specifically, blood flow was significantly reduced in 8 of 24 individual muscles or muscle parts whereas VC was reduced in 13 of 24 of these tissues (Table 2.1). The absolute Δ blood flow and Δ VC after SMTC were significantly correlated with the percent sum of type I and IIa fibers found in the individual muscles or muscle parts (Δ blood flow: $r = 0.85$, Δ VC: $r = 0.87$, $p < 0.001$ for both, Figure 2.2) such that the greatest effect of SMTC administration occurred in those muscles or muscle parts containing primarily oxidative muscle fibers. There were no significant correlations between the relative Δ blood flow and Δ VC after SMTC administration and the percent sum of type I and IIa muscle fibers in the individual tissues examined. The absolute Δ blood flow and Δ VC after SMTC increased as a function of the relative resting blood flow ($r = 0.97$, $p < 0.001$) and VC ($r = 0.95$, $p < 0.001$) under control conditions, respectively, to the individual muscles or muscle parts of hindlimb (Figure 2.3).

In marked contrast to the resting condition, total hindlimb muscle blood flow (control: 108 ± 7 , SMTC: 105 ± 8 ml/min/100g, $p > 0.05$) and VC (control: 0.77 ± 0.06 ; SMTC: 0.70 ± 0.05 ml/min/100g/mmHg, $p > 0.05$) during exercise were not different between control and SMTC conditions (Figure 2.1). Moreover, blood flow and VC were not reduced ($p > 0.05$) in any of the 24 individual muscles or muscle parts of the hindlimb musculature.

Effects of SMTC on kidney and splanchnic organ blood flow

During both rest and exercise SMTC administration reduced ($p < 0.05$) blood flow and VC in the right and left kidney, adrenal glands, and liver but not in the small or large intestine, pancreas, spleen or stomach (Table 2.2).

Effects of SMTC and L-NAME on MAP, HR, and hypotensive response to ACh injections

The effects of SMTC and L-NAME administration on resting and exercising MAP and HR are presented in Figure 2.4. At rest, SMTC increased MAP and reduced HR compared to the control condition. The administration of L-NAME further elevated MAP and decreased HR such that the values attained were significantly different ($p < 0.05$) from both the control and SMTC conditions. In the exercising rats, MAP and HR measured during exercise immediately prior to microsphere injection were elevated above resting values in the control condition, whereas after SMTC administration exercising HR was significantly elevated ($p < 0.05$) above rest but MAP was not. More importantly, the MAP and HR measured during exercise were not different between control and SMTC conditions.

The absolute and relative hypotensive responses (Δ MAP) to ACh injection are presented in Figure 2.5. The absolute Δ MAP was increased after SMTC administration compared to control whereas after L-NAME it was reduced compared to SMTC but not control. Conversely, there were no differences in the relative Δ MAP after ACh injections between control and SMTC conditions and L-NAME resulted in significant blunting of relative Δ MAP compared to both control and SMTC.

Discussion

The present investigation is the first of its kind to investigate systematically the effects of selective nNOS inhibition on inter- and intramuscular hindlimb muscle(s) blood flow at rest and during submaximal treadmill exercise in the conscious rat. Consistent with our hypothesis, total hindlimb muscle blood flow and VC were reduced at rest after SMTC. The absolute, but not relative, Δ blood flow and Δ VC to the individual tissues after nNOS inhibition were correlated with muscle fiber-type such that the greatest reductions occurred in individual muscles and muscle parts with the greatest proportion of oxidative fibers. However, contrary to our hypothesis there was no effect of nNOS inhibition on exercising blood flow or VC in the total hindlimb or any of the individual muscles or muscle parts. In addition, nNOS inhibition reduced right and left kidney, adrenal and liver blood flow both at rest and during exercise. The present study demonstrates that nNOS-derived NO plays an integral role in regulating basal (i.e., resting) locomotory skeletal muscle blood flow but appears not to be obligatory for achieving the exercise hyperemic response, at least during these submaximal running speeds (equivalent to ~55-65% of $\dot{V}O_2 peak$) in the rat.

Relationship with the literature

Presently, we found that SMTC administration reduced resting total hindlimb muscle blood flow and VC by 38% and 47%, respectively. These results are consistent with recent reports from Seddon and colleagues of 30% (39) and 36% (38) SMTC-induced blood flow reductions in the human forearm. In those same investigations from Seddon *et al.* infusion of the non-selective NOS inhibitor N^G -monomethyl-L-arginine (L-NMMA) reduced blood flow by only marginally higher values of 37% (39) and 40% (38), respectively. Taken together, these data suggest that at rest nNOS may supply the bulk of the NO-mediated blood flow regulatory signal (38, 39). Furthermore, our data demonstrate that within the hindlimb musculature the greatest reductions in resting blood flow and VC occurred in the muscles composed of primarily oxidative muscle fibers. This was somewhat surprising given that previous *in vitro* (33) and histochemical (22) data in rodents suggests that nNOS is the predominant NOS isoform in less-oxidative fast-twitch muscle but not in more oxidative muscle fibers. The different implications

from those reports and our current study are likely due to our ability to measure specifically blood flow within an intact physiological model. For example, we demonstrate a strong correlation between the Δ blood flow and VC after SMTC and the relative blood flow and VC, respectively, measured during control conditions (Figure 2.4). This may indicate that it is not fiber-type composition *per se*, but rather the relatively high resting muscle blood flows and VCs that drive the effects of SMTC in the primarily oxidative muscles.

Previously, our laboratory has utilized the conscious rat model of treadmill exercise in the presence of the non-selective NOS inhibitor L-NAME to demonstrate that NO plays an important role in the regulation of hindlimb muscle blood flow during locomotory exercise (3, 12, 30). While those studies and others using non-selective NOS inhibition cannot identify the specific isoform from which the NO originates, eNOS-derived NO has traditionally been considered to be responsible for most, if not all, of the NO response. However, evidence in contracting mouse (8, 10, 42) and human (36) muscle in which nNOS is absent provides support for nNOS-derived NO as a key component in NO-mediated blood flow control during muscle contractions. Specifically, in healthy subjects, nNOS-derived NO attenuates norepinephrine-induced vasoconstriction in active muscle vascular beds whereas this sympathetic modulation is absent in skeletal muscle that lacks nNOS (36, 42). More recently, novel work in transgenic *mdx* mice (a model of Duchenne muscular dystrophy with transplanted nNOS anchoring proteins) indicates that these animals have greater active locomotor muscle blood flow and thus enhanced treadmill exercise performance compared to their non-transgenic *mdx* counterparts (2, 26). While these observations have important clinical significance for a variety of chronic pathological conditions in which nNOS structure or function is altered, our current study is the first to test the hypothesis that, during physiological exercise nNOS-derived NO contributes to the regulation of active muscle blood flow in healthy individuals. However, contrary to our hypothesis, our data demonstrate that nNOS inhibition does not alter the hyperemic response to exercise.

The control of blood flow within active skeletal muscle is hallmarked by substantial redundancy and synergy (14). For example, when one NOS isoform is chronically disrupted (i.e., eNOS or nNOS knockout models) compensatory mechanisms may increase NO production from existing isoforms (1, 21, 41). Additionally, there is evidence that NO is not the sole mediator of sympathetic modulation within active skeletal muscle vascular beds (5, 6, 35) and

the roles of other substances may increase when nNOS is inhibited. Until any such redundancy of the NO sympathetic-inhibitory and/or vasodilatory signal in healthy subjects is dissected systematically, it may be inappropriate to conclude that NO derived from nNOS does not contribute to locomotor skeletal muscle blood flow regulation during exercise under normal physiological conditions (i.e., in the absence of SMTC administration). Rather, the present investigation indicates that nNOS participation may not be obligatory for the exercise hyperemic response.

At rest, the splanchnic and renal circulations may account for nearly 50% of the total cardiac output and thus serve as important controllers of MAP and constitute a vast blood volume reservoir for the active skeletal muscle to draw upon during dynamic exercise (17). Previous investigations have indicated that NO is an important blood flow regulator in these circulations (15, 34). The present investigation identifies nNOS-derived NO as an important mediator of kidney, adrenal and liver blood flow at rest and during exercise which is consistent with *in vitro* (18) and anesthetized (45) rodent models after SMTC administration. The ~35% reduction in liver blood flow and VC found herein is in agreement with the presence of nNOS in the liver vasculature of the rat (28). However, it is important to note that the human liver is thought to lack nNOS (25). Collectively, the literature supports a crucial role of nNOS in the regulation of the kidney, adrenal, and liver circulations and, accordingly, diseases affecting these circulations have been associated with impaired nNOS function (23, 34).

Experimental considerations

The interpretation of the present results depends highly on the efficacy of the current dose of SMTC ($2.1 \pm 0.1 \mu\text{mol/kg}$ or $0.56 \pm 0.02 \text{ mg/kg}$) to block nNOS without affecting eNOS-mediated function. We believe that the selected dose was appropriate for the following reasons: First, the SMTC dose utilized presently was selected based on previous investigations in rats reporting selective nNOS inhibition with SMTC *in vivo* (15, 42, 44) and preliminary studies from our laboratory which attempted to elucidate the highest SMTC dose that did not affect endothelial-mediated NO function (Copp, Hirai, Schwagerl, Musch, Poole, unpublished observations). Indeed, the SMTC dose utilized in the present investigation is slightly greater than the highest *in vivo* doses of SMTC that achieved selective nNOS inhibition in rats reported by Wakefield *et al.* (44, 0.3 mg/kg) and Komers *et al.* (23, 0.5 mg/kg). Second, it is important to

note the similar reductions in blood flow and VC observed in the kidneys, adrenals and liver both at rest and during exercise. This suggests that the SMTC dose was sufficient to inhibit nNOS under both conditions and the lack of an effect observed during exercise in the hindlimb musculature results from the obligatory role of nNOS-derived NO at rest but not during exercise. Third, to confirm that the SMTC dose utilized presently did not affect endothelial-mediated NO function we examined the hypotensive responses to ACh injections before and after SMTC and after L-NAME administration (which is expected to inhibit endothelial-mediated vasodilation). We considered that if SMTC did not affect eNOS function the hypotensive response to ACh would not be attenuated when compared to control conditions. Conversely, we anticipated that eNOS function and, therefore, the hypotensive response to ACh would be attenuated after L-NAME. As anticipated, SMTC did not attenuate the absolute or relative hypotensive responses to ACh compared to control. Furthermore, the absolute hypotensive response after L-NAME was attenuated compared to SMTC but not control and the relative hypotensive response was attenuated compared to both control and SMTC conditions. Taking into account the primary comparison of interest (control vs. SMTC) and the considerations presented above, our results support that SMTC administration in the present study effectively inhibited nNOS but did not inhibit eNOS.

NO has many diverse roles in intact biological systems. For example, NO derived from nNOS has been implicated in the metabolic inhibition of sympathetically-mediated vasoconstriction (i.e., functional sympatholysis; 11) as well as regulation of regional sympathetic nerve activity (13), the modulation of skeletal muscle force production (10), and the direct relaxation of vascular smooth muscle. Given that the same absolute treadmill speed was utilized before and after SMTC, the power output necessary to sustain running was the same during the two exercise bouts. Therefore, muscle force production likely changed little, if at all, between control and SMTC conditions. In addition, given that SMTC increased MAP at rest we report both resting blood flow and VC. The fact that SMTC reduced blood flow and VC at rest provides convincing evidence that nNOS-derived NO is an obligatory controller of local resting muscle perfusion. However, the present *in vivo* model does not allow for the determination of the specific mechanisms by which bioavailable nNOS-derived NO exerts its influence on the regulation of blood flow and VC. Notwithstanding this model limitation, a major strength of the

present study is that it presents the first evaluation of the effects of selective nNOS inhibition on circulatory control in a healthy, intact biological system performing locomotory exercise.

Summary and conclusions

This study investigated the effects of selective nNOS inhibition via SMTC on hindlimb muscle(s) blood flow and VC at rest and during submaximal treadmill exercise in the healthy conscious rat. We have identified that nNOS inhibition reduces blood flow and VC in the skeletal muscle of the hindlimb at rest, however, nNOS inhibition had no effect on hindlimb musculature blood flow and VC during exercise. These results enhance our understanding of the role of nNOS in circulatory control by demonstrating that nNOS-derived NO is not obligatory for achieving the hyperemic response in healthy rats performing whole-body dynamic exercise. Moreover, our data may be directly relevant to a growing number of clinical populations in which impaired vascular control and reduced NO bioavailability are hallmarks of disease pathology.

Table 2.1. Effects of nNOS inhibition on resting skeletal muscle blood flow and VC

	Blood flow		Vascular conductance	
	<u>Control</u>	<u>SMTC</u>	<u>Control</u>	<u>SMTC</u>
<u>Ankle extensors</u>				
Soleus	87±14	46±8*	0.70±0.11	0.38±0.07*
Plantaris	17±3	12±4	0.13±0.02	0.08±0.02
Red gastrocnemius	51±12	20±6*	0.40±0.09	0.15±0.03*
White gastrocnemius	15±2	9±2*	0.12±0.01	0.07±0.02*
Mixed gastrocnemius	19±4	9±2*	0.15±0.03	0.06±0.01*
Tibialis posterior	28±7	14±4	0.22±0.05	0.10±0.03*
Flexor digitorum longus	50±11	32±15	0.40±0.09	0.21±0.11
Flexor halicis longus	19±3	10±3*	0.15±0.02	0.07±0.02*
<u>Ankle flexors</u>				
Tibialis anterior, red	64±9	35±14	0.50±0.06	0.31±0.04
Tibialis anterior, white	23±3	16±4	0.18±0.02	0.13±0.03
Extensor digitorum longus	21±3	14±5	0.16±0.02	0.09±0.03
Peroneals	25±5	12±4	0.20±0.05	0.08±0.02*
<u>Knee extensors</u>				
Vastus intermedius	83±13	46±9*	0.65±0.09	0.34±0.06*
Vastus medialis	14±3	11±2	0.11±0.02	0.08±0.01
Vastus lateralis, red	73±14	41±14	0.57±0.10	0.33±0.12
Vastus lateralis, white	9±1	9±2	0.07±0.01	0.06±0.01
Vastus lateralis, mixed	19±3	15±3	0.15±0.02	0.10±0.02
Rectus femoris, red	54±14	18±6*	0.42±0.10	0.14±0.04*
Rectus femoris, white	16±2	13±3	0.12±0.01	0.09±0.02
<u>Knee flexors</u>				
Biceps femoris anterior	11±1	8±1	0.09±0.01	0.06±0.01*
Biceps femoris posterior	18±3	10±2	0.14±0.03	0.07±0.01*
Semitendinosus	20±3	10±2*	0.16±0.03	0.07±0.01*
Semimembranosus, red	14±1	11±2	0.11±0.01	0.07±0.01*
Semimembranosus, white	9±1	8±1	0.07±0.01	0.06±0.01

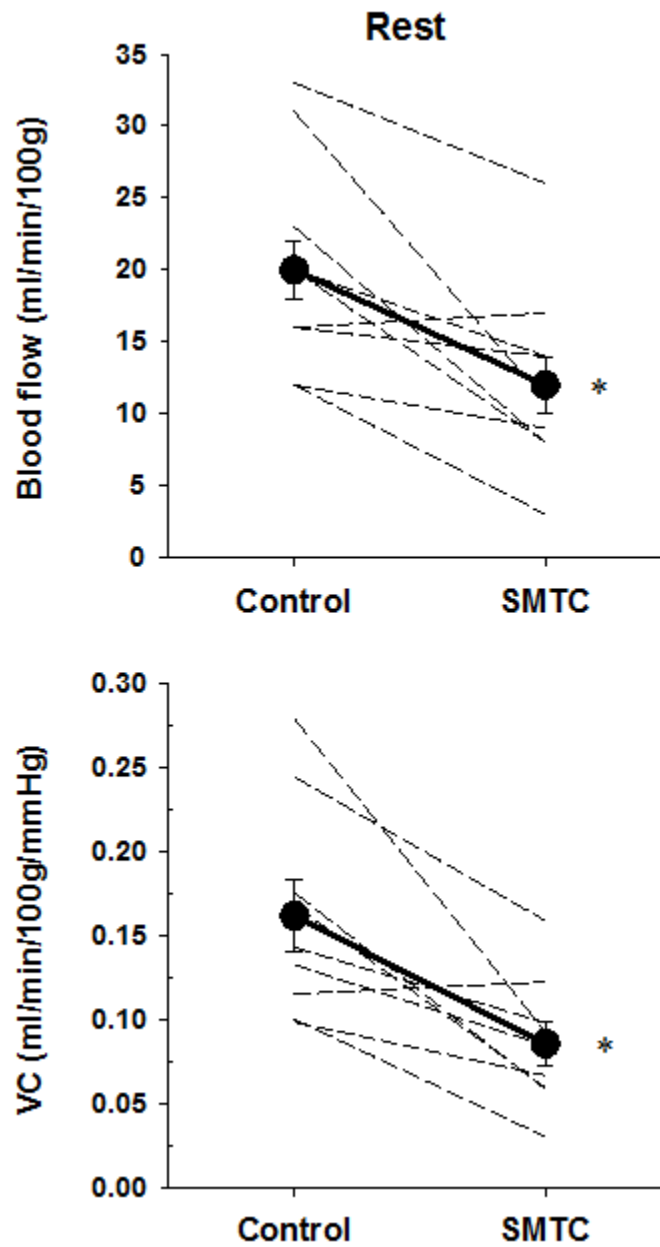
Effects of SMTC (2.1±0.1 µmol/kg) on resting blood flow (ml/min/100g) and vascular conductance (ml/min/100g/mmHg) to the individual muscles or muscle parts of the rat hindlimb. Data are mean±SEM. n=9, *p<0.05 versus control.

Table 2.2. Effects of nNOS inhibition on kidney and splanchnic organ blood flow and VC

	At rest		During exercise	
	<u>Control</u>	<u>SMTC</u>	<u>Control</u>	<u>SMTC</u>
<u>Blood flow</u>				
Right kidney	871±92	514±45*	666±74	452±30*
Left kidney	880±101	499±65*	666±79	431±31*
Stomach	137±24	111±20	71±12	61±12
Adrenals	736±103	443±74*	653±85	261±25*
Spleen	269±32	310±30	60± 14	73±19
Pancreas	240±42	180±29	132± 27	85±20
Sm. intestine	539±80	502±76	366± 60	395±55
Lg. intestine	309±43	287±34	194± 44	179±43
Liver	26±3	17±3*	30± 8	11±1*
<u>VC</u>				
Right kidney	6.92±0.68	3.89±0.40*	4.73±0.60	3.03±0.18*
Left kidney	6.98±0.73	3.71±0.50*	4.75±0.67	2.90±0.20*
Stomach	1.08±0.18	0.80±0.16	0.51±0.10	0.42±0.09
Adrenals	6.35±0.60	3.71±0.68*	4.64±0.69	1.77±0.19*
Spleen	2.13±0.26	2.21±0.26	0.43±0.10	0.49±0.12
Pancreas	1.88±0.31	1.35±0.21	0.94±0.19	0.60±0.15
Sm. intestine	4.24±0.58	4.09±0.55	2.61±0.45	2.66±0.38
Lg. intestine	2.47±0.35	2.19±0.25	1.71±0.28	1.42±0.21
Liver	0.22±0.02	0.14±0.03*	0.21±0.06	0.07±0.01*

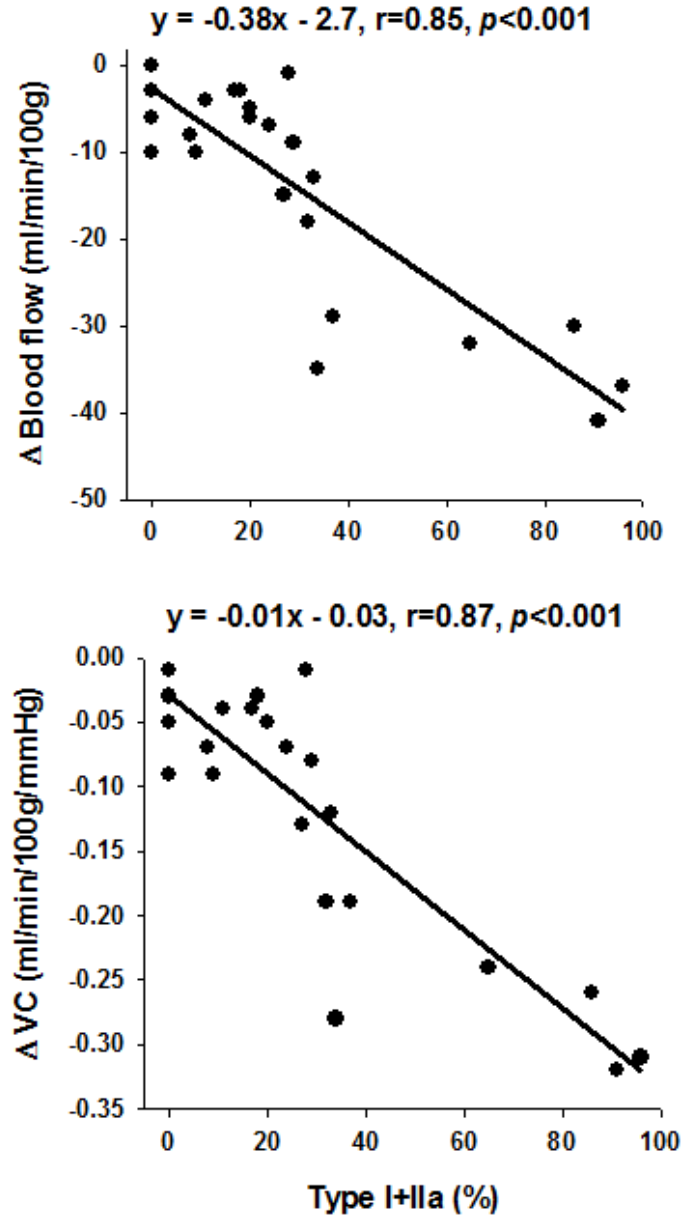
Effects of SMTC (2.1±0.1 µmol/kg) on resting (n=9) and exercising (n=10) blood flow (ml/min/100g) and vascular conductance (ml/min/100g/mmHg) to the kidneys and organs of the splanchnic region. Data are mean±SEM. *p<0.05 versus control.

Figure 2.1. Effects of nNOS inhibition on resting skeletal muscle blood flow and VC



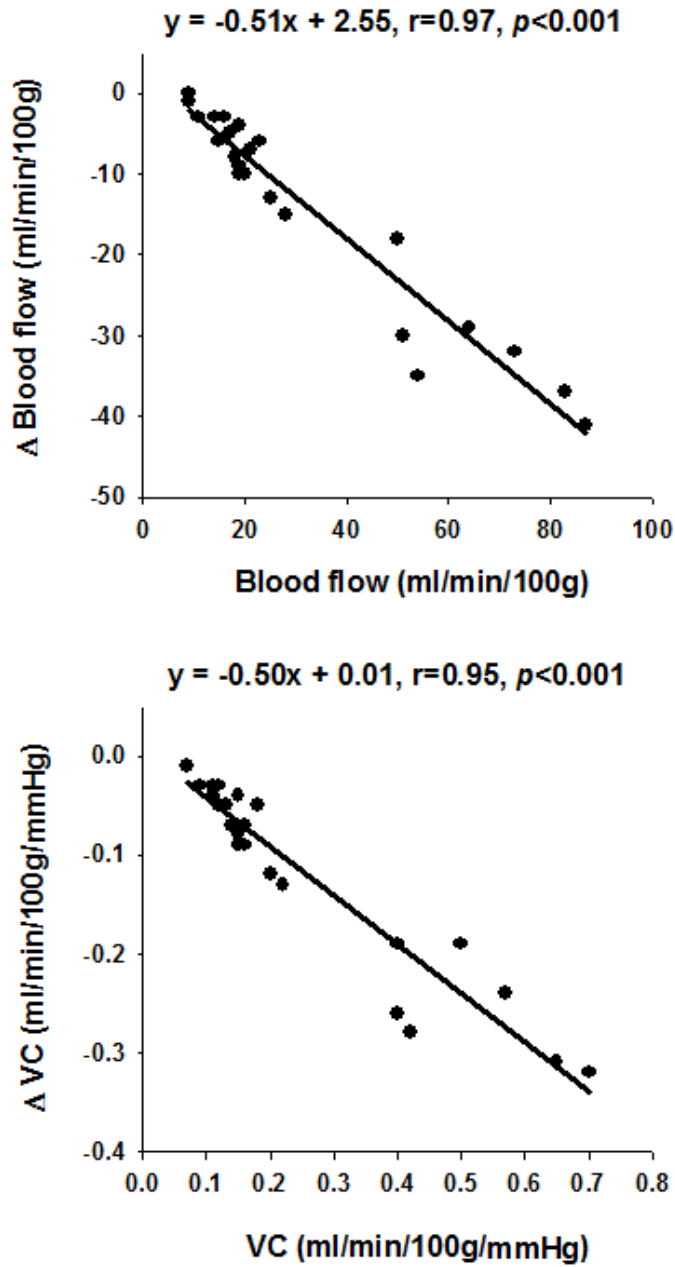
Effects of SMTC ($2.1 \pm 0.1 \mu\text{mol/kg}$) on resting total hindlimb blood flow and vascular conductance (VC). Individual animals and group means \pm SEM are shown. $n=9$, $*p < 0.05$ vs. control.

Figure 2.2. Relationships between changes in resting blood flow and VC following SMTC and muscle fiber-type composition



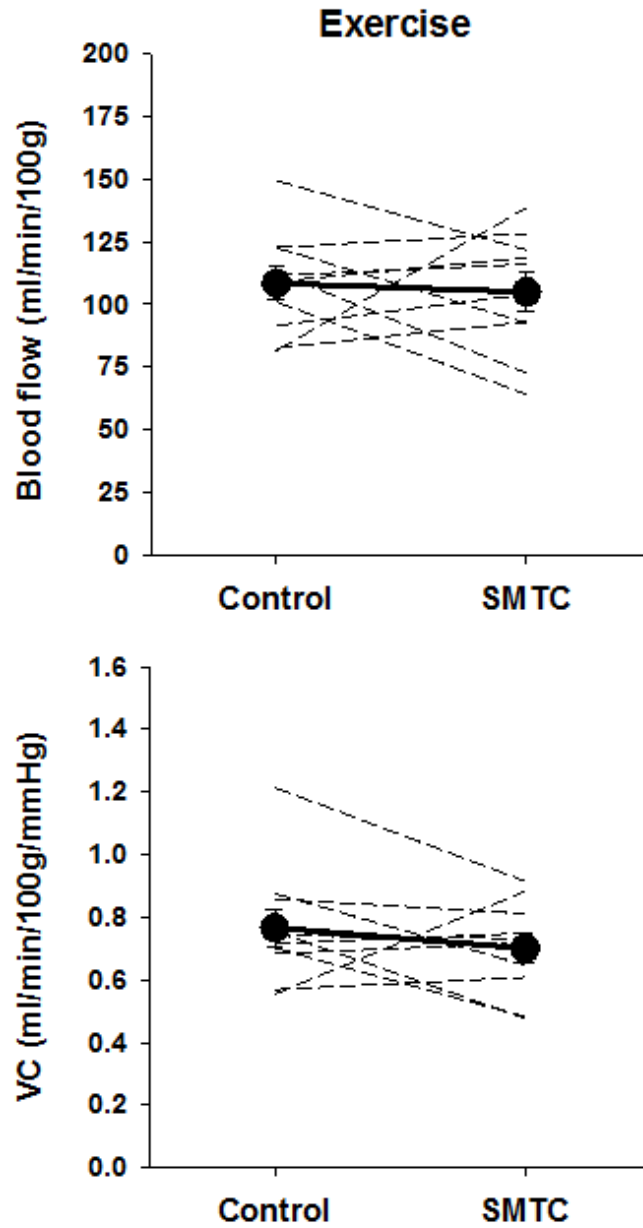
Correlations between the percent sum of type I and IIa fibers in the individual muscles and muscle parts of the rat hindlimb and the absolute changes in resting blood flow (Δ blood flow) and vascular conductance (Δ VC) after SMTC infusion ($2.1 \pm 0.1 \mu\text{mol/kg}$).

Figure 2.3. Relationships between resting blood flow and VC and the changes in resting blood flow and VC



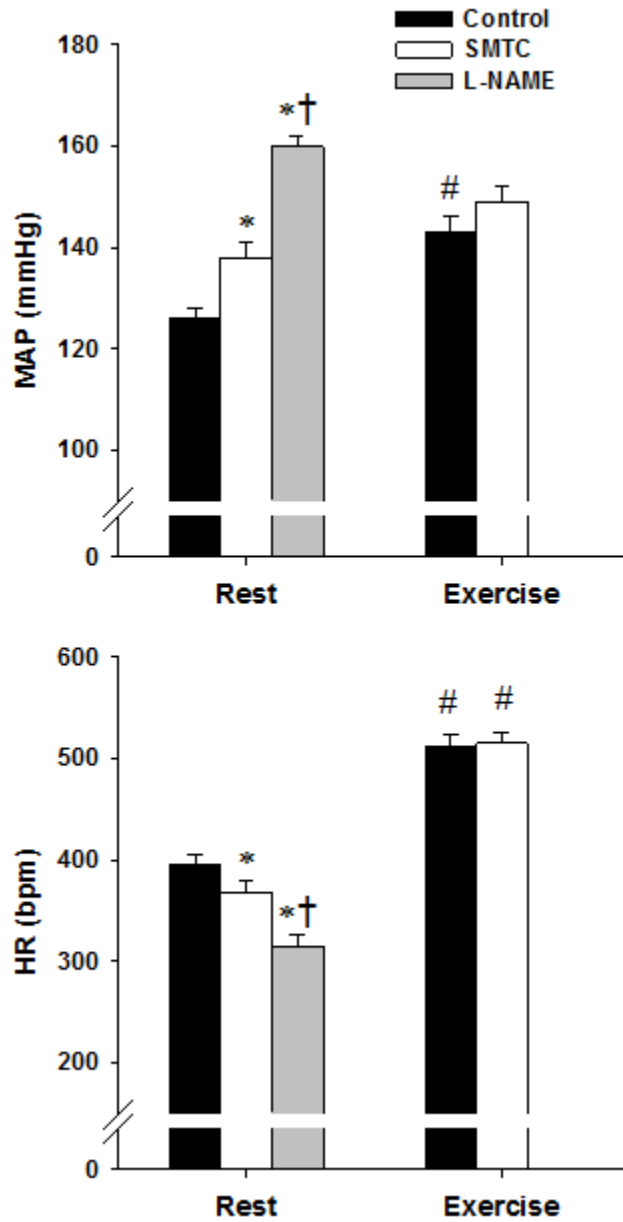
Correlations between the relative resting blood flow and vascular conductance (VC) to the individual muscles or muscle parts of the rat hindlimb and the absolute change in relative resting blood flow (Δ blood flow) and VC (Δ VC) after SMTC infusion ($2.1 \pm 0.1 \mu\text{mol/kg}$).

Figure 2.4. Effects of nNOS inhibition on exercising skeletal muscle blood flow and VC



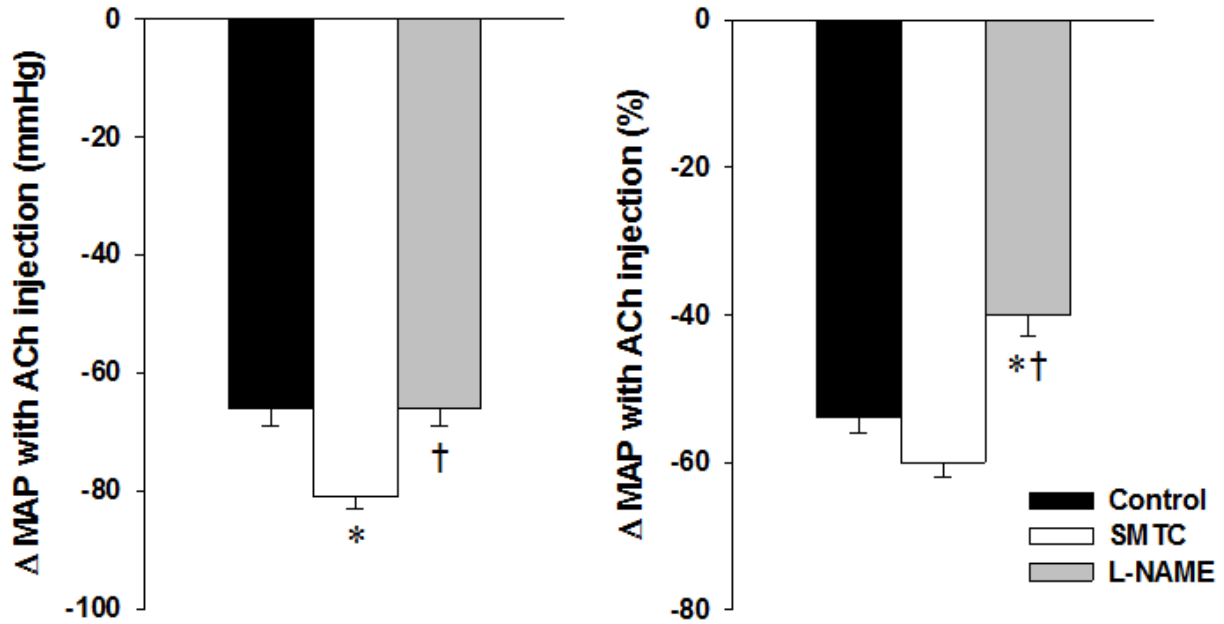
Effects of SMTC ($2.1 \pm 0.1 \mu\text{mol/kg}$) on exercising total hindlimb blood flow and vascular conductance (VC). Individual animals and group means \pm SEM are shown. $n=9$. There were no significant differences between control and SMTC.

Figure 2.5. Effects of nNOS inhibition on resting and exercising MAP and HR



Mean arterial pressure (MAP, top panel) and heart rate (HR, bottom panel) during control and after SMTC ($2.1 \pm 0.1 \mu\text{mol/kg}$) and L-NAME (10 mg/kg) administration. Rest: $n=19$, Exercise: $n=10$, * $p < 0.05$ vs. control, † $p < 0.05$ vs. SMTC, # $p < 0.05$ vs. same condition at rest.

Figure 2.6. Effects of SMTC and L-NAME on the hypotensive response to ACh



Absolute and relative hypotensive responses to acetylcholine injection (10 $\mu\text{g}/\text{kg}$) for control condition and after SMTC ($2.1 \pm 0.1 \mu\text{mol}/\text{kg}$) and L-NAME (10 mg/kg) administration. $n=19$, $*p < 0.05$ vs. control, $†p < 0.05$ vs. SMTC.

References

1. **Buckwalter JB, Taylor JC, Hamann JJ, and Clifford PS.** Role of nitric oxide in exercise sympatholysis. *J Appl Physiol* 97: 417-423., 2004.
2. **Clifford PS and Hellsten Y.** Vasodilatory mechanisms in contracting skeletal muscle. *J Appl Physiol* 97: 393-403, 2004.
3. **Copp SW, Hirai DM, Hageman KS, Poole DC, and Musch TI.** Nitric oxide synthase inhibition during treadmill exercise reveals fiber-type specific vascular control in the rat hindlimb. *Am J Physiol Regul Integr Comp Physiol* 298: R478-485, 2010.
4. **Delp MD and Duan C.** Composition and size of type I, IIA, IID/X, and IIB fibers and citrate synthase activity of rat muscle. *J Appl Physiol* 80: 261-270, 1996.
5. **Dineno FA and Joyner MJ.** Blunted sympathetic vasoconstriction in contracting skeletal muscle of healthy humans: is nitric oxide obligatory? *J Physiol* 553: 281-292, 2003.
6. **Dineno FA and Joyner MJ.** Combined NO and PG inhibition augments alpha-adrenergic vasoconstriction in contracting human skeletal muscle. *Am J Physiol Heart Circ Physiol* 287: H2576-2584, 2004.
7. **Drummond GB.** Reporting ethical matters in the Journal of Physiology: standards and advice. *J Physiol* 587: 713-719, 2009.
8. **Fadel PJ, Zhao W, and Thomas GD.** Impaired vasomodulation is associated with reduced neuronal nitric oxide synthase in skeletal muscle of ovariectomized rats. *J Physiol* 549: 243-253, 2003.
9. **Furfine ES, Harmon MF, Paith JE, Knowles RG, Salter M, Kiff RJ, Duffy C, Hazelwood R, Oplinger JA, and Garvey EP.** Potent and selective inhibition of human nitric oxide synthases. Selective inhibition of neuronal nitric oxide synthase by S-methyl-L-thiocitrulline and S-ethyl-L-thiocitrulline. *J Biol Chem* 269: 26677-26683, 1994.
10. **Grange RW, Isotani E, Lau KS, Kamm KE, Huang PL, and Stull JT.** Nitric oxide contributes to vascular smooth muscle relaxation in contracting fast-twitch muscles. *Physiol Genomics* 5: 35-44, 2001.

11. **Hirai T, Musch TI, Morgan DA, Kregel KC, Claassen DE, Pickar JG, Lewis SJ, and Kenney MJ.** Differential sympathetic nerve responses to nitric oxide synthase inhibition in anesthetized rats. *Am J Physiol* 269: R807-813, 1995.
12. **Hirai T, Visneski MD, Kearns KJ, Zelis R, and Musch TI.** Effects of NO synthase inhibition on the muscular blood flow response to treadmill exercise in rats. *J Appl Physiol* 77: 1288-1293, 1994.
13. **Hirschfield W, Moody MR, O'Brien WE, Gregg AR, Bryan RM, Jr., and Reid MB.** Nitric oxide release and contractile properties of skeletal muscles from mice deficient in type III NOS. *Am J Physiol Regul Integr Comp Physiol* 278: R95-R100, 2000.
14. **Huang A, Sun D, Shesely EG, Levee EM, Koller A, and Kaley G.** Neuronal NOS-dependent dilation to flow in coronary arteries of male eNOS-KO mice. *Am J Physiol Heart Circ Physiol* 282: H429-436, 2002.
15. **Ichihara A, Inscho EW, Imig JD, and Navar LG.** Neuronal nitric oxide synthase modulates rat renal microvascular function. *Am J Physiol* 274: F516-524, 1998.
16. **Ikenaga H, Fallet RW, and Carmines PK.** Basal nitric oxide production curtails arteriolar vasoconstrictor responses to ANG II in rat kidney. *Am J Physiol* 271: F365-373, 1996.
17. **Jankord R, McAllister RM, Ganjam VK, and Laughlin MH.** Chronic inhibition of nitric oxide synthase augments the ACTH response to exercise. *Am J Physiol Regul Integr Comp Physiol* 296: R728-734, 2009.
18. **Jansson L, Carlsson PO, Bodin B, Andersson A, and Kallskog O.** Neuronal nitric oxide synthase and splanchnic blood flow in anaesthetized rats. *Acta Physiol Scand* 183: 257-262, 2005.
19. **Johnstone MT, Creager SJ, Scales KM, Cusco JA, Lee BK, and Creager MA.** Impaired endothelium-dependent vasodilation in patients with insulin-dependent diabetes mellitus. *Circulation* 88: 2510-2516, 1993.
20. **Joyner MJ and Dietz NM.** Nitric oxide and vasodilation in human limbs. *J Appl Physiol* 83: 1785-1796, 1997.
21. **Kavdia M and Popel AS.** Contribution of nNOS- and eNOS-derived NO to microvascular smooth muscle NO exposure. *J Appl Physiol* 97: 293-301, 2004.

22. **Kobzik L, Reid MB, Bredt DS, and Stamler JS.** Nitric oxide in skeletal muscle. *Nature* 372: 546-548, 1994.
23. **Komers R, Oyama TT, Chapman JG, Allison KM, and Anderson S.** Effects of systemic inhibition of neuronal nitric oxide synthase in diabetic rats. *Hypertension* 35: 655-661, 2000.
24. **Kubo SH, Rector TS, Bank AJ, Williams RE, and Heifetz SM.** Endothelium-dependent vasodilation is attenuated in patients with heart failure. *Circulation* 84: 1589-1596, 1991.
25. **Kwon O, Hong SM, and Ramesh G.** Diminished NO generation by injured endothelium and loss of macula densa nNOS may contribute to sustained acute kidney injury after ischemia-reperfusion. *Am J Physiol Renal Physiol* 296: F25-33, 2009.
26. **Lai Y, Thomas GD, Yue Y, Yang HT, Li D, Long C, Judge L, Bostick B, Chamberlain JS, Terjung RL, and Duan D.** Dystrophins carrying spectrin-like repeats 16 and 17 anchor nNOS to the sarcolemma and enhance exercise performance in a mouse model of muscular dystrophy. *J Clin Invest* 119: 624-635, 2009.
27. **Lau KS, Grange RW, Isotani E, Sarelus IH, Kamm KE, Huang PL, and Stull JT.** nNOS and eNOS modulate cGMP formation and vascular response in contracting fast-twitch skeletal muscle. *Physiol Genomics* 2: 21-27, 2000.
28. **McNaughton L, Puttagunta L, Martinez-Cuesta MA, Kneteman N, Mayers I, Moqbel R, Hamid Q, and Radomski MW.** Distribution of nitric oxide synthase in normal and cirrhotic human liver. *Proc Natl Acad Sci USA* 99: 17161-17166, 2002.
29. **Musch TI, Bruno A, Bradford GE, Vayonis A, and Moore RL.** Measurements of metabolic rate in rats: a comparison of techniques. *J Appl Physiol* 65: 964-970, 1988.
30. **Musch TI, McAllister RM, Symons JD, Stebbins CL, Hirai T, Hageman KS, and Poole DC.** Effects of nitric oxide synthase inhibition on vascular conductance during high speed treadmill exercise in rats. *Exp Physiol* 86: 749-757, 2001.
31. **Musch TI and Terrell JA.** Skeletal muscle blood flow abnormalities in rats with a chronic myocardial infarction: rest and exercise. *Am J Physiol* 262: H411-419, 1992.
32. **Radegran G and Hellsten Y.** Adenosine and nitric oxide in exercise-induced human skeletal muscle vasodilatation. *Acta Physiol Scand* 168: 575-591, 2000.

33. **Roberts CK, Barnard RJ, Jasman A, and Balon TW.** Acute exercise increases nitric oxide synthase activity in skeletal muscle. *Am J Physiol* 277: E390-394, 1999.
34. **Rockey DC and Chung JJ.** Reduced nitric oxide production by endothelial cells in cirrhotic rat liver: endothelial dysfunction in portal hypertension. *Gastroenterology* 114: 344-351, 1998.
35. **Rowell L.** *Human cardiovascular control.* New York, NY: Oxford University Press, Inc., 1993.
36. **Sander M, Chavoshan B, Harris SA, Iannaccone ST, Stull JT, Thomas GD, and Victor RG.** Functional muscle ischemia in neuronal nitric oxide synthase-deficient skeletal muscle of children with Duchenne muscular dystrophy. *Proc Natl Acad Sci USA* 97: 13818-13823, 2000.
37. **Schrage WG, Eisenach JH, and Joyner MJ.** Ageing reduces nitric-oxide- and prostaglandin-mediated vasodilatation in exercising humans. *J Physiol* 579: 227-236, 2007.
38. **Seddon M, Melikian N, Dworakowski R, Shabeeh H, Jiang B, Byrne J, Casadei B, Chowienczyk P, and Shah AM.** Effects of neuronal nitric oxide synthase on human coronary artery diameter and blood flow in vivo. *Circulation* 119: 2656-2662, 2009.
39. **Seddon MD, Chowienczyk PJ, Brett SE, Casadei B, and Shah AM.** Neuronal nitric oxide synthase regulates basal microvascular tone in humans in vivo. *Circulation* 117: 1991-1996, 2008.
40. **Stamler JS and Meissner G.** Physiology of nitric oxide in skeletal muscle. *Physiol Rev* 81: 209-237, 2001.
41. **Talukder MA, Fujiki T, Morikawa K, Motoishi M, Kubota H, Morishita T, Tsutsui M, Takeshita A, and Shimokawa H.** Up-regulated neuronal nitric oxide synthase compensates coronary flow response to bradykinin in endothelial nitric oxide synthase-deficient mice. *J Cardiovasc Pharmacol* 44: 437-445, 2004.
42. **Thomas GD, Sander M, Lau KS, Huang PL, Stull JT, and Victor RG.** Impaired metabolic modulation of alpha-adrenergic vasoconstriction in dystrophin-deficient skeletal muscle. *Proc Natl Acad Sci USA* 95: 15090-15095, 1998.
43. **Thomas GD, Shaul PW, Yuhanna IS, Froehner SC, and Adams ME.** Vasomodulation by skeletal muscle-derived nitric oxide requires alpha-syntrophin-

- mediated sarcolemmal localization of neuronal Nitric oxide synthase. *Circ Res* 92: 554-560, 2003.
44. **Wakefield ID, March JE, Kemp PA, Valentin JP, Bennett T, and Gardiner SM.** Comparative regional haemodynamic effects of the nitric oxide synthase inhibitors, S-methyl-L-thiocitrulline and L-NAME, in conscious rats. *Br J Pharmacol* 139: 1235-1243, 2003.
45. **Wei CL, Khoo HE, Lee KH, and Hon WM.** Differential expression and localization of nitric oxide synthases in cirrhotic livers of bile duct-ligated rats. *Nitric Oxide* 7: 91-102, 2002.

Chapter 3 - Muscle fiber-type dependence of neuronal nitric oxide synthase-mediated vascular control in the rat during high-speed treadmill running

Summary

Nitric oxide (NO) derived from neuronal NO synthase (nNOS) does not contribute to the hyperemic response within rat hindlimb skeletal muscle during low-speed treadmill running. This may be attributed to low exercise intensities recruiting primarily oxidative muscle and that vascular effects of nNOS-derived NO are manifest principally within glycolytic muscle. We tested the hypothesis that selective nNOS inhibition via S-methyl-L-thiocitrulline (SMTC) would reduce rat hindlimb skeletal muscle blood flow and vascular conductance (VC) during high-speed treadmill running above critical speed (asymptote of the hyperbolic speed versus time-to-exhaustion relationship for high-speed running and an important glycolytic fast-twitch fiber recruitment boundary in the rat) principally within glycolytic fast-twitch muscle. 6 rats performed 3 high speed treadmill runs to exhaustion to determine critical speed. Subsequently, hindlimb skeletal muscle blood flow (radiolabelled microspheres) and VC (blood flow/mean arterial pressure) were determined during supra-critical speed treadmill running (critical speed+15%, 52.5 ± 1.3 m/min) before (control) and after selective nNOS inhibition with 0.56 mg/kg SMTC. SMTC reduced total hindlimb skeletal muscle blood flow (control: 241 ± 23 , SMTC: 204 ± 13 ml/min/100g, $p < 0.05$) and VC (control: 1.88 ± 0.20 , SMTC: 1.48 ± 0.13 ml/min/100g/mmHg, $p < 0.05$) during high-speed running. The relative reductions in blood flow and VC were greater in the highly glycolytic muscles and muscle parts consisting of 100% type IIb+d/x fibers compared to the highly oxidative muscles and muscle parts consisting of $\leq 35\%$ type IIb+d/x muscle fibers ($p < 0.05$). These results extend our understanding of vascular control during exercise by identifying fiber-type selective peripheral vascular effects of nNOS-derived NO during high-speed treadmill running.

Introduction

The ability of the cardiovascular system to increase skeletal muscle blood flow and, therefore, O₂ delivery during exercise is accomplished via neurohumoral activation (to increase cardiac output and initiate blood flow redistribution) and local mechanical and vasomotor control mechanisms (19). The robust active muscle blood flow response supports sustained exercise performance whereas many disease processes are hallmarked by O₂ delivery impairment and exercise intolerance (e.g., heart failure, 30).

Nitric oxide (NO) is an important cardiovascular signaling molecule that has been reported to play an integral role in promoting exercise hyperemia in animals (17, 20) and humans (33). In healthy subjects NO is synthesized enzymatically via neuronal NO synthase (nNOS or type I NOS) or endothelial NO synthase (eNOS or type III NOS). The vasodilatory contributions of eNOS-derived NO secondary, at least in part, to vascular endothelial shear stress during exercise are well known (15). The peripheral vascular effects of nNOS-derived NO, particularly during dynamic exercise, remain controversial. For example, our laboratory reported recently that acute administration of the selective nNOS inhibitor S-methyl-L-thiocitrulline (SMTC) reduced rat hindlimb skeletal muscle blood flow at rest but not during low-speed treadmill running (6). Conversely, nNOS-derived NO attenuates skeletal muscle sympathetic vasoconstriction during muscle contractions in both rats (39, 40) and humans (32). Importantly, this “functional sympatholysis” may occur within glycolytic but not oxidative skeletal muscle and at high contraction intensities only (38). The fiber-type and contraction-intensity dependent vascular effects of nNOS-derived NO may account for the unchanged skeletal muscle blood flow following nNOS inhibition during low-speed treadmill running (6) which recruits primarily oxidative slow- and fast-twitch muscle (13, 23). It is possible that high-speed treadmill running which additively recruits highly glycolytic fast-twitch muscle may unmask obligatory nNOS-derived NO vasomotor control during dynamic exercise. This information would have important implications for diseased (3, e.g., heart failure, 41) and aged (16) populations which have been associated with impaired nNOS-mediated function.

Our laboratory has demonstrated recently that critical speed (the asymptote of the hyperbolic speed versus time-to-exhaustion relationship for high-speed running) can be

determined empirically in the rat and that running above, relative to below, critical speed recruits glycolytic fast-twitch muscle to a greater extent than oxidative slow- and fast-twitch muscle (5). In this regard, the ability to accurately measure blood flow distribution among and within active skeletal muscles during high-speed running (1, 26) specifically above critical speed (5) makes the rat an ideal model to examine the fiber-type dependency of nNOS-mediated vascular control during exercise. Therefore, the present investigation tested the hypothesis that selective nNOS inhibition with S-methyl-L-thiocitrulline (SMTC) would reduce rat hindlimb skeletal muscle blood flow and (vascular conductance) VC during treadmill running above critical speed whereas there would be no effects of SMTC during low-speed treadmill running. Furthermore, we hypothesized that during supra-critical speed running the greatest relative reductions in blood flow and VC would occur principally within the muscles and muscle parts composed of highly glycolytic type IIb and d/x fibers.

Methods

Ethical approval

The experimental procedures described in the present investigation were approved by the Institutional Animal Care and Use Committee of Kansas State University and were conducted according to the animal use guidelines mandated by *The Journal of Physiology* (8).

A total of 17 male Sprague-Dawley rats (~4 months old, body mass 387 ± 13 g, Charles River Laboratories, Wilmington, MA, USA) were utilized in the present investigation. Rats were housed 2 per cage in accredited facilities (Association for the Assessment and Accreditation of Laboratory Animal Care) with food and water provided *ad libitum*. 12 rats were assigned initially to either the high-speed (n=6) or low-speed (n=6) group and acclimatized to running on a custom built motor-driven treadmill over 1 week (5-6 days up to 5 min/day). The treadmill was set to a 5% incline which was maintained throughout the experimental protocol.

Determination of critical speed

Rats in the high-speed group performed a peak $\dot{V}O_2$ test as described previously (25). Rats performed a progressive ramp-style treadmill test inside a metabolic chamber which was placed on the treadmill belt. Ambient air was drawn through the chamber via a vacuum pump (Neptune-Dyna model 4K, Dover, NJ, USA), through drierite (anhydrous CaSO_4), through a flowmeter (Fischer-Porter model 10A1378, Burr Ridge, IL, USA) and delivered subsequently to inline O_2 and CO_2 analyzers (O_2 : model S-3A/I, CO_2 : model CD-3A AEI Technologies, Pittsburgh, PA, USA). The speed of the treadmill and corresponding $\dot{V}O_2$ and $\dot{V}CO_2$ were monitored and recorded continuously throughout the test. The test was terminated when the rat was unable or unwilling to keep pace with the treadmill belt.

Critical speed was determined as described previously (5). Rats in the high-speed group performed at least 3 runs to exhaustion, in random order, at a range of speeds corresponding to 90-115% of the speed that elicited $\dot{V}O_2$ peak. For each constant-speed test rats were given a 2 minute warm-up at 20-25 m/min which was followed by 1 minute of quiet resting. The treadmill speed was then increased rapidly over an ~10 s period to the pre-determined speed. Rats were

encouraged to run by applying manual bursts of high pressure air at the hindlimbs whenever they drifted towards the back of the treadmill lane. Tests were terminated when the rat could not maintain pace with the treadmill belt despite obvious exertion. Time-to-exhaustion was measured to the nearest tenth of a second. The following criteria constituted a successful constant-speed test: 1) the ability of the rat to quickly settle into a normal running gait at the beginning of the test, 2) a noticeable change in gait (i.e., lowering of the hindquarters and a rising of the snout) preceding exhaustion, and 3) marked attenuation of the righting reflex when placed in the supine position. A minimum of 24 hours rest was given between consecutive exercise tests. Following completion of the constant-speed tests, the individual critical speeds were determined by 1) the hyperbolic speed-time model ($\text{time} = D' / (\text{speed} - \text{critical speed})$) where the asymptote of the hyperbolic curve is the critical speed and the curvature constant is D' and 2) the linear $1/\text{time}$ model ($\text{speed} = D' * 1/\text{time} + \text{critical speed}$) where speed is plotted as a function of the inverse of time (s)-to-exhaustion and the intercept of the regression line is the critical speed and the slope is D' (12). For both models, D' (vertical distance in meters) was multiplied by the rats' average weight in kg for the constant-speed tests to determine m·kg, then converted to W' in joules (J) using the relationship: $1 \text{ J} = 0.103155 \text{ m}\cdot\text{kg}$. Both the hyperbolic and linear $1/\text{time}$ models were utilized to ensure accuracy and robustness of the critical speed estimation.

Measurement of hindlimb skeletal muscle blood flow

On the final experimental day anesthesia was induced with a 5% isoflurane- O_2 mixture with maintenance on 2-3% isoflurane- O_2 . Subsequently, one catheter (PE-10 connected to PE-50, Clay Adams Brand, Sparks, MD, USA) was placed in the ascending aorta via the right carotid artery and a second catheter was placed in the caudal (tail) artery. The catheters were tunneled subcutaneously to the dorsal cervical region and exteriorized through a puncture wound in the skin. Anesthesia was terminated and the animal was given ≥ 1 hour to recover prior to blood flow measurement.

Following recovery, each rat (high-speed group) was placed on the treadmill and the tail artery catheter was connected to a 1 ml plastic syringe and a Harvard infusion/withdrawal pump while the carotid artery catheter was connected to a pressure transducer (Gould Statham P23ID, Valley View, OH, USA) and chart recorder for continuous monitoring of mean arterial pressure (MAP) and heart rate (HR). Exercise was then initiated and each rat ran at a speed of 25 m/min

for 1 min. At the 1 min mark the speed of the treadmill was increased to the speed equaling 15% above each individual rat's critical speed determined from the linear 1/time model (selected for the slightly, but not significantly, higher average critical speed estimation from this model, see *Results*). After 1.5 minutes of running at this speed (2.5 minutes of total exercise time) blood withdrawal from the tail artery catheter was initiated at a rate of 0.25 ml/min while MAP and HR were measured and recorded simultaneously via the carotid artery catheter. The carotid artery catheter was then disconnected from the pressure transducer and $0.5\text{-}0.6 \times 10^6$ microspheres (^{85}Sr or ^{57}Co in random order, Perkin Elmer, Waltham, MA, USA) were injected via carotid catheter into the aortic arch. Following microsphere injection and while the rat was still running a 0.3 ml blood sample was taken from the carotid artery catheter for determination of arterial pH, blood gases, and [lactate]. Exercise was then terminated and blood withdrawal from the caudal artery catheter (which was occurring simultaneous with microsphere injection) was stopped. The reference blood sample was collected and rats were then given 1 hour to recover.

After the 1 hour recovery period, 0.56 mg/kg (dissolved in 0.5 ml of heparinized saline) of the selective nNOS inhibitor SMTC (11, 28) was infused as a bolus into the caudal artery catheter (see below and Discussion for details regarding assessment of the efficacy and selectivity of nNOS inhibition). The tail catheter was then connected to a 1 ml syringe which was placed in the Harvard pump for blood withdrawal. 2 min following SMTC infusion a second bout of exercise, microsphere injection (differently labeled from the first run), and blood sample collection were performed exactly as described above for the control condition. ~10-15 min following exercise cessation the non-selective NOS inhibitor N^G -arginine-methyl-ester (L-NAME) was administered and MAP and HR were monitored and recorded for an additional ~10 min (see below for more details).

Low-speed group

For rats in the low-speed group MAP, HR and skeletal muscle, kidney, and splanchnic organ blood flow were measured before and after nNOS inhibition with SMTC exactly as described above for the high-speed group except the treadmill speed was set to 20 m/min for both the control and SMTC exercise bouts (i.e., same experimental protocol as ref. 6).

Assessment of efficacy and selectivity of nNOS inhibition with SMTC

To confirm that SMTC was mediating effects via nNOS inhibition (as opposed to some unknown/unexpected non-specific effect), MAP was measured in 5 additional rats (instrumented as described above) in which drug administration order was reversed such that non-selective NOS inhibition with L-NAME preceded SMTC. We reasoned that if SMTC was indeed acting via nNOS inhibition there would be no additional SMTC-induced MAP increase in the presence of prior L-NAME administration. In the rats from the exercise groups the selectivity of SMTC for nNOS versus eNOS was assessed via measurement of the hypotensive responses to rapid acetylcholine (ACh) infusions (10 µg/kg in 0.2 ml saline into the tail artery catheter) while the rats sat quietly on the treadmill belt under control, SMTC, and L-NAME conditions. The magnitude and recovery time of the hypotensive response to ACh was utilized as an index of eNOS-mediated function. The absence of any blunting of the hypotensive response to ACh following SMTC was considered consistent with the notion that SMTC did not impact eNOS-mediated function (see Discussion for more details).

Determination of blood flow and VC

Following the experimental protocol each animal was euthanized by pentobarbital overdose (≥ 100 mg/kg) administered via the carotid artery catheter. The thorax was opened, and placement of the carotid artery catheter into the aortic arch was confirmed by anatomical dissection. Organs of the splanchnic region, the kidneys, diaphragm, intercostal muscles, and the 28 individual muscles and muscle portions of the rat hindlimb were identified and removed. The tissues were blotted, weighed, and placed immediately into counting vials.

The radioactivity of each tissue was determined on a gamma scintillation counter (Packard Auto Gamma Spectrometer model 5230, Downers Grove, IL, USA). Accounting for cross-talk between isotopes, blood flows to each tissue were determined using the reference sample method (27) and expressed as milliliters per minute per 100 g of tissue (ml/min/100g). Adequate microsphere mixing was verified for each injection by the demonstration of a <15% difference between blood flow to the right and left kidneys and/or to the right and left hindlimb musculature. Blood flows were normalized to the MAP measured immediately preceding microsphere injection and expressed as VC (ml/min/100g/mmHg).

Data analyses

All data are presented as mean \pm SEM. MAP, HR and ACh responses were compared via ANOVAs with Student-Newman-Keuls *post hoc* tests where appropriate. Blood flow, VC, and blood sample variables were compared with paired Student's t-tests. z-tests were used to determine when reductions in blood flow and VC were different from zero. Significance was accepted at $p < 0.05$.

Results

High-speed group

$\dot{V}O_2$ peak and critical speed estimation

The average $\dot{V}O_2$ peak was 86 ± 1 ml/kg/min (RER = 1.07 ± 0.03) with a peak speed of 54.4 ± 2.4 m/min. The times to exhaustion at 90, 100, and 115% of peak speed and the hyperbolic and linear 1/time model fits and estimated critical speeds for a representative rat are shown in Figure 3.1. The coefficient of determination (r^2 , hyperbolic: 0.96 ± 0.03 , linear 1/time: 0.96 ± 0.02 , $p > 0.05$), W' (hyperbolic: 162 ± 67 J, linear: 139 ± 66 , $p > 0.05$) and estimated critical speed (hyperbolic: 44.0 ± 1.8 , linear 1/time: 45.6 ± 1.2 m/min, $p > 0.05$) were not different between models. The average running speed at which blood flow measurements were performed was 52.5 ± 1.3 m/min (15% above critical speed from the 1/time model).

Effects of SMTC on MAP, HR, and blood sample variables

At rest, SMTC increased MAP and reduced HR compared to control. During exercise, SMTC increased MAP whereas HR was not different between conditions (Table 3.1). Exercising arterial blood pH (control: 7.39 ± 0.02 , SMTC: 7.40 ± 0.02), PO_2 (control: 85.2 ± 2.1 , SMTC: 88.3 ± 3.3 mmHg), and [lactate] (control: 6.1 ± 0.4 , SMTC: 6.7 ± 0.8 mmol/L) were not different ($p > 0.05$ for all) between conditions. SMTC significantly reduced PCO_2 (control: 21.7 ± 0.8 , SMTC: 19.8 ± 0.8 mmHg, $p < 0.05$).

Effects of SMTC on hindlimb skeletal muscle blood flow and VC

In marked contrast to low-speed running (see below and also ref. 6), SMTC reduced total hindlimb skeletal muscle blood flow and VC during high-speed running above critical speed ($p < 0.05$, Figure 3.2). Specifically, blood flow was reduced in 14, and VC in 22, of the 28 individual muscles or muscle parts of the rat hindlimb (Table 3.2). Reductions in blood flow and VC were found in some muscles across the spectrum of oxidative capacities and muscle fiber-type compositions. However, the relative reductions in blood flow and VC following SMTC were greater in the highly glycolytic (100% type IIB+d/x fibers, $n=5$) compared to the highly oxidative ($\leq 35\%$ type IIB+d/x fibers, $n=5$, Figure 3.3) muscles and muscle portions. Moreover,

note in Figure 4.4 that within representative individual muscles containing distinct red and white portions the relative reductions in blood flow and VC following SMTC were greater in the glycolytic white versus the oxidative red portions of those muscles.

Effects of SMTC on respiratory skeletal muscle, kidney and splanchnic organ blood flow and VC

Blood flow and VC were reduced in the diaphragm and intercostal muscles following SMTC compared to control (Table 3.3, $p < 0.05$). Blood flow and VC to the kidneys and all organs of the splanchnic region were not different between control and SMTC conditions (Table 3.3, $p > 0.05$ for all)

Low-speed group

Similar to both the high-speed group and our previous report (6), SMTC increased resting MAP ($\uparrow 11 \pm 2$ mmHg, $p < 0.05$) and reduced HR ($\downarrow 38 \pm 16$ bpm) compared to control. In marked contrast to the high-speed group, during treadmill running at 20 m/min SMTC had no effects on MAP, HR, or blood flow and VC to the total hindlimb musculature (Figure 3.2) or any individual muscle or muscle part compared to control ($p > 0.05$ for all). Similarly, diaphragm and intercostal muscle blood flow and VC were not different between conditions ($p > 0.05$). SMTC reduced blood flow and VC to the kidneys, adrenals, stomach, and small intestine ($p < 0.05$ for all). As these data replicated closely those published previously (6), in the interests of brevity and clarity herein the reader is referred to that publication.

Efficacy and selectivity of nNOS inhibition with SMTC

SMTC followed by L-NAME administration produced a step-like increase in MAP above control values (Figure 3.5A, left panel). Conversely, when the drug administration order was reversed, SMTC administered in the presence of prior L-NAME administration produced no further MAP increase (Figure 3.5A, right panel). The magnitude (Δ MAP, Figure 5B, left panel) and recovery speed (time to 50% MAP recovery, Figure 5B, right panel) of the hypotensive response to ACh infusions were not different between control and SMTC conditions whereas they were blunted significantly following L-NAME.

Discussion

Consistent with our hypothesis, nNOS inhibition with SMTC reduced rat hindlimb skeletal muscle blood flow and VC during high-speed treadmill running (52.5 ± 1.3 m/min) above critical speed. Reductions in blood flow and VC were found in some muscles and muscle portions across the range of oxidative capacities and fiber-type compositions, however, the greatest relative reductions were found predominantly within glycolytic muscles composed primarily of type IIB+d/x fibers. The SMTC-induced reductions in skeletal muscle blood flow and VC during high-speed running directly oppose the lack of effects of nNOS inhibition with SMTC on blood flow or VC in any individual muscle or muscle part during low-speed (20 m/min) running. The present data reveal important fiber-type and exercise intensity dependent peripheral vascular effects of nNOS-derived NO during whole-body locomotory exercise.

Relationship with the literature

Low-intensity exercise recruits primarily motor units innervating oxidative slow- and fast-twitch muscle fibers whereas motor units innervating glycolytic fast-twitch muscle fibers are recruited additively as exercise intensity increases (13, 23). For high-intensity exercise the critical speed (or power) represents an important metabolic rate where exercise performed above critical speed/power systematically drives $\dot{V}O_2$ toward its maximum value (2, 31). In the rat, supra-critical speed treadmill running elicits marked preferential type IIB and d/x fast-twitch muscle fiber recruitment (5). That nNOS inhibition reduced relative blood flow and VC during supra-critical speed running to the greatest extent in glycolytic fast-twitch muscles in the present investigation is a crucial extension of the previous findings that nNOS-derived NO attenuates sympathetic vasoconstriction in glycolytic but not oxidative muscles during electrically-induced rat muscle contractions (38-40). Moreover, artificial simultaneous recruitment of all motor units may explain why nNOS inhibition reduced skeletal muscle blood flow and VC during electrically-induced contractions of the mixed muscle-fiber type rats spinotrapezius muscle (4). A fiber-type selective vascular effect of nNOS-derived NO is consistent with the identification of greater nNOS activity in predominantly type II, compared to type I, rat muscles (21) although human oxidative type I muscle may actually contain more nNOS than type II muscle (10). The

mechanisms of nNOS-mediated vasomotor control within glycolytic type II muscle during high-speed running likely involves attenuation of the exercise-induced augmented sympathetic vasoconstrictor signal (i.e., functional sympatholysis) mediated via α_2 -adrenergic receptors (38, 39). Although a more direct vasodilatory role for nNOS-derived NO has also been identified in rat fast-twitch muscle (14) acting presumably via alterations in intra-smooth muscle cell cyclic guanosine monophosphate (cGMP) concentration.

In the present investigation the absolute magnitude of SMTC-induced reductions in BF and VC were similar between some oxidative and glycolytic muscles. However, those reductions were not consistent or statistically significant in the majority of the oxidative muscles. A noted exception is the adductor longus which is only 5% type IIB+d/x muscle fibers according to the histochemical analysis of Delp and Duan (7). Interestingly, using immunological methods, Eng and colleagues (9) reported that the adductor longus is comprised of ~97% type IIB+d/x fibers. Thus, our present conclusion of a selective, but not exclusive, influence of nNOS inhibition within glycolytic fast-twitch muscles during high-speed running (as depicted, for example, in Figure 3.3) may actually be an underestimation. Furthermore, emphasis is placed on the relative reductions in blood flow and VC following SMTC herein because this designates the magnitude of the nNOS-derived NO signal relative to other vasodilator candidates within the individual muscles. Any pathological disruption in nNOS-mediated function (and resultant impairments in O₂ delivery) would lower the microvascular PO₂ in proportion to its relative vasomotor contribution. Thus, dysfunctional nNOS signaling would reduce microvascular PO₂ to the greatest extent in glycolytic muscles. This would presumably incur major negative consequences for capillary-myocyte O₂ flux, metabolic control, and contractile performance within those fibers (37); especially considering that glycolytic muscles evidence lower microvascular PO₂ values compared to oxidative muscles in the control condition (24).

In addition to muscle metabolic and contractile characteristics as reported presently, it is likely that other factors, for example, muscle contraction intensity (38), metabolic rate, and/or muscle function also influence the presence and extent of nNOS-derived NO vasomotor control. In support of the latter, nNOS inhibition with SMTC reduced blood flow and VC within predominantly oxidative rat hindlimb muscles at rest where muscle function (i.e., postural recruitment) may dictate nNOS-mediated vascular control. It is also noteworthy that blood flow and VC were reduced following SMTC in the intercostals and highly oxidative diaphragm

(although comprised of 50% type IIb+d/x muscle fibers) muscles during high-speed but not low-speed running. Admittedly, force generation by these respiratory muscles was not necessarily matched before and after SMTC (as it was for the hindlimb muscles, a key feature of the current experimental design). Force generation/recruitment was, if anything, likely enhanced given the well-characterized inhibitory effects of nNOS-derived NO on skeletal muscle contractile function (21) and the lower arterial PCO₂ which indicates a greater exercise-induced hyperventilation likely increasing respiratory muscle work. Therefore, the lower blood flow and VC following nNOS inhibition within the diaphragm and intercostals may well reflect a particularly important vasodilatory role for nNOS-derived NO in those muscles.

In the present investigation nNOS inhibition with SMTC did not reduce blood flow or VC to the kidneys or any splanchnic organs during high-speed running. This contrasts with the obligatory nNOS-derived NO renal vascular control reported by our laboratory (present data, 6) and others (18, 42). However, high exercise intensities elicit marked sympathetically-induced vasoconstriction within non-muscular tissues and inactive muscle thereby promoting cardiac output redistribution towards active skeletal muscle. This is evidenced by the lower kidney and splanchnic organ blood flows and VCs compared to that found in the rat at rest and during low-speed treadmill running (6). At high exercise intensities obligatory nNOS-derived NO kidney and splanchnic organ vascular control may be obviated in order to facilitate this blood flow redistribution.

nNOS has been identified within nerves, skeletal muscle, and key cardiovascular control centers in the brain (29, 36). Importantly, an identical systemic SMTC dose as used herein does not impact lumbar or renal sympathetic nerve discharge (author's unpublished observations). This supports that the effects of SMTC observed presently reflect peripheral nNOS-derived NO vascular control specifically.

Efficacy and selectivity of nNOS inhibition with SMTC

The efficacy and selectivity of nNOS inhibition herein is supported by: 1) the lack of further MAP increase with SMTC in the presence of prior L-NAME administration (Figure 5A, right panel), 2) the previously reported 17-fold selectivity of SMTC for nNOS over eNOS in rat tissue *in vivo* (11), 3) a comprehensive SMTC dose-response analysis indicating marked selectivity of SMTC for nNOS over eNOS at low doses (i.e., <1.0 mg/kg; 42), and 4) the present

demonstration that 0.56 mg/kg of SMTC did not alter the hypotensive response to ACh whereas it was blunted significantly following non-selective NOS inhibition with L-NAME. Importantly, higher SMTC doses also blunt the hypotensive response to ACh (22, 42) thus supporting the sensitivity of this assessment as an indicator of nNOS selectivity. Analysis of the hypotensive response to ACh has been utilized extensively to assess the selectivity of SMTC for nNOS in conscious rats (6, 42) and humans (34, 35) although we acknowledge that systemic ACh infusion may not necessarily impact eNOS exclusively. However, it is also compelling that non-selective NOS inhibition with L-NAME in the rat running at low (17) and high (26) speeds markedly reduces blood flow and VC with the greatest effects observed in highly oxidative muscles. In direct contrast, 0.56 mg/kg of SMTC did not impact blood flow or VC whatsoever during low-speed running and the greatest relative reductions during high-speed running were found primarily within glycolytic fast-twitch muscles. Had the SMTC dose utilized herein been so high as to inhibit eNOS at least some effects would have been anticipated during low-speed running. Therefore, we believe that SMTC as used presently did not impact eNOS-mediated function.

Conclusions

In the present investigation, selective nNOS inhibition with SMTC reduced skeletal muscle blood flow and VC principally within highly glycolytic fast-twitch muscle during high-speed treadmill running above critical speed. These pronounced effects of nNOS inhibition during supra-critical speed exercise differ dramatically from the lack of effects observed at low running speeds (present data, 6). This identifies, for the first time, that nNOS-derived NO is an integral controller of skeletal muscle blood flow and in a fiber-type and exercise intensity dependent manner during whole-body locomotory exercise that contrasts markedly from eNOS-derived NO. Specifically, eNOS (plus nNOS) blockade with L-NAME induces the greatest blood flow and VC decrements in the most highly oxidative fibers and, as such, is manifested at both low and high running speeds. The present investigation has important implications for cardiovascular disorders associated with reduced NO bioavailability and blood flow impairments during exercise and diseases associated specifically with altered nNOS structure and/or function.

Table 3.1. Effects of nNOS inhibition on MAP and HR

	<i>Control</i>	<i>SMTC</i>
<u>Rest</u>		
MAP (mmHg)	125±4	137±5*
HR (bpm)	410±9	393±11*
<u>Exercise</u>		
MAP (mmHg)	130±4	139±4*
HR (bpm)	538±6 [†]	555±11 [†]

Effects of nNOS inhibition with SMTC on MAP and HR at rest and during high-speed treadmill running (15% above critical speed, 52.5±1.3 m/min). Data are mean±SEM, * p <0.05 versus control. [†] p <0.05 versus rest.

Table 3.2. Effects of nNOS inhibition on blood flow and VC

	<i>Blood flow</i>		<i>VC</i>	
	<i>Control</i>	<i>SMTC</i>	<i>Control</i>	<i>SMTC</i>
<u>Ankle extensors</u>				
Soleus (21.3, 9%)	366±37	309±14	2.87±0.37	2.23±0.11*
Plantaris (21.8, 80%)	394±29	382±16	3.04±0.20	2.75±0.11
Gastrocnemius, red (36.2, 14%)	566±48	533±22	4.40±0.42	3.85±0.22*
Gastrocnemius, white (8.1, 100%)	141±24	99±12*	1.10±0.19	0.71±0.09*
Gastrocnemius, mixed (25.7, 91%)	284±25	255±6	2.21±0.22	1.84±0.09*
Tibialis posterior (18.3, 73%)	347±41	334±26	2.70±0.33	2.41±0.21
Flexor digitorum longus (10.6, 68%)	187±47	145±20	1.46±0.37	1.06±0.17
Flexor halicis longus (12.3, 71%)	183±18	153±9*	1.42±0.14	1.10±0.07*
<u>Ankle flexors</u>				
Tibialis anterior, red (39.3, 63%)	572±79	429±44*	4.50±0.76	3.12±0.40*
Tibialis anterior, white (18.4, 80%)	222±42	156±22*	1.75±0.40	1.14±0.19*
Extensor digitorum longus (21.6, 76%)	107±19	90±18	0.84±0.16	0.66±0.15*
Peroneals (20.3, 67%)	222±26	143±15*	1.73±0.21	1.05±0.13*
<u>Knee extensors</u>				
Vastus intermedius (33.2, 4%)	585±50	520±33	4.52±0.34	3.76±0.28*
Vastus medialis (20.2, 82%)	424±36	383±12	3.27±0.21	2.76±0.09*
Vastus lateralis, red (42.3, 35%)	482±99	476±72	3.61±0.67	3.39±0.50
Vastus lateralis, white (8.3, 100%)	188±24	144±19*	1.47±0.21	1.05±0.16*
Vastus lateralis, mixed (19.2, 89%)	336±29	325±13	2.60±0.22	2.35±0.14
Rectus femoris, red (25.6, 66%)	458±50	399±33	3.51±0.32	2.89±0.28*
Rectus femoris, white (15.1, 100%)	267±29	218±18*	2.06±0.20	1.58±0.15*
<u>Knee flexors</u>				
Biceps femoris, anterior (8.4, 100%)	127±26	95±19*	1.01±0.23	0.70±0.16*
Biceps femoris, posterior (14.0, 92%)	191±23	150±11*	1.50±0.21	1.09±0.11*
Semitendinosus (12.6, 83%)	88±15	55±7*	0.69±0.13	0.40±0.06*
Semimembranosus, red (20.6, 72%)	316±46	259±21	2.47±0.40	1.88±0.17*
Semimembranosus, white (10.2, 100%)	135±32	95±17*	1.06±0.27	0.69±0.13
<u>Thigh adductors</u>				
Adductor longus (18.9, 5%) ¹	378±70	269±44*	2.98±0.64	1.94±0.31*
Adductor magnus & brevis (18.5, 89%)	204±38	158±22*	1.60±0.33	1.14±0.16*
Gracilis (15.4, 77%)	89±25	53±9*	0.69±0.19	0.38±0.07*
Pectinius (20.2, 69%)	176±73	136±81	1.43±0.66	1.04±0.65*

(Table 3.2 continued)

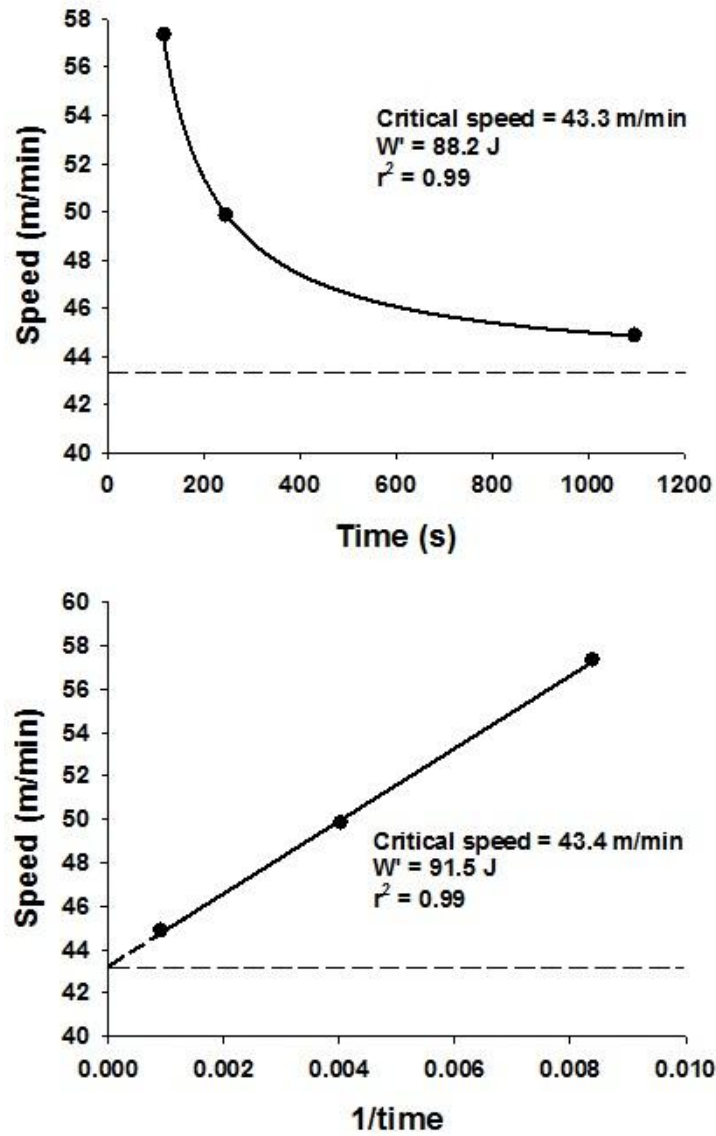
Effects of nNOS inhibition with SMTC on individual hindlimb muscle or muscle part blood flow (ml/min/100g) and vascular conductance (VC, ml/min/100g/mmHg) during high-speed treadmill running (15% above critical speed, 52.5 ± 1.3 m/min). Data are mean \pm SEM. Numbers in parentheses represent the citrate synthase activity ($\mu\text{mol}/\text{min}/\text{g}$) and percent sum of type IIb+d/x muscle fibers, respectively, as reported previously by Delp and Duan (7). ¹See text for comments regarding contrasting report of the adductor longus muscle fiber-type composition by Eng et al. (9). * $p < 0.05$ versus control.

Table 3.3. Effects of nNOS inhibition on blood flow and VC

	<i>Blood flow</i>		<i>VC</i>	
	<i>Control</i>	<i>SMTC</i>	<i>Control</i>	<i>SMTC</i>
Diaphragm (39.1, 50%)	355±55	267±27*	2.76±0.43	1.94±0.23*
Intercostals (12.0, ~82%)	60±7	47±4*	0.47±0.06	0.34±0.03*
Kidney	318±65	255±57	2.46±0.48	1.81±0.38
Stomach	35±5	29±4	0.28±0.05	0.20±0.03
Adrenals	227±51	158±28	1.77±0.40	1.13±0.19
Spleen	19±5	24±6	0.15±0.04	0.17±0.04
Pancreas	59±10	42±4	0.47±0.09	0.30±0.02
Small intestine	164±32	141±16	1.29±0.27	1.00±0.10
Large intestine	97±17	86±12	0.76±0.14	0.61±0.08
Liver ²	18±4	21±4	0.14±0.03	0.15±0.03

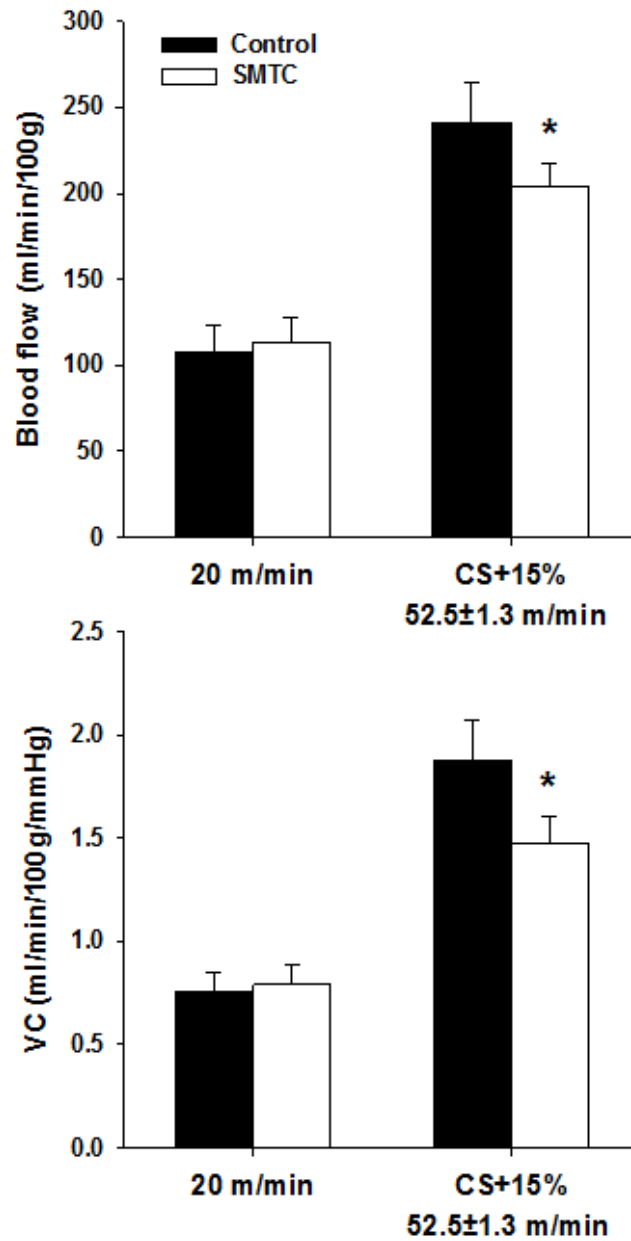
Effects of nNOS inhibition with SMTC on respiratory skeletal muscle, kidney, and splanchnic organ blood flow (ml/min/100g) and vascular conductance (VC, ml/min/100g/mmHg) during high-speed treadmill running (15% above critical speed, 52.5±1.3 m/min). Data are mean±SEM. Numbers in parentheses represent the citrate synthase activity (μmol/min/g) and percent sum of type IIb+d/x muscle fibers, respectively, as reported previously by Delp and Duan (7). ²Denotes arterial, not portal, blood flow and VC. **p*<0.05 versus control.

Figure 3.1. Estimation of critical speed for a representative rat



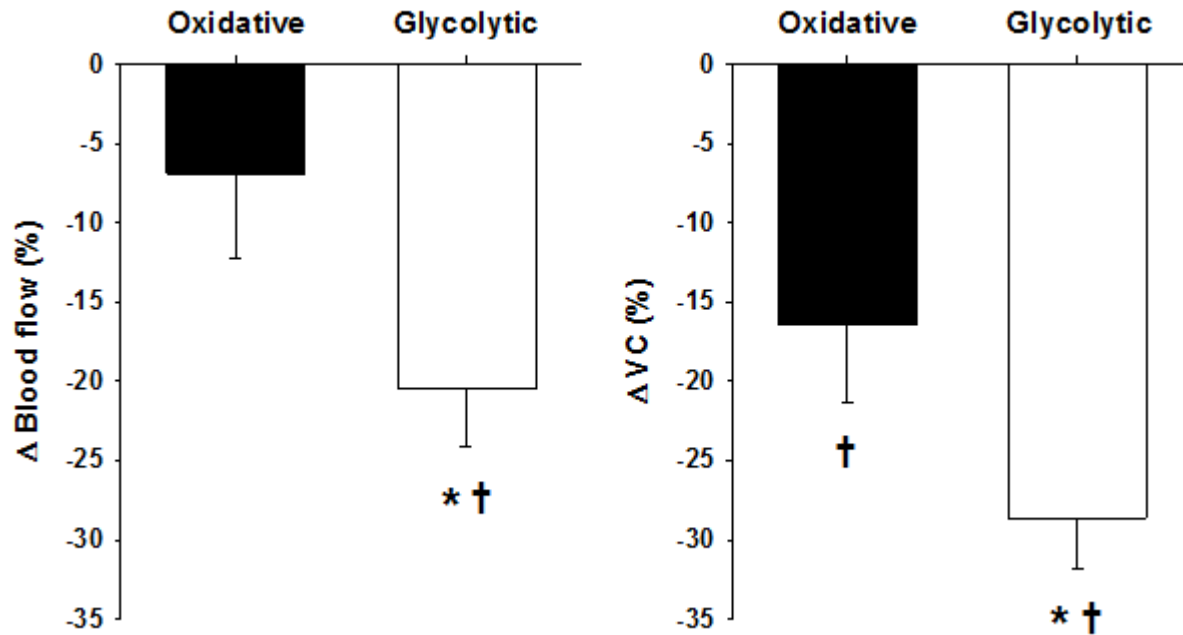
Estimation of critical speed (represented by the horizontal dashed lines) via the hyperbolic and linear 1/time models for a representative rat.

Figure 3.2. Effects of nNOS inhibition on hindlimb skeletal muscle blood flow and VC



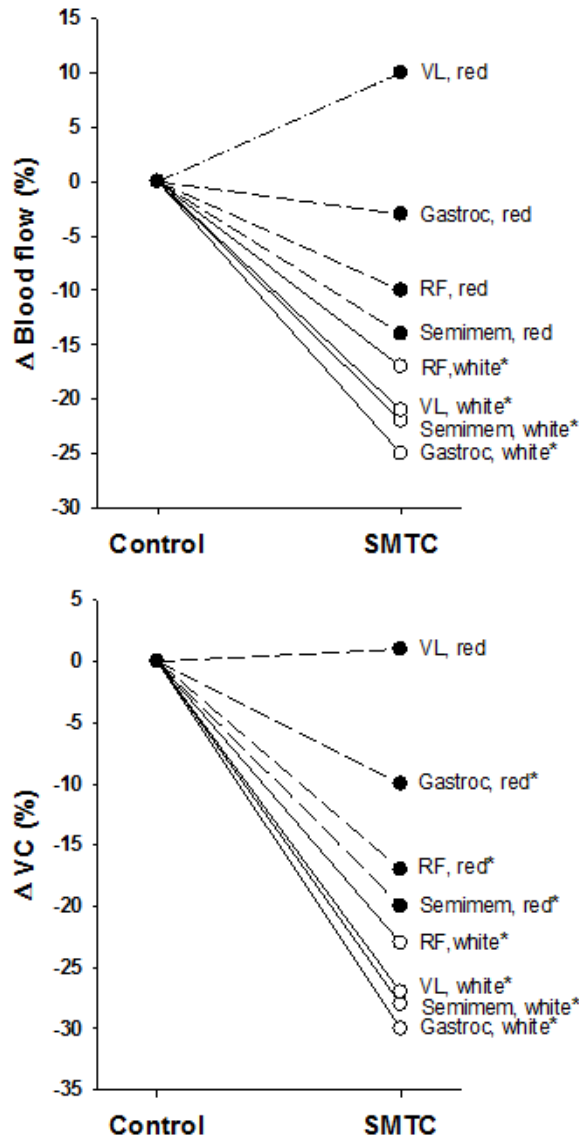
Effects of nNOS inhibition with SMTC (0.56 mg/kg) on hindlimb skeletal muscle blood flow and vascular conductance (VC) during treadmill running at 20 m/min (from present low-speed group) and 15% above critical speed (CS+15%, 52.5±1.3 m/min). * $p < 0.05$ versus control.

Figure 3.3. Relative changes in blood flow and VC following nNOS inhibition



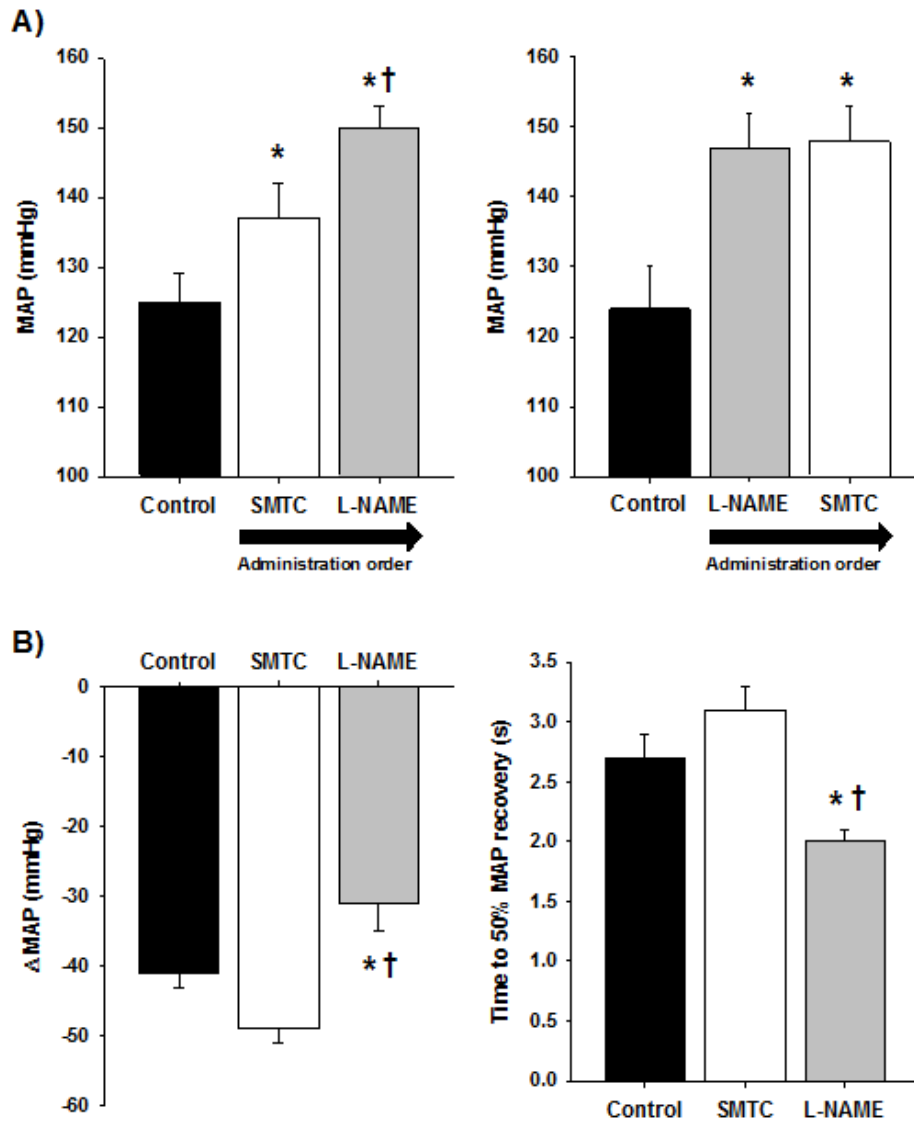
Relative changes in blood flow (Δ blood flow) and VC (Δ VC) following nNOS inhibition with SMTc (0.56 mg/kg) in the highly oxidative and highly glycolytic muscles and muscle parts during high-speed treadmill running. Oxidative muscles (n=5, adductor longus, red portion of the vastus lateralis, vastus intermedius, soleus, and red portion of the gastrocnemius) are comprised of $\leq 35\%$ type IIb+d/x fibers and have 3-fold higher citrate synthase activity versus glycolytic muscles (7). Glycolytic muscles (n=5, anterior portion of the biceps femoris, white portions of the semimembranosus, rectus femoris, gastrocnemius, and vastus lateralis) are comprised of 100% type IIb+d/x fibers (7). * $p < 0.05$ versus oxidative, † $p < 0.05$ versus zero.

Figure 3.4. Relative changes in blood flow and VC following nNOS inhibition



Relative changes in blood flow (Δ blood flow) and vascular conductance (Δ VC) following nNOS inhibition with SMTC (0.56 mg/kg) for oxidative red and glycolytic white portions of representative individual muscles during high-speed treadmill running. Oxidative red (dashed lines and filled circles): $47 \pm 14\%$ type IIB+d/x muscle fibers and 3-fold higher citrate synthase activity versus glycolytic white portions (7). Glycolytic white (solid lines and open circles): all 100% type IIB+d/x muscle fibers (7). VL, vastus lateralis; Semim, semimembranosus; RF, rectus femoris; Gastroc, gastrocnemius. SEM bars are omitted for clarity (range across all muscles 4-12%). * $p < 0.05$ versus control.

Figure 3.5. MAP data demonstrating the efficacy and selectivity of nNOS inhibition



A) The step-like MAP increase when SMTC preceded L-NAME (left panel, high-speed group, n=6) and the lack of any further MAP increase when SMTC followed L-NAME (right panel, n=5) confirm that SMTC mediated its effects via nNOS inhibition. B) The lack of effects of SMTC on the magnitude (left panel) and recovery speed (right panel) of the hypotensive response to ACh is consistent with intact eNOS-mediated function (high-speed group, n=6). * $p < 0.05$ versus control, † $p < 0.05$ versus SMTC.

References

1. **Armstrong RB and Laughlin MH.** Rat muscle blood flows during high-speed locomotion. *J Appl Physiol* 59: 1322-1328, 1985.
2. **Broxterman RM, Ade CJ, Poole DC, Harms CA, and Barstow TJ.** A single test for the determination of parameters of the speed-time relationship for running. *Respir Physiol Neurobiol* 185: 380-385, 2013.
3. **Copp SW, Hirai DM, Ferguson SK, Holdsworth CT, Musch TI, and Poole DC.** Effects of chronic heart failure on neuronal nitric oxide synthase-mediated control of microvascular O₂ pressure in contracting rat skeletal muscle. *J Physiol* 590: 3585-3596, 2012.
4. **Copp SW, Hirai DM, Ferguson SK, Musch TI, and Poole DC.** Role of neuronal nitric oxide synthase in modulating microvascular and contractile function in rat skeletal muscle. *Microcirculation* 18: 501-511, 2011.
5. **Copp SW, Hirai DM, Musch TI, and Poole DC.** Critical speed in the rat: implications for hindlimb muscle blood flow distribution and fiber recruitment. *J Physiol* 588: 5077-5087, 2010.
6. **Copp SW, Hirai DM, Schwagerl PJ, Musch TI, and Poole DC.** Effects of neuronal nitric oxide synthase inhibition on resting and exercising hindlimb muscle blood flow in the rat. *J Physiol* 588: 1321-1331, 2010.
7. **Delp MD and Duan C.** Composition and size of type I, IIA, IID/X, and IIB fibers and citrate synthase activity of rat muscle. *J Appl Physiol* 80: 261-270, 1996.
8. **Drummond GB.** Reporting ethical matters in the Journal of Physiology: standards and advice. *J Physiol* 587: 713-719, 2009.
9. **Eng CM, Smallwood LH, Rainiero MP, Lahey M, Ward SR, and Lieber RL.** Scaling of muscle architecture and fiber types in the rat hindlimb. *J Exp Biol* 211: 2336-2345, 2008.
10. **Frandsen U, Lopez-Figueroa M, and Hellsten Y.** Localization of nitric oxide synthase in human skeletal muscle. *Biochem Biophys Res Commun* 227: 88-93, 1996.

11. **Furfine ES, Harmon MF, Paith JE, Knowles RG, Salter M, Kiff RJ, Duffy C, Hazelwood R, Oplinger JA, and Garvey EP.** Potent and selective inhibition of human nitric oxide synthases. Selective inhibition of neuronal nitric oxide synthase by S-methyl-L-thiocitrulline and S-ethyl-L-thiocitrulline. *J Biol Chem* 269: 26677-26683, 1994.
12. **Gaesser GA, Carnevale TJ, Garfinkel A, Walter DO, and Womack CJ.** Estimation of critical power with nonlinear and linear models. *Med Sci Sports Exerc* 27: 1430-1438, 1995.
13. **Gollnick PD, Piehl K, and Saltin B.** Selective glycogen depletion pattern in human muscle fibers after exercise of varying intensity and at varying pedalling rates. *J Physiol* 241: 45-57, 1974.
14. **Grange RW, Isotani E, Lau KS, Kamm KE, Huang PL, and Stull JT.** Nitric oxide contributes to vascular smooth muscle relaxation in contracting fast-twitch muscles. *Physiol Genomics* 5: 35-44, 2001.
15. **Green DJ, O'Driscoll G, Blanksby BA, and Taylor RR.** Control of skeletal muscle blood flow during dynamic exercise: contribution of endothelium-derived nitric oxide. *Sports Med* 21: 119-146, 1996.
16. **Hirai DM, Copp SW, Holdsworth CT, Ferguson SK, Musch TI, and Poole DC.** Effects of neuronal nitric oxide synthase inhibition on microvascular and contractile function in skeletal muscle of aged rats. *Am J Physiol Heart Circ Physiol* 303: H1076-1084, 2012.
17. **Hirai T, Visneski MD, Kearns KJ, Zelis R, and Musch TI.** Effects of NO synthase inhibition on the muscular blood flow response to treadmill exercise in rats. *J Appl Physiol* 77: 1288-1293, 1994.
18. **Ichihara A, Inscho EW, Imig JD, and Navar LG.** Neuronal nitric oxide synthase modulates rat renal microvascular function. *Am J Physiol* 274: F516-524, 1998.
19. **Joyner MJ and Wilkins BW.** Exercise hyperaemia: is anything obligatory but the hyperaemia? *J Physiol* 583: 855-860, 2007.
20. **King CE, Melinyshyn MJ, Mewburn JD, Curtis SE, Winn MJ, Cain SM, and Chapler CK.** Canine hindlimb blood flow and O₂ uptake after inhibition of EDRF/NO synthesis. *J Appl Physiol* 76: 1166-1171, 1994.

21. **Kobzik L, Reid MB, Bredt DS, and Stamler JS.** Nitric oxide in skeletal muscle. *Nature* 372: 546-548, 1994.
22. **Komers R, Oyama TT, Chapman JG, Allison KM, and Anderson S.** Effects of systemic inhibition of neuronal nitric oxide synthase in diabetic rats. *Hypertension* 35: 655-661, 2000.
23. **Laughlin MH and Armstrong RB.** Muscular blood flow distribution patterns as a function of running speed in rats. *Am J Physiol* 243: H296-306, 1982.
24. **McDonough P, Behnke BJ, Padilla DJ, Musch TI, and Poole DC.** Control of microvascular oxygen pressures in rat muscles comprised of different fiber types. *J Physiol* 563: 903-913, 2005.
25. **Musch TI, Bruno A, Bradford GE, Vayonis A, and Moore RL.** Measurements of metabolic rate in rats: a comparison of techniques. *J Appl Physiol* 65: 964-970, 1988.
26. **Musch TI, McAllister RM, Symons JD, Stebbins CL, Hirai T, Hageman KS, and Poole DC.** Effects of nitric oxide synthase inhibition on vascular conductance during high speed treadmill exercise in rats. *Exp Physiol* 86: 749-757, 2001.
27. **Musch TI and Terrell JA.** Skeletal muscle blood flow abnormalities in rats with a chronic myocardial infarction: rest and exercise. *Am J Physiol* 262: H411-419, 1992.
28. **Narayanan K and Griffith OW.** Synthesis of L-thiocitrulline, L-homothiocitrulline, and S-methyl-L-thiocitrulline: a new class of potent nitric oxide synthase inhibitors. *J Med Chem* 37: 885-887, 1994.
29. **Patel KP, Li YF, and Hirooka Y.** Role of nitric oxide in central sympathetic outflow. *Exper Biol Med* 226: 814-824, 2001.
30. **Poole DC, Hirai DM, Copp SW, and Musch TI.** Muscle oxygen transport and utilization in heart failure: implications for exercise (in)tolerance. *Am J Physiol Heart Circ Physiol* 302: H1050-1063, 2012.
31. **Poole DC, Ward SA, Gardner GW, and Whipp BJ.** Metabolic and respiratory profile of the upper limit for prolonged exercise in man. *Ergonomics* 31: 1265-1279, 1988.
32. **Sander M, Chavoshan B, Harris SA, Iannaccone ST, Stull JT, Thomas GD, and Victor RG.** Functional muscle ischemia in neuronal nitric oxide synthase-deficient skeletal muscle of children with Duchenne muscular dystrophy. *Proc Natl Acad Sci USA* 97: 13818-13823, 2000.

33. **Schrage WG, Joyner MJ, and Dinunno FA.** Local inhibition of nitric oxide and prostaglandins independently reduces forearm exercise hyperaemia in humans. *J Physiol* 557: 599-611, 2004.
34. **Seddon M, Melikian N, Dworakowski R, Shabeeh H, Jiang B, Byrne J, Casadei B, Chowienczyk P, and Shah AM.** Effects of neuronal nitric oxide synthase on human coronary artery diameter and blood flow in vivo. *Circulation* 119: 2656-2662, 2009.
35. **Seddon MD, Chowienczyk PJ, Brett SE, Casadei B, and Shah AM.** Neuronal nitric oxide synthase regulates basal microvascular tone in humans in vivo. *Circulation* 117: 1991-1996, 2008.
36. **Stamler JS and Meissner G.** Physiology of nitric oxide in skeletal muscle. *Physiol Rev* 81: 209-237, 2001.
37. **Stary CM and Hogan MC.** Effect of varied extracellular PO₂ on muscle performance in *Xenopus* single skeletal muscle fibers. *J Appl Physiol* 86: 1812-1816, 1999.
38. **Thomas GD, Hansen J, and Victor RG.** Inhibition of alpha 2-adrenergic vasoconstriction during contraction of glycolytic, not oxidative, rat hindlimb muscle. *Am J Physiol* 266: H920-929, 1994.
39. **Thomas GD, Sander M, Lau KS, Huang PL, Stull JT, and Victor RG.** Impaired metabolic modulation of alpha-adrenergic vasoconstriction in dystrophin-deficient skeletal muscle. *Proc Natl Acad Sci USA* 95: 15090-15095, 1998.
40. **Thomas GD, Shaul PW, Yuhanna IS, Froehner SC, and Adams ME.** Vasomodulation by skeletal muscle-derived nitric oxide requires alpha-syntrophin-mediated sarcolemmal localization of neuronal Nitric oxide synthase. *Circ Res* 92: 554-560, 2003.
41. **Thomas GD, Zhang W, and Victor RG.** Impaired modulation of sympathetic vasoconstriction in contracting skeletal muscle of rats with chronic myocardial infarctions: role of oxidative stress. *Circ Res* 88: 816-823, 2001.
42. **Wakefield ID, March JE, Kemp PA, Valentin JP, Bennett T, and Gardiner SM.** Comparative regional haemodynamic effects of the nitric oxide synthase inhibitors, S-methyl-L-thiocitrulline and L-NAME, in conscious rats. *Br J Pharmacol* 139: 1235-1243, 2003.

Chapter 4 - Role of neuronal nitric oxide synthase in modulating skeletal muscle microvascular and contractile function

Summary

The present study tested the hypothesis that selective neuronal nitric oxide synthase (nNOS) inhibition would lower the dynamic microvascular O₂ delivery/utilization ($\dot{V}O_2$) balance (which sets the microvascular O₂ partial pressure; PO_{2mv}) in rat skeletal muscle at rest and during contractions. Anesthetized male Sprague-Dawley rats had their spinotrapezius muscles exposed for blood flow (radiolabelled microspheres), $\dot{V}O_2$ (direct Fick calculation), PO_{2mv} (phosphorescence quenching), or exteriorized for force production measurement during electrically-induced contractions (1 Hz, 6-8 V, 180 s) pre- and post-nNOS inhibition with 2.1 μ mol/kg of S-methyl-L-thiocitrulline (SMTC). At rest, spinotrapezius blood flow was not different whereas SMTC reduced $\dot{V}O_2$ ($\downarrow 27\%$) resulting in an elevated pre-contracting baseline PO_{2mv} (control: 31.2 ± 1.6 , SMTC: 37.1 ± 2.0 mmHg, $p < 0.05$). Following contractions onset SMTC speeded the time to reach 63% of the overall PO_{2mv} kinetics response (control: 22.5 ± 1.6 , SMTC: 16.9 ± 1.4 s, $p < 0.05$). During the contracting steady-state, SMTC reduced spinotrapezius blood flow ($\downarrow 17\%$) and $\dot{V}O_2$ ($\downarrow 17\%$) such that PO_{2mv} was not different (control: 22.8 ± 1.6 , SMTC: 22.7 ± 2.1 mmHg, $p > 0.05$) which occurred despite an elevated ($\uparrow \sim 8\%$) muscle force production. These data demonstrate important physiological roles for nNOS-derived NO during contractions in healthy rat skeletal muscle and implicate maladaptations in nNOS function in pathological conditions associated with reduced NO bioavailability.

Introduction

Nitric oxide (NO) derived from constitutively expressed neuronal (type I) and endothelial (type III) NO synthase (NOS) has been identified as an important signaling molecule with a vast array of physiological functions. Given that global endothelial dysfunction represents an important biomarker and predictor of functional capacity and quality of life (2), the potential role of endothelial NOS (eNOS) rather than neuronal NOS (nNOS) in modulating peripheral vascular tone has been a principal focus of experimental enquiry.

More recently, however, novel investigations have identified specific roles for nNOS-derived NO in the regulation of vascular function and O₂ delivery (12, 23, 32, 48, 49, 51). For example, mice lacking nNOS evince impaired modulation of sympathetic vasoconstrictor influence (i.e., functional sympatholysis; 15, 51, 52) and augmented smooth muscle contractile protein phosphorylation (21) which culminates in reduced active skeletal muscle blood flow during treadmill exercise (35). Furthermore, in healthy subjects pharmacological selective nNOS blockade reduced resting blood flow in humans (48, 49) and animals (12) but, contrary to data from mice lacking nNOS, did not alter active skeletal muscle blood flow during treadmill running exercise in the rat hindlimb (12). Thus, the precise role of nNOS-derived NO in regulating O₂ delivery to active skeletal muscle remains controversial. One important consideration in this regard is that nNOS-derived NO may modulate a variety of intramyocyte processes. For example, within skeletal muscle it has been shown that NO may exert inhibitory influences on both contractile function (3, 45) and mitochondrial respiration (9). In light of these diverse NO-mediated effects, it is surprising that no study has yet investigated the precise role(s) of nNOS-derived NO in regulating O₂ delivery in specific relation to local O₂ demand. Within the skeletal muscle microvasculature the local O₂ delivery-to-O₂ utilization ($\dot{V}O_2$) ratio sets the microvascular partial pressure of O₂, PO_{2mv} and constitutes the sole pressure-head for capillary-myocyte O₂ flux according to Fick's law of diffusion. An enhanced understanding of the role of nNOS-derived NO in controlling the dynamic and steady-state PO_{2mv} response during muscle contractions would be particularly important given the crucial role of O₂ availability in determining muscle performance. This information would be beneficial for the many chronic clinical conditions are associated with derangements in nNOS structure and/or function (53).

Therefore, the purpose of the present investigation was to explore the effects of nNOS inhibition via the selective nNOS inhibitor S-methyl-L-thiocitrulline (SMTC, which possesses a 17-fold selectivity for nNOS versus eNOS; 19) administered prior to contractions of an *in situ* skeletal muscle on the regulation of dynamic skeletal muscle PO_{2mv} response during contractions. Based on the evidence summarized above, we tested the hypothesis that selective nNOS inhibition via SMTC would: 1) reduce resting but not contracting muscle blood flow, 2) increase resting and contracting muscle $\dot{V}O_2$, 3) lower the muscle O_2 delivery/ $\dot{V}O_2$ ratio (i.e., PO_{2mv}) at rest and during the rest-contractions transition, and 4) increase muscle force production.

Methods

Animals

26 total young (4-5 months, body mass 459 ± 14 g) male Sprague-Dawley rats (Charles River Laboratories, Wilmington, MA, USA) were housed 2 per cage in accredited facilities and maintained on a 12:12 hour light-dark cycle with food and water provided *ad libitum*. All experimental protocols described presently were approved by the Institutional Animal Care and Use Committee of Kansas State University and conducted in accordance with federally mandated guidelines.

Surgical preparation

All rats were anesthetized initially with a 5% isoflurane-O₂ mixture and maintained on 2-3% isoflurane-O₂. The carotid and caudal (tail) arteries were cannulated (Polyethelene-50, Intra-Medic Tubing, Clay Adams Brand, Becton, Dickinson and Company, Sparks, MD, USA) for continuous monitoring of heart rate (HR) and mean arterial pressure (MAP), infusion of the phosphorescent probe, and/or blood flow measurement via radiolabelled microsphere injection (see below). Following placement of the catheters, the animals were gradually transitioned to pentobarbital sodium (administered i.a. to effect). The level of anesthesia was monitored continuously throughout the experiment via toe-pinch and blink reflexes and was supplemented as necessary. Anesthetized rats were placed on a heating pad to maintain core temperature, measured via rectal probe, at ~ 37 - 38 °C.

For PO_2mv measurement, overlying skin and adipose tissue was removed surgically from the right side of the dorsal, mid-caudal region of each rat exposing the right spinotrapezius muscle in a manner preserving the muscles vascular and neural supply. For example, our laboratory has demonstrated previously similar blood flow responses may be obtained among intact (non-exposed), exposed, and exteriorized spinotrapezius muscles (4) indicating that potential inflammatory responses as a result of surgical preparation do not confound data interpretation at least in regards to the principal measurements made herein. Exposed muscle was moistened constantly throughout the surgery and experimental protocol via superfusion of Krebs-Henseleit bicarbonate-buffered solution (equilibrated with 5% CO₂, 95% N₂, pH 7.4,

warmed to 37 °C) and surrounding tissue was covered with Saran™ wrap (Dow Brands, Indianapolis, IN, USA). Silver wire electrodes were sutured to the rostral (cathode) and caudal (anode) region of the muscle to elicit electrically-induced muscle contractions. The spinotrapezius muscle is ideal for investigations of microvascular and metabolic function given that it is optimally located for surgical exposure/exteriorization and possesses a mosaic of muscle-fiber types and a citrate synthase activity similar to the human quadriceps (13, c.f., 36).

Measurement of PO_2mv

In 10 rats, the phosphorescent probe palladium meso-tetra (4-carboxyphenyl) porphyrin dendrimer (R2: 15-20 mg/kg dissolved in saline) was infused via the carotid artery catheter. After a ~10-15 minute stabilization, the carotid artery catheter was connected to a pressure transducer for continuous monitoring of HR and MAP, PO_2mv measurement (see below) was initiated. Confirmation of a valid preparation with intact arteriolar tone required a stable PO_2mv for a minimum of 30 s and within ± 10 mmHg of the value established for this measurement in the young healthy rat (i.e., 31.4 mmHg; 8). Subsequently, 1.2 ml of heparinized saline was infused at a rate of 0.2 ml/min into the caudal artery catheter to serve as a control infusion. Following the infusion the caudal artery catheter was connected to a 1 ml plastic syringe and placed in a withdrawal pump (model 907, Harvard Apparatus, Cambridge, MA, USA). Subsequently, 1 Hz (~6-8 V, 2 ms pulse duration) twitch contractions were elicited via a stimulator (model S88, Grass Instrument Co., Quincy, MA, USA). At 180 seconds of contractions blood withdrawal from the tail catheter was initiated at a rate of 0.25 ml/min, the carotid catheter was disconnected from the pressure transducer, and $\sim 0.5-0.6 \times 10^6$ $15 \mu\text{m}$ radiolabelled microspheres (^{46}Sc or ^{85}Sr in random order, Perkin Elmer Life and Analytical Sciences, Boston, MA, USA) were injected into the aortic arch for determination of blood flow (see below for details), and contractions were then terminated. Following a minimum 20 minute recovery period, 0.56 mg/kg (2.1 $\mu\text{mol/kg}$) of SMTC was dissolved in 1.2 ml of heparinized saline and infused as described above. Following the infusion and once it was observed that PO_2mv was stable for at least 30 seconds, contraction and microsphere injection protocols were performed exactly as described for control. Blood samples were taken after each contraction protocol to determine arterial PO_2 , O_2 saturation, pH, and blood [lactate]. In a separate group of animals (n=5) acetylcholine (ACh) infusions (10 $\mu\text{g/kg}$ in 0.2 ml of saline) were performed

under control and SMTC conditions as well as following non-selective NOS inhibition with 10 mg/kg of N^G-nitro-L-arginine-methyl-ester (L-NAME) administered into the caudal artery. The hypotensive responses to these infusions were recorded in order to confirm the efficacy of selective nNOS inhibition in the presence of SMTC in anesthetized rats. At the end of each experiment, rats were euthanized via an intra-arterial pentobarbital overdose (~50 mg/kg).

Determination of muscle blood flow and calculation of $\dot{V}O_2$

Upon completion of each experiment, the right and left spinotrapezius muscles and kidneys were carefully dissected, removed and weighed. The radioactivity of the individual tissues and reference blood samples taken from the tail artery catheter during microsphere injections were determined via a gamma scintillation counter (Auto Gamma Spectrometer, Cobra model 5003, Hewlett-Packard, Downers Grove, IL, USA) and individual tissue blood flows were determined by the reference sample method (26) and expressed in milliliters per minute per 100 grams of tissue. In each condition (control and SMTC) the stimulated right, and non-stimulated left spinotrapezius muscles represented the contracting and resting blood flow measurements, respectively. Vascular conductance (VC) was determined as the ratio of blood flow to MAP using the MAP measured immediately prior to microsphere injection. All rats exhibited <15% difference in blood flow between the right and left kidneys which indicated an adequate mixing of microspheres during the blood flow determinations.

$\dot{V}O_2$ was calculated from blood flow and PO_{2mv} as described previously (6). Arterial O₂ concentration (CaO₂) was calculated directly from arterial blood samples and venous muscle effluent blood O₂ concentration (CvO₂) was estimated from either the baseline (rest) or the contracting steady-state (contractions) PO_{2mv} using the rat dissociation curve (Hill's coefficient of 2.6), the measured hemoglobin (Hb) concentration, a P₅₀ of 38 mmHg, and an O₂ carrying capacity of 1.34 ml O₂/g Hb (1). The measures of the resting and contracting spinotrapezius blood flows were then used to determine $\dot{V}O_2$ via the direct Fick calculation (i.e., $\dot{V}O_2 = \text{blood flow} \times (\text{CaO}_2 - \text{CvO}_2)$).

Measurement of PO_{2mv} and curve-fitting

The principles of the phosphorescence quenching technique have been discussed previously (8). The Stern-Volmer relationship allows the calculation of PO_2mv through the direct measurement of a phosphorescence lifetime via the following equation (46):

$$PO_2mv = [(\tau^\circ / \tau) - 1] / (k_Q \times \tau^\circ)$$

where k_Q is the quenching constant (expressed in $\text{mmHg}^{-1}/\text{s}$) and τ° and τ are the phosphorescence lifetimes in the absence of O_2 and the ambient O_2 concentration, respectively. For R2, k_Q is $409 \text{ mmHg}^{-1}/\text{s}$ and τ° is $601 \mu\text{s}$ (37) and these characteristics do not change over the physiological range of pH and temperature in the rat *in vivo* and, therefore, the phosphorescence lifetime is determined directly by the O_2 pressure (37, 46).

The R2 phosphorescent probe binds to albumin, and consequently, is uniformly distributed throughout the plasma. In rat skeletal muscle albumin has a reflection coefficient of 0.98-0.99 (43, 44) thus limiting its filtration into surrounding tissue. A previous study from our laboratory investigated systematically the compartmentalization of R2 and confirmed that it remains within the microvasculature of exposed muscle over the duration considered in the present experiments, thereby ensuring a valid measurement of PO_2mv (39). The PO_2mv was determined with a PMOD 5000 Frequency Domain Phosphorometer (Oxygen Enterprises, Philadelphia, PA, USA). The common end of the light guide was placed ~2-4 mm superficial to the dorsal surface of the exposed right spinotrapezius muscle. The randomly selected muscle field was comprised principally of capillary blood and PO_2mv was measured continuously and recorded at 2 second intervals throughout the duration of the contraction periods.

For the measured PO_2mv responses, curve-fitting was performed with commercially available software (SigmaPlot 11.2, Systat Software, San Jose, CA, USA) and the data were fit with either a one- or two-component model as described below:

$$\text{One component: } PO_2mv(t) = PO_2mv_{(BL)} - \Delta PO_2mv (1 - e^{-(t - TD)/\tau})$$

$$\text{Two component: } PO_2mv(t) = PO_2mv_{(BL)} - \Delta_1 PO_2mv (1 - e^{-(t - TD_1)/\tau_1}) + \Delta_2 PO_2mv (1 - e^{-(t - TD_2)/\tau_2})$$

where $PO_2mv(t)$ represents the PO_2mv at any given time t , $PO_2mv_{(BL)}$ corresponds to the pre-contracting resting PO_2mv , Δ_1 and Δ_2 are the amplitudes for the first and second component,

respectively, TD_1 and TD_2 are the time delays for each component, and τ_1 and τ_2 are the time constants (i.e., time to 63% of the final response value) for each component. Goodness of fit was determined using the following criteria: 1) the coefficient of determination (r^2), 2) sum of the squared residuals, and 3) visual inspection and analysis of the model fits to the data and the residuals. The mean response time (MRT, time taken to reach 63% of the overall dynamic response) of the kinetics response was calculated for the first component in order to provide an index of the overall principal kinetics response according to the following equation (25, 38):

$$MRT = TD_1 + \tau_1$$

where TD and τ are as described above. The time taken to reach 63% of the final response PO_{2mv} was determined independent of modeling procedures (T_{63}) to ensure appropriateness of the model fits. Specifically, the raw PO_{2mv} data was interpolated and the time coinciding with 63% of the initial amplitude was determined. The delta of the initial PO_{2mv} fall following contractions onset was normalized to τ ($\Delta_1 PO_{2mv} / \tau_1$) to provide an index of the relative rate of fall.

Measurement of muscle force production

Due to differences in the surgical preparation required between measurements of muscle force production and PO_{2mv} , an additional group of rats (n=5) was utilized to determine the effects of SMTC on muscle contractile function. In these animals, the caudal end of the exposed spinotrapezius muscle was exteriorized and sutured to a thin, wire horseshoe manifold attached to a swivel apparatus and a non-distensible light-weight (0.4 g) cable which linked the muscle to a force transducer (model FTO3, Grass Instrument Co., Quincy, MA, USA). The pre-load tension of the muscle was set at ~4-5 g which elicited the muscle's optimum length for twitch force production. Muscle force production was measured throughout control and SMTC contraction bouts which were identical to the contraction protocols described for the measurement of PO_{2mv} .

Control experiments

The reproducibility of spinotrapezius muscle measurements has been addressed previously (10, 24) and was reconfirmed in the present study via time control experiments (n=6). The average coefficient of variation for PO_2mv kinetics parameters and muscle force production was $12\pm 4\%$ with no ordering effects for any parameter ($p > 0.05$ versus zero for all). These data provide confidence that the significant effects detected herein were the direct result of SMTC administration.

Statistical analysis

Data are presented as mean \pm SEM. All comparisons between or among control, SMTC, and L-NAME conditions were made using paired Students *t*-tests or repeated measures ANOVAs (Student-Newman-Keuls post-hoc where appropriate). When a directional hypothesis was tested a one-tail test was performed. The significance level was set at $p < 0.05$.

Results

Blood sampling, hemodynamic variables and ACh injections

There were no differences in arterial blood PO_2 (control: 99.6 ± 1.4 , SMTC: 99.4 ± 1.5 mmHg), O_2 saturation (control: 91.4 ± 0.7 , SMTC: $91.4 \pm 1.4\%$), or pH (control: 7.37 ± 0.01 , SMTC: 7.38 ± 0.01) between conditions ($p > 0.05$ for all). Blood [lactate] was significantly different between control (0.99 ± 0.08 mmol/L) and SMTC (1.12 ± 0.08 mmol/L, $p < 0.05$).

HR and MAP did not change during the control saline infusion; however, MAP increased and HR decreased during the infusion of SMTC. The effects of SMTC on MAP and HR at the end of infusion, at rest immediately prior to contractions onset, and during the contracting steady-state are displayed in Table 1.

The time to 50% recovery of the hypotensive response to ACh injections was not different ($p > 0.05$) between control and SMTC conditions (Figure 4.1). Conversely, the recovery was speeded significantly compared to control and SMTC ($p < 0.05$ for both) following L-NAME administration which is consistent with a lack of effect of SMTC on eNOS.

PO_2mv

Average PO_2mv during control and SMTC infusions are displayed in Figure 4.2. PO_2mv was not different between control and SMTC at the start or during the first 5 min of infusion ($p > 0.05$ for all time points) but was significantly elevated by the end of infusion (6th min) (35.5 ± 2.1 mmHg) versus control (30.7 ± 1.3 mmHg, $p < 0.05$). Average absolute and normalized PO_2mv profiles during contractions are depicted in Figure 4.3 with average kinetics parameters displayed in Table 2. The principal effects of SMTC were to increase the resting baseline PO_2mv and reduce the time delay of the PO_2mv fall which resulted in a speeding of the principal kinetics response (i.e., reduced MRT and T_{63} and increased $\Delta_1 PO_2mv / \tau_1$, $p < 0.05$ between control and SMTC for all). Within control and SMTC conditions there were no differences ($p > 0.05$) between MRT and T_{63} which indicates that modeling procedures did not bias the kinetics analyses. SMTC increased ($p < 0.05$) the amplitude of the PO_2mv fall during contractions such that steady-state PO_2mv was not different ($p > 0.05$) from control. For both control and SMTC conditions the post-contractions PO_2mv recovered to values that were not different ($p > 0.05$ for

both) from their respective pre-contracting values which is consistent with a valid and stable preparation.

Blood flow and $\dot{V}O_2$

Resting and contracting spinotrapezius muscle blood flow and VC are displayed in Figure 4.4. Blood flow at rest was not different ($p>0.05$) whereas VC was significantly lower ($p<0.05$) following SMTC compared to control. During contractions SMTC reduced significantly ($p<0.05$ for both) spinotrapezius muscle blood flow and VC. Delta blood flow and VC between rest and contractions were reduced ($p<0.05$ for both) after SMTC versus control. Resting and contracting spinotrapezius muscle $\dot{V}O_2$ are displayed in Figure 4.5. SMTC reduced spinotrapezius muscle $\dot{V}O_2$ at rest and during contractions as well as the delta $\dot{V}O_2$ between rest and contractions ($p<0.05$ for all).

Muscle force production

Average spinotrapezius muscle force-time integrals are displayed in Figure 4.6. SMTC increased significantly ($p<0.05$) the force-time integral by ~8% in the absence of altered baseline tension. The average steady-state (180 second) force production-to- $\dot{V}O_2$ ratio was increased by ~31% following SMTC (control: 0.21 ± 0.02 , SMTC: 0.27 ± 0.03 g/ μ l/min, $p<0.05$).

Discussion

The present study has identified novel roles for nNOS-derived NO in healthy resting and contracting rat skeletal muscle. Specifically, when compared to control, systemic selective nNOS inhibition via SMTC reduced resting spinotrapezius muscle $\dot{V}O_2$ resulting in an elevated resting baseline PO_{2mv} . During the contracting steady-state spinotrapezius blood flow and $\dot{V}O_2$ were reduced in similar proportion such that PO_{2mv} was not different between control and SMTC. Moreover, blood flow and $\dot{V}O_2$ were reduced during contractions in the presence of an elevated muscle force production thereby increasing the economy ($\text{force}/\dot{V}O_2$) of contractions. The present data unveil that, via marked effects on both metabolic and microvascular control, nNOS-derived NO has an integral role in setting the PO_{2mv} during electrically-induced skeletal muscle contractions. These data are consistent with observations that impaired nNOS-mediated structure and/or function is associated with alterations in the regulation of O_2 delivery, $\dot{V}O_2$ and contractile function and have important implications for the litany of chronic clinical populations where the pathology is associated with reduced NO bioavailability.

Comparison with the literature

Despite the absence of effects on blood flow *per se*, in the present investigation nNOS inhibition with SMTC reduced resting spinotrapezius muscle VC which is generally consistent with observations that nNOS-derived NO regulates resting vascular tone in the human forearm (49), coronary arteries (48), and rat hindlimb muscle (12). However, it is also worth considering that the lack of increase in blood flow in the face of increased muscle perfusion pressure may represent simply an autoregulatory mechanism that maintains O_2 delivery. Upon the initiation of contractions the time delay, and therefore MRT, of the PO_{2mv} fall was reduced indicating that nNOS-derived NO mediates, in part, the rapid dynamic O_2 delivery adjustment and/or limits the rate of $\dot{V}O_2$ increase upon contractions onset (17, 27, 28). Importantly, the faster rate of PO_{2mv} fall observed presently with nNOS inhibition resembles faster on-transient PO_{2mv} responses reported in aged (7, 25) and chronic heart failure (14) rats; conditions which are associated with reduced NO bioavailability. During the contracting steady-state SMTC reduced blood flow and

VC; effects which were not evident when SMTC was administered prior to conscious whole-body treadmill exercise when speed and grade were independent variables (12). It is possible the effects of anesthesia and/or the use of an isolated electrically-induced contractions protocol of a small muscle mass blunted redundant O₂ delivery regulatory mechanisms that were present during conscious exercise. More importantly, it is noteworthy that blood flow was reduced in direct proportion (i.e., both reduced by 17%) such that steady-state PO_{2mv} was similar between conditions. This may be interpreted to suggest that the effects on blood flow were secondary to alterations in metabolic rate and do not indicate specific vascular effects *per se* during contractions. Therefore, the present data qualify and extend our previous findings in conscious rats running on a treadmill by unveiling a role for nNOS-derived NO in the regulation of active skeletal muscle vascular tone in healthy subjects when force production is allowed to change during electrically-induced muscle contractions.

It may also be argued that the reduced blood flow during contractions simply reflects the increased vascular tone at rest limiting the contractions-induced vasodilation. Intriguingly, it has been demonstrated that, in highly oxidative muscles, blood flow during treadmill running is better preserved when L-NAME is infused during rather than prior to exercise (11). Whereas this was not the case for less oxidative muscle fibers in that instance (a category encompassing the spinotrapezius muscle) it should not be discounted that infusion of SMTC during contractions may potentially evoke a different response than observed herein.

In contrast to our hypothesis, SMTC reduced resting and contracting spinotrapezius muscle $\dot{V}O_2$ which contrasts with the reported potential for NO to inhibit cytochrome *c* oxidase in the mitochondrial respiratory chain (9) and observations that non-selective NOS inhibition with L-NAME does not alter resting or contracting steady-state $\dot{V}O_2$ in dogs (22, 31) and humans (17, 27). However, others have reported that L-NAME may attenuate the delta $\dot{V}O_2$ between rest and contractions (22) and steady-state $\dot{V}O_2$ (30) during isolated contractions of the canine hindlimb. Moreover, isolated contracting rat hindlimb $\dot{V}O_2$ was reduced following L-NAME (5, 34) even at matched convective O₂ delivery (34). Our findings extend the observations in rat muscle by identifying that at least a portion of this influence is directly attributable to nNOS-derived NO. Presently, SMTC reduced spinotrapezius $\dot{V}O_2$ at rest despite maintenance of blood flow and, therefore, O₂ delivery, suggesting a stimulatory influence of

NOS-derived NO on mitochondrial function directly. During contractions SMTC reduced $\dot{V}O_2$ in direct proportion to blood flow such that PO_{2mv} was unchanged. This later observation makes interpretations concerning the influence of nNOS-derived NO on mitochondrial function *per se* during contractions challenging. However, given that metabolic demand during contractions is influenced directly by the rate of ATP hydrolysis at the myofibrillar contractile elements, it is important to note that SMTC increased the contracting spinotrapezius muscle force-time integral identifying a contractile-inhibitory influence for nNOS-derived NO likely via alterations of sarcoplasmic reticulum calcium release (41), myofibrillar calcium sensitivity (3), and/or direct myofibrillar protein redox modification (20). Accordingly, we speculate that the economy of contractions (average steady-state force production-to- $\dot{V}O_2$ ratio) was therefore increased through the combination of attenuation of inhibitory effects on muscle force production and stimulatory effects on $\dot{V}O_2$ in the present model. These findings are consistent with observations that non-selective NOS inhibition reduces the O₂ cost of tension development in the contracting rat (5, 34) and dog (30) hindlimb and implicates specifically nNOS-derived NO as a principal mediator.

Efficacy of selective nNOS inhibition

Despite the obvious scientific utility of genetically-altered nNOS knockout models, we chose to utilize acute selective nNOS inhibition to examine the role of nNOS-mediated function in healthy rats where there is no opportunity for chronic compensation of nNOS absence. Thus, the efficacy of the selected SMTC dose (0.56 mg/kg or 2.1 μ mol/kg) to inhibit nNOS without affecting eNOS-mediated function is crucial. Several points support that this was successfully accomplished: 1) SMTC did not alter the hypotensive response to ACh injections whereas it was blunted (i.e., faster time to 50% recovery) after L-NAME (a non-selective inhibitor of nNOS and eNOS) which is consistent with previous reports from our laboratory in conscious rats (12). 2) The dose used presently is similar to other studies reporting selective nNOS inhibition with SMTC in rats *in vivo* (i.e., 0.5 mg/kg; 33, 0.3 mg/kg; 54). 3) The modest SMTC-induced MAP increases observed presently are substantially lower than those observed when L-NAME is administered following SMTC in these same rats where values may reach >150 mmHg (authors' unpublished observations). While we are confident that the present data reflect selective nNOS inhibition (i.e., eNOS inhibition was absent), it must also be considered that it is presently

impossible to determine if nNOS was fully inhibited. Thus the present results may actually represent an underestimation of the full contribution of nNOS in modulating microvascular function.

Experimental considerations

Stimulation paradigm: During voluntary muscle contractions the magnitude of the hyperemia reflects the competition between enhanced neural vasoconstrictor tone (50, which may be offset by sympatholysis in active muscle; 42) and contractions-mediated vasodilation as well as mechanical factors relating to muscle pumping action. The stimulation paradigm used herein was selected based upon its ability to: 1. Provide reproducible contraction bouts without fatigue. 2. Induce hyperemic response kinetics at the capillary level (29) that match those observed across muscles performing voluntary exercise (47). 3. Reproduce the proportional matching of blood flow and O₂ delivery to $\dot{V}O_2$ as that present in animal and human muscles during voluntary exercise (16, 40). The 2 ms pulse duration employed herein is expected to activate sympathetic perivascular nerves concomitant with inducing muscle fiber contraction, and, as such may help re-create the vasoconstriction/vasodilation competition found *in vivo*. That conditions 2 and 3 above are satisfied may reflect either a fortuitous/coincidental outcome or, more likely, that essential control features of the *in vivo* response are preserved despite the electrical stimulation necessary to evoke muscle contractions.

Systemic versus local SMTC application: The mandate to demonstrate selectivity of nNOS blockade (as opposed to eNOS) precluded local application (i.e., superfusion) of SMTC. Specifically, for any superfused preparation the rapid ACh infusion test, utilized herein to provide confidence that eNOS had not been blocked, is not valid. Thus, whereas it must be acknowledged that the protocol used presently does not provide a rigorous discrimination between systemic versus local effects in all respects: there was clear evidence of nNOS selectivity (Figure 4.1). Insofar as contractile force and the ability to match O₂ delivery with $\dot{V}O_2$ are regulated by local events there can be confidence that SMTC-induced nNOS blockade within the muscle is responsible for the effects observed (i.e., increased tension and altered PO_{2mv} at rest). However, in the contracting muscle where both blood flow and $\dot{V}O_2$ were decreased, such that PO_{2mv} was unaltered, more proximal (central) effects of SMTC on blood pressure regulation and possibly the neural regulation of vascular conductance including sympatholysis

cannot be discounted. Given this situation it is intriguing that, although O_2 delivery and $\dot{V}O_2$ were both altered, their proportionality (as evidenced by the constancy of PO_{2mv}) during contractions (but not at rest) was unperturbed.

Conclusions

The present investigation has identified that nNOS-derived NO sets the O_2 delivery/utilization balance (i.e., PO_{2mv}) during contractions under the specific experimental conditions used presently via mirrored effects on metabolic ($\dot{V}O_2$) and vascular (blood flow and VC) control. Specifically, during electrically-induced twitch contractions when force output is allowed to change, nNOS inhibition reduced blood flow in proportion to $\dot{V}O_2$ such that the steady-state PO_{2mv} was unaltered compared to the control condition. These effects may be masked during conscious whole-body treadmill exercise when force output or work is a set independent variable (12). In the present investigation force output was increased which, in conjunction with the SMTC-induced $\dot{V}O_2$ reduction, increased the economy of muscle contractions. The present novel findings in healthy skeletal muscle further identify nNOS as a potential target for physiological and possibly pathological modulation of systemic hemodynamics as well as muscle metabolic and microvascular function. These data carry important implications suggesting that future therapeutic interventions targeting nNOS may be successful in alleviating dysfunction in populations where the pathology is associated with reduced NO bioavailability.

Table 4.1. Effects of nNOS inhibition on HR and MAP

	Control	SMTC
<u>End-infusion</u>		
HR (bpm)	345±9	330±7*
MAP (mmHg)	113±6	130±7*
<u>Rest (pre-contractions)</u>		
HR (bpm)	339±11	319±7*
MAP (mmHg)	111±6	135±6*
<u>Contractions (steady-state)</u>		
HR (bpm)	340±11	323±9*
MAP (mmHg)	112±6	134±6*

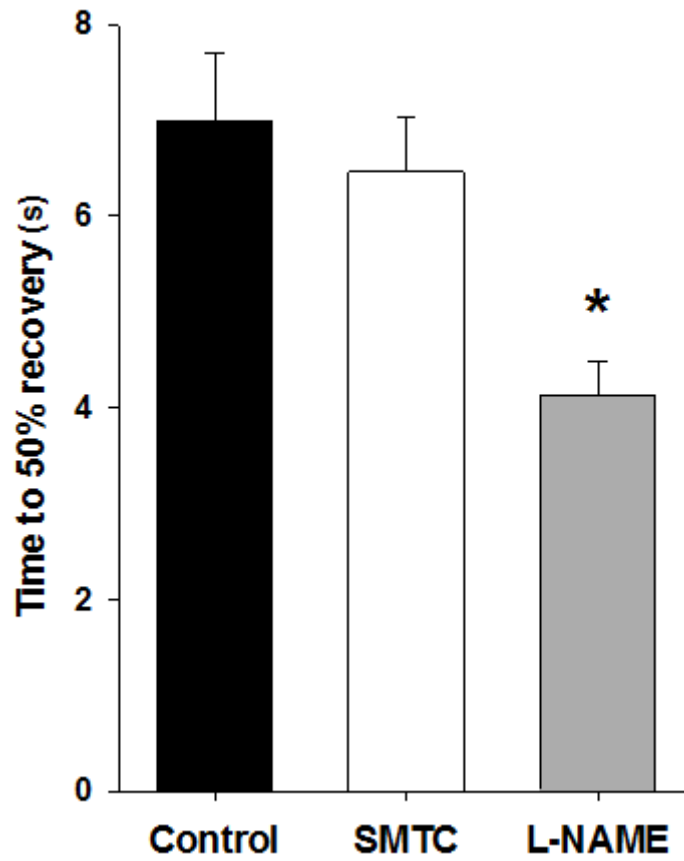
HR and MAP at rest prior to and during the steady-state of electrically-induced muscle contractions before (control) and after selective nNOS inhibition with SMTC. Values are mean±SEM, * $p < 0.05$ versus control. Within each condition there were no differences among end-infusion, rest, or contractions HR and MAP.

Table 4.2. Effects of nNOS inhibition on contracting skeletal muscle PO_2mv parameters

	Control	SMTC
$PO_2mv_{(BL)}$, mmHg	31.2±1.6	37.1±2.0*
Δ_1PO_2mv , mmHg	10.2±0.4	14.7±1.4*
Δ_2PO_2mv , mmHg	1.9±0.6	-
$\Delta_{total}PO_2mv$, mmHg	8.4±0.4	14.4±1.5*
$PO_2mv_{(steady-state)}$, mmHg	22.8±1.6	22.7±2.1
TD₁ , s	8.2±0.8	5.1±0.6*
TD₂ , s	27.8±4.4	-
τ_1 , s	14.3±1.4	11.7±1.5
τ_2 , s	29.7±1.4	-
MRT , s	22.5±1.6	16.9±1.4*
T₆₃ , s	21.1±1.8	17.3±1.6*
Δ_1PO_2mv/τ_1 , mmHg/s	0.8±0.1	1.6±0.3*

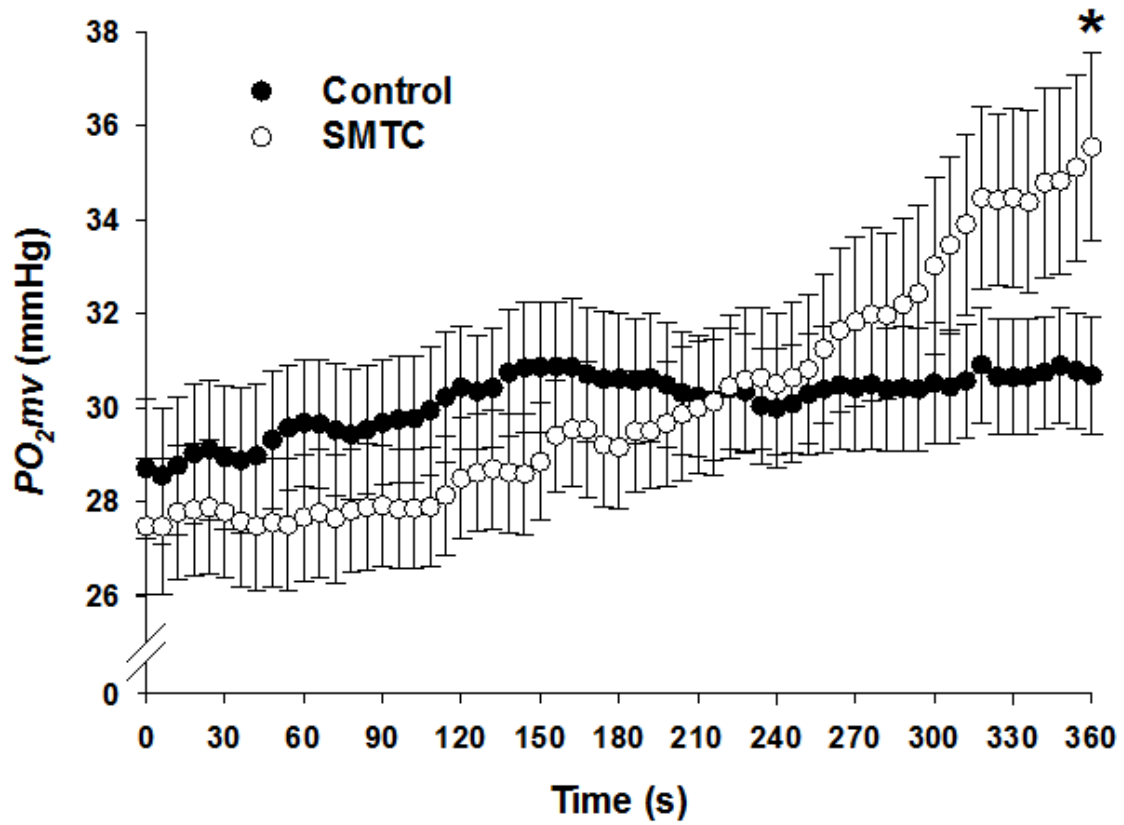
Microvascular partial pressure of O₂ (PO_2mv) kinetics parameters during contractions before (control) and after selective nNOS inhibition with SMTC. Values are mean±SEM. $PO_2mv_{(BL)}$, pre-contracting PO_2mv ; Δ_1PO_2mv , amplitude of the first component; Δ_2PO_2mv , amplitude of the second component; $\Delta_{total}PO_2mv$; overall amplitude regardless of one- or two-component model fit; $PO_2mv_{(steady-state)}$, contracting steady-state PO_2mv ; TD₁, time delay for the first component; TD₂, time delay for the second component; τ_1 , time constant for the first component; τ_2 , time constant for the second component; MRT, mean response time describing the overall kinetics response; T₆₃, time to reach 63% of the overall response determined independent of modeling procedures; Δ_1PO_2mv/τ_1 , parameter describing the relative rate of PO_2mv fall. * $p<0.05$ versus control.

Figure 4.1. Effects SMTC and L-NAME on the hypotensive response to ACh



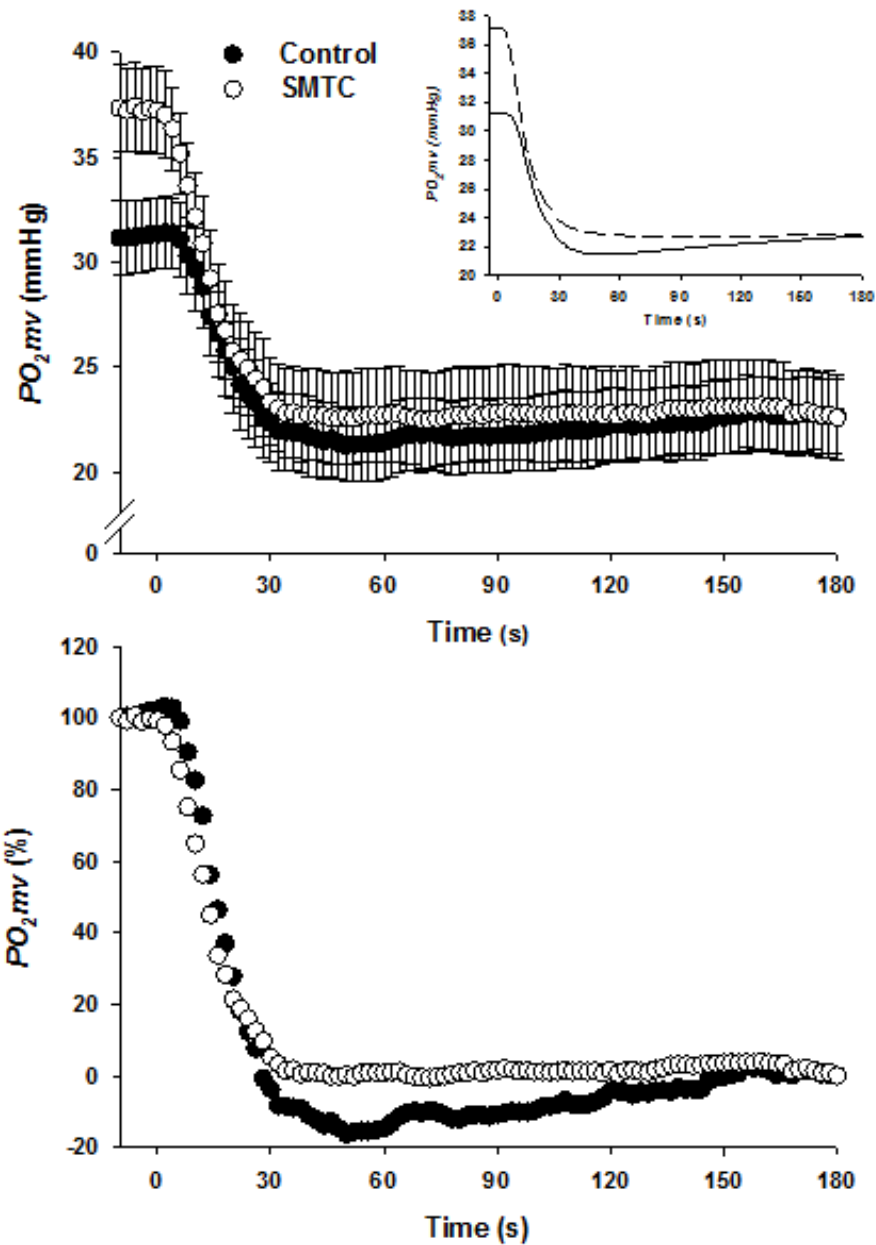
Effects of SMTC (0.56 mg/kg) and L-NAME (10 mg/kg) on the time to 50% recovery of the hypotensive response to ACh injections. * $p < 0.05$ versus control and SMTC.

Figure 4.2. Effects of SMTC infusion on PO_2mv



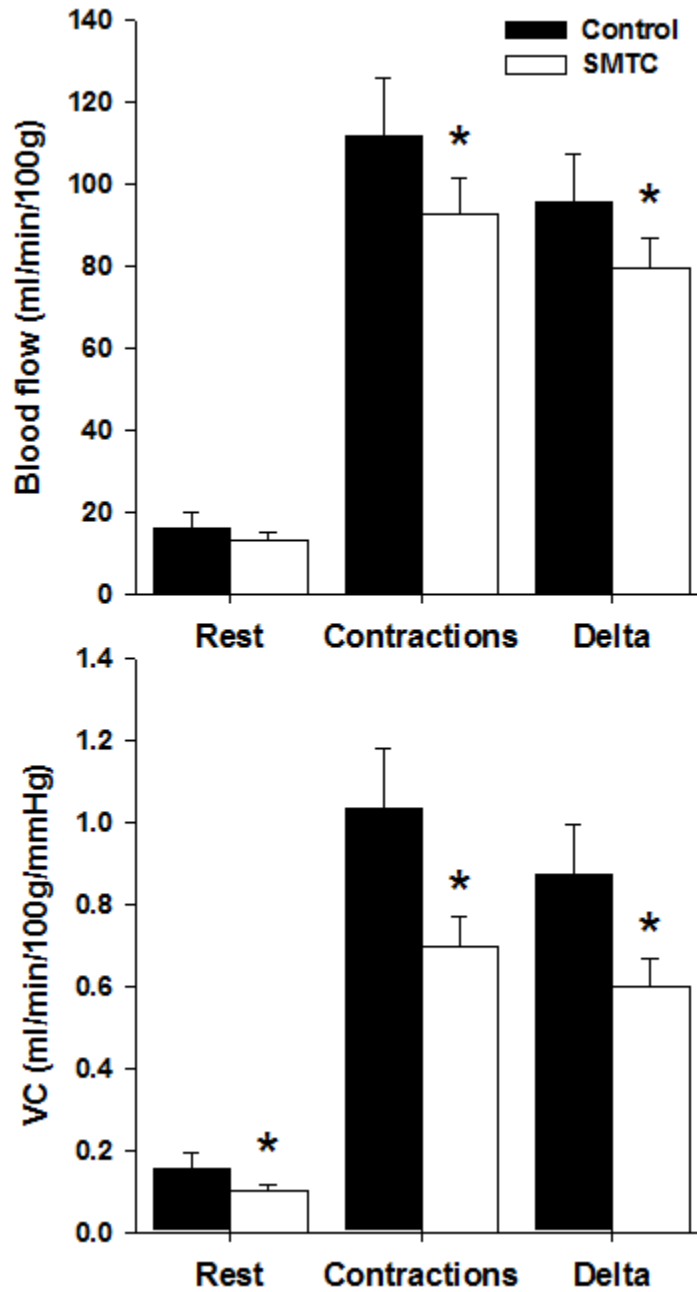
Average PO_2mv during infusion for control and SMTC (0.56 mg/kg) conditions. * $p < 0.05$ versus control for end-infusion PO_2mv . Time “0” depicts initiation of saline (control) or SMTC infusion. 6 second averages are shown.

Figure 4.3. Effects of nNOS inhibition on contracting muscle PO_2mv



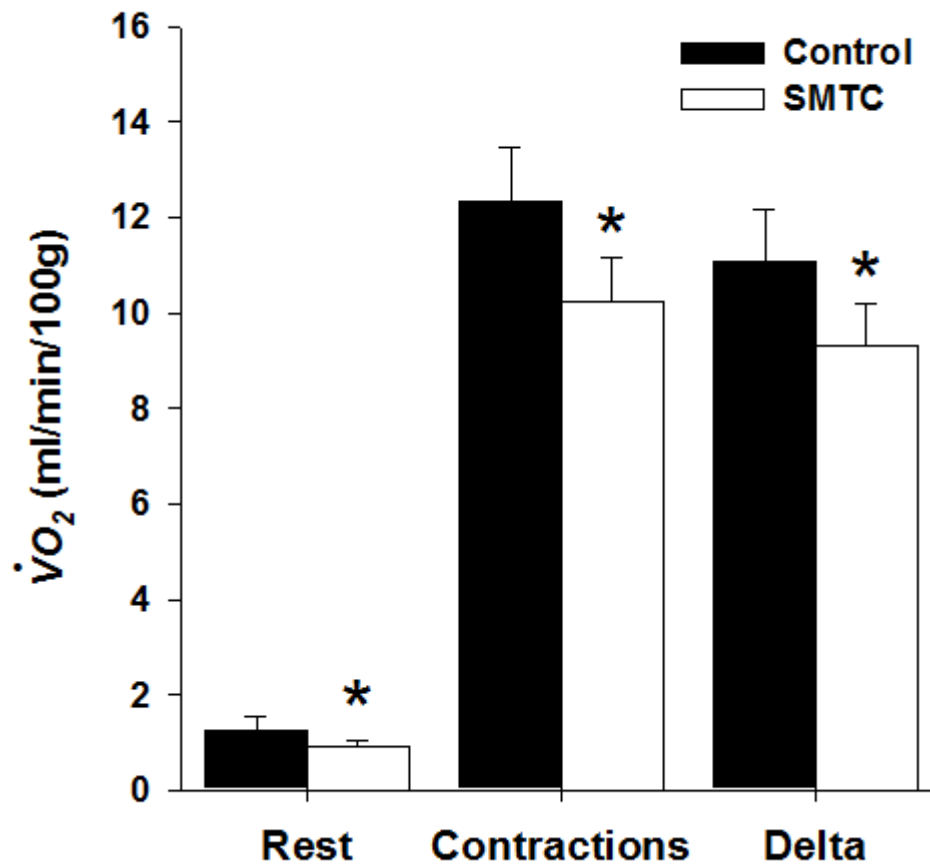
Average absolute (top panel) and normalized (bottom panel) PO_2mv profiles during contractions for control and SMTC (0.56 mg/kg) conditions. The inset shows the average model fits for control (solid line) and SMTC (dashed line) conditions. Time “0” depicts onset of contractions.

Figure 4.4. Effects of nNOS inhibition on spinotrapezius muscle blood flow and VC



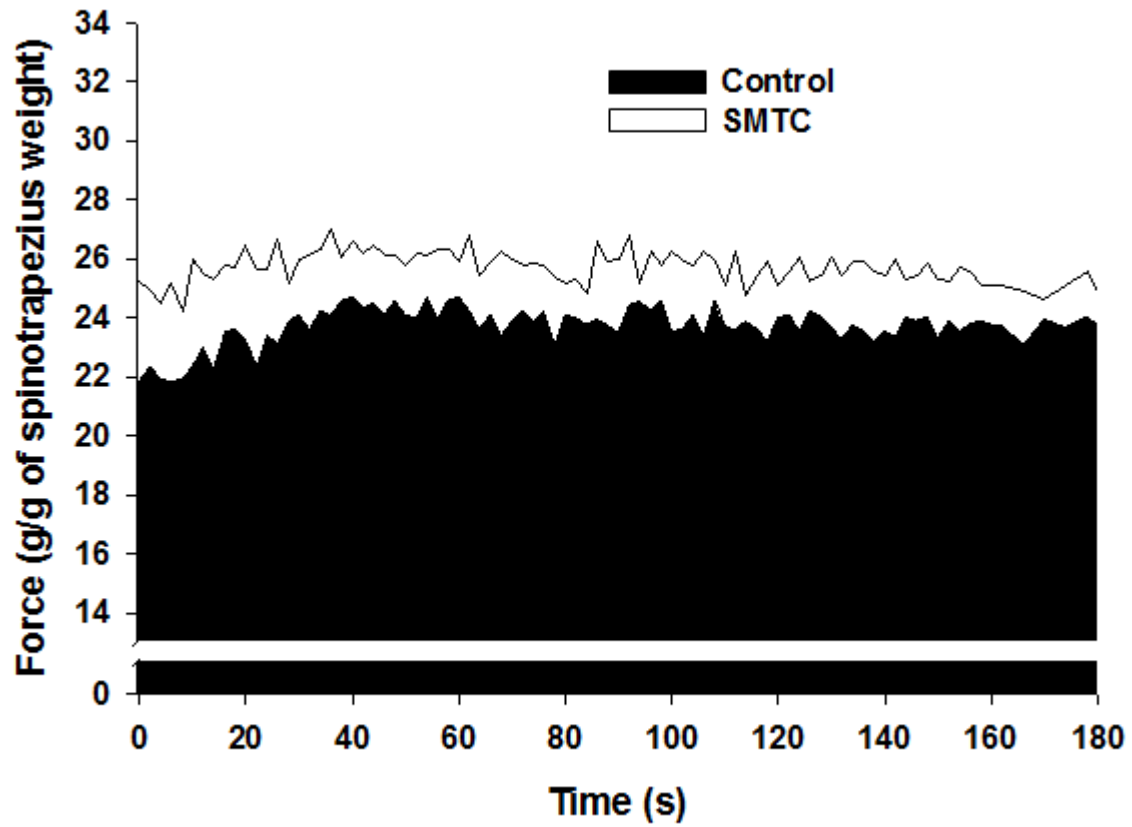
Effects of SMTC (0.56 mg/kg) on spinotrapezius muscle blood flow (top panel) and vascular conductance (VC, bottom panel) at rest and during contractions. * $p < 0.05$ versus control.

Figure 4.5. Effects of nNOS inhibition on spinotrapezius muscle $\dot{V}O_2$



Effects of SMTC (0.56 mg/kg) on spinotrapezius muscle O_2 consumption ($\dot{V}O_2$) at rest and during contractions. * $p < 0.05$ versus control.

Figure 4.6. Effects of nNOS inhibition on spinotrapezius muscle force production



Effects of SMTC (0.56 mg/kg) on spinotrapezius muscle force production. The force-time integral was increased significantly ($p < 0.05$) after SMTC versus control.

References

1. **Altman P and Dittmer D.** Biological Data Book (2nd ed.) Bethesda, MD: FASEB, 1974.
2. **Anderson TJ.** Nitric oxide, atherosclerosis and the clinical relevance of endothelial dysfunction. *Heart Failure Reviews* 8: 71-86, 2003.
3. **Andrade FH, Reid MB, Allen DG, and Westerblad H.** Effect of nitric oxide on single skeletal muscle fibres from the mouse. *J Physiol* 509 (Pt 2): 577-586, 1998.
4. **Bailey JK, Kindig CA, Behnke BJ, Musch TI, Schmid-Schoenbein GW, and Poole DC.** Spinotrapezius muscle microcirculatory function: effects of surgical exteriorization. *Am J Physiol Heart Circ Physiol* 279: H3131-3137, 2000.
5. **Baker DJ, Krause DJ, Howlett RA, and Hepple RT.** Nitric oxide synthase inhibition reduces O₂ cost of force development and spares high-energy phosphates following contractions in pump-perfused rat hindlimb muscles. *Exp Physiol* 91: 581-589, 2006.
6. **Behnke BJ, Barstow TJ, Kindig CA, McDonough P, Musch TI, and Poole DC.** Dynamics of oxygen uptake following exercise onset in rat skeletal muscle. *Respir Physiol Neurobiol* 133: 229-239, 2002.
7. **Behnke BJ, Delp MD, Dougherty PJ, Musch TI, and Poole DC.** Effects of aging on microvascular oxygen pressures in rat skeletal muscle. *Respir Physiol Neurobiol* 146: 259-268, 2005.
8. **Behnke BJ, Kindig CA, Musch TI, Koga S, and Poole DC.** Dynamics of microvascular oxygen pressure across the rest-exercise transition in rat skeletal muscle. *Respir Physiol* 126: 53-63, 2001.
9. **Brown GC.** Nitric oxide regulates mitochondrial respiration and cell functions by inhibiting cytochrome oxidase. *FEBS Lett* 369: 136-139, 1995.
10. **Copp SW, Ferreira LF, Herspring KF, Hirai DM, Snyder BS, Poole DC, and Musch TI.** The effects of antioxidants on microvascular oxygenation and blood flow in skeletal muscle of young rats. *Exp Physiol* 94: 961-971, 2009.

11. **Copp SW, Hirai DM, Hageman KS, Poole DC, and Musch TI.** Nitric oxide synthase inhibition during treadmill exercise reveals fiber-type specific vascular control in the rat hindlimb. *Am J Physiol Regul Inter Comp Physiol* 298: R478-85, 2010.
12. **Copp SW, Hirai DM, Schwagerl PJ, Musch TI, and Poole DC.** Effects of neuronal nitric oxide synthase inhibition on resting and exercising hindlimb muscle blood flow in the rat. *J Physiol* 588: 1321-1331, 2010.
13. **Delp MD and Duan C.** Composition and size of type I, IIA, IID/X, and IIB fibers and citrate synthase activity of rat muscle. *J Appl Physiol* 80: 261-270, 1996.
14. **Diederich ER, Behnke BJ, McDonough P, Kindig CA, Barstow TJ, Poole DC, and Musch TI.** Dynamics of microvascular oxygen partial pressure in contracting skeletal muscle of rats with chronic heart failure. *Cardiovasc Res* 56: 479-486, 2002.
15. **Fadel PJ, Zhao W, and Thomas GD.** Impaired vasomodulation is associated with reduced neuronal nitric oxide synthase in skeletal muscle of ovariectomized rats. *J Physiol* 549: 243-253, 2003.
16. **Ferreira LF, McDonough P, Behnke BJ, Musch TI, and Poole DC.** Blood flow and O₂ extraction as a function of O₂ uptake in muscles composed of different fiber types. *Respir Physiol Neurobiol* 153: 237-249, 2006.
17. **Ferreira LF, Padilla DJ, Williams J, Hageman KS, Musch TI, and Poole DC.** Effects of altered nitric oxide availability on rat muscle microvascular oxygenation during contractions. *Acta Physiol* 186: 223-232, 2006.
18. **Frandsen U, Bangsbo J, Sander M, Hoffner L, Betak A, Saltin B, and Hellsten Y.** Exercise-induced hyperaemia and leg oxygen uptake are not altered during effective inhibition of nitric oxide synthase with N^G-nitro-L-arginine methyl ester in humans. *J Physiol* 531: 257-264, 2001.
19. **Furfine ES, Harmon MF, Paith JE, Knowles RG, Salter M, Kiff RJ, Duffy C, Hazelwood R, Oplinger JA, and Garvey EP.** Potent and selective inhibition of human nitric oxide synthases. Selective inhibition of neuronal nitric oxide synthase by S-methyl-L-thiocitrulline and S-ethyl-L-thiocitrulline. *J Biol Chem* 269: 26677-26683, 1994.
20. **Galler S, Hilber K, and Gobesberger A.** Force-generating proteins of skeletal muscle. *Pflugers Arch* 434: 242-245, 1997.

21. **Grange RW, Isotani E, Lau KS, Kamm KE, Huang PL, and Stull JT.** Nitric oxide contributes to vascular smooth muscle relaxation in contracting fast-twitch muscles. *Physiol Genomics* 5: 35-44, 2001.
22. **Grassi B, Hogan MC, Kelley KM, Howlett RA, and Gladden LB.** Effects of nitric oxide synthase inhibition by L-NAME on oxygen uptake kinetics in isolated canine muscle in situ. *J Physiol* 568: 1021-1033, 2005.
23. **Hansen J, Sander M, and Thomas GD.** Metabolic modulation of sympathetic vasoconstriction in exercising skeletal muscle. *Acta Physiol Scand* 168: 489-503, 2000.
24. **Herspring KF, Ferreira LF, Copp SW, Snyder BS, Poole DC, and Musch TI.** Effects of antioxidants on contracting spinotrapezius muscle microvascular oxygenation and blood flow in aged rats. *J Appl Physiol* 105: 1889-1896, 2008.
25. **Hirai DM, Copp SW, Herspring KF, Ferreira LF, Poole DC, and Musch TI.** Aging impacts microvascular oxygen pressures during recovery from contractions in rat skeletal muscle. *Respir Physiol Neurobiol* 169: 315-322, 2009.
26. **Ishise S, Pegram BL, Yamamoto J, Kitamura Y, and Frohlich ED.** Reference sample microsphere method: cardiac output and blood flows in conscious rat. *Am J Physiol* 239: H443-H449, 1980.
27. **Jones AM, Wilkerson DP, Koppo K, Wilmshurst S, and Campbell IT.** Inhibition of nitric oxide synthase by L-NAME speeds phase II pulmonary VO_2 kinetics in the transition to moderate-intensity exercise in man. *J Physiol* 552: 265-272, 2003.
28. **Kindig CA, McDonough P, Erickson HH, and Poole DC.** Nitric oxide synthase inhibition speeds oxygen uptake kinetics in horses during moderate domain running. *Respir Physiol Neurobiol* 132: 169-178, 2002.
29. **Kindig CA, Richardson TE, and Poole DC.** Skeletal muscle capillary hemodynamics from rest to contractions: implications for oxygen transfer. *J Appl Physiol* 92: 2513-2520, 2002.
30. **King-VanVlack CE, Mewburn JD, Chapler CK, and MacDonald PH.** Endothelial modulation of skeletal muscle blood flow and VO_2 during low- and high-intensity contractions. *J Appl Physiol* 92: 461-468, 2002.

31. **King CE, Melinyshyn MJ, Mewburn JD, Curtis SE, Winn MJ, Cain SM, and Chapler CK.** Canine hindlimb blood flow and O₂ uptake after inhibition of EDRF/NO synthesis. *J Appl Physiol* 76: 1166-1171, 1994.
32. **Kobayashi YM, Rader EP, Crawford RW, Iyengar NK, Thedens DR, Faulkner JA, Parikh SV, Weiss RM, Chamberlain JS, Moore SA, and Campbell KP.** Sarcolemma-localized nNOS is required to maintain activity after mild exercise. *Nature* 456: 511-515, 2008.
33. **Komers R, Oyama TT, Chapman JG, Allison KM, and Anderson S.** Effects of systemic inhibition of neuronal nitric oxide synthase in diabetic rats. *Hypertension* 35: 655-661, 2000.
34. **Krause DJ, Hagen JL, Kindig CA, and Hepple RT.** Nitric oxide synthase inhibition reduces the O₂ cost of force development in rat hindlimb muscles pump perfused at matched convective O₂ delivery. *Exp Physiol* 90: 889-900, 2005.
35. **Lai Y, Thomas GD, Yue Y, Yang HT, Li D, Long C, Judge L, Bostick B, Chamberlain JS, Terjung RL, and Duan D.** Dystrophins carrying spectrin-like repeats 16 and 17 anchor nNOS to the sarcolemma and enhance exercise performance in a mouse model of muscular dystrophy. *J Clin Invest* 119: 624-635, 2009.
36. **Leek BT, Mudaliar SR, Henry R, Mathieu-Costello O, and Richardson RS.** Effect of acute exercise on citrate synthase activity in untrained and trained human skeletal muscle. *Am J Physiol Regul Integr Comp Physiol* 280: R441-447, 2001.
37. **Lo LW, Vinogradov SA, Koch CJ, and Wilson DF.** A new, water soluble, phosphor for oxygen measurements in vivo. *Adv Exp Med Biol* 428: 651-656, 1997.
38. **Macdonald M, Pedersen PK, and Hughson RL.** Acceleration of VO₂ kinetics in heavy submaximal exercise by hyperoxia and prior high-intensity exercise. *J Appl Physiol* 83: 1318-1325, 1997.
39. **Poole DC, Behnke BJ, McDonough P, McAllister RM, and Wilson DF.** Measurement of muscle microvascular oxygen pressures: compartmentalization of phosphorescent probe. *Microcirculation* 11: 317-326, 2004.
40. **Poole DC, Copp SW, Hirai DM, and Musch TI.** Dynamics of muscle microcirculatory blood-myocyte O₂ flux during contractions. *Acta Physiol* 202(3): 292-310, 2011.

41. **Pouvreau S and Jacquemond V.** Nitric oxide synthase inhibition affects sarcoplasmic reticulum Ca²⁺ release in skeletal muscle fibres from mouse. *J Physiol* 567: 815-828, 2005.
42. **Remensnyder JP, Mitchell JH, and Sarnoff SJ.** Functional sympatholysis during muscular activity. Observations on influence of carotid sinus on oxygen uptake. *Circ Res* 11: 370-380, 1962.
43. **Renkin EM.** Relation of capillary morphology to transport of fluid and large molecules: a review. *Acta Physiol Scand (Suppl)* 463: 81-91, 1979.
44. **Renkin EM and Tucker VL.** Measurements of microvascular transport parameters of macromolecules in tissues and organs of intact animals. *Microcirculation* 5: 139-152, 1998.
45. **Reid MB, Kobzik L, Brecht DS, and Stamler JS.** Nitric oxide modulates excitation-contraction coupling in the diaphragm. *Comp Biochem Physiol A Mol Integr Physiol* 119: 211-218, 1998.
46. **Rumsey WL, Vanderkooi JM, and Wilson DF.** Imaging of phosphorescence: a novel method for measuring oxygen distribution in perfused tissue. *Science* 241: 1649-1651, 1988.
47. **Saunders NR, and Tschakovsky ME.** Evidence for a rapid vasodilatory contribution to immediate hyperemia in rest-to-mild and mild-to-moderate forearm exercise transitions in humans. *J Appl Physiol* 97: 1143-51, 2004.
48. **Seddon M, Melikian N, Dworakowski R, Shabeeh H, Jiang B, Byrne J, Casadei B, Chowienczyk P, and Shah AM.** Effects of neuronal nitric oxide synthase on human coronary artery diameter and blood flow in vivo. *Circulation* 119: 2656-2662, 2009.
49. **Seddon MD, Chowienczyk PJ, Brett SE, Casadei B, and Shah AM.** Neuronal nitric oxide synthase regulates basal microvascular tone in humans in vivo. *Circulation* 117: 1991-1996, 2008.
50. **Somers VK, Leo KC, Shields R, Clary M, and Mark AL.** Forearm endurance training attenuates sympathetic nerve response to isometric handgrip in normal humans. *J Appl Physiol* 72: 1039-1043, 1992.

51. **Thomas GD, Sander M, Lau KS, Huang PL, Stull JT, and Victor RG.** Impaired metabolic modulation of alpha-adrenergic vasoconstriction in dystrophin-deficient skeletal muscle. *Proc Natl Acad Sci USA* 95: 15090-15095, 1998.
52. **Thomas GD, Shaul PW, Yuhanna IS, Froehner SC, and Adams ME.** Vasomodulation by skeletal muscle-derived nitric oxide requires alpha-syntrophin-mediated sarcolemmal localization of neuronal Nitric oxide synthase. *Circ Res* 92: 554-560, 2003.
53. **Villanueva C and Giulivi C.** Subcellular and cellular locations of nitric oxide synthase isoforms as determinants of health and disease. *Free Radic Biol Med* 49: 307-316, 2010.
54. **Wakefield ID, March JE, Kemp PA, Valentin JP, Bennett T, and Gardiner SM.** Comparative regional haemodynamic effects of the nitric oxide synthase inhibitors, S-methyl-L-thiocitrulline and L-NAME, in conscious rats. *Br J Pharmacol* 139: 1235-1243, 2003.

Chapter 5 - Neuronal nitric oxide synthase inhibition and regional sympathetic nerve discharge: implications for peripheral vascular control

Summary

Neuronal nitric oxide (NO) synthase (nNOS) inhibition with systemically-administered S-methyl-L-thiocitrulline (SMTC) elevates mean arterial pressure (MAP) and reduces rat hindlimb skeletal muscle and renal blood flow. We tested the hypothesis that those SMTC-induced cardiovascular effects resulted, in part, from increased sympathetic nerve discharge (SND). MAP, HR, and lumbar and renal SND (direct nerve recordings) were measured in 9 baroreceptor (sino-aortic)-denervated rats for 20 minutes each following both saline and SMTC (0.56 mg/kg i.v.). SMTC increased MAP (peak Δ MAP: 50 ± 8 mmHg, $p < 0.01$) compared to saline. Lumbar and renal SND were not different between saline and SMTC conditions at any time ($p > 0.05$). The Δ SND between saline and SMTC conditions for the lumbar and renal nerves were not different from zero (peak Δ SND, lumbar: $2.0 \pm 6.8\%$; renal: $9.7 \pm 9.0\%$, $p > 0.05$ versus zero for both). These data support that SMTC-induced reductions in skeletal muscle and renal blood flow reported previously reflect peripheral nNOS-derived NO vascular control as opposed to increased sympathetic vasoconstriction.

Introduction

Nitric oxide (NO) is an important biological signaling molecule that exerts profound cardiovascular influences. In healthy subjects NO is produced from two distinct constitutively expressed NO synthase (NOS) isoforms: endothelial NOS (eNOS) and neuronal NOS (nNOS). Since the identification of endothelial-derived relaxing factor as NO (14), NO-mediated peripheral vascular modulation is often attributed to eNOS (6, 19). However, studies utilizing mice lacking nNOS (7, 22, 23) and acute pharmacological selective nNOS inhibition (13, 15) have unveiled novel cardiovascular roles specifically for nNOS-derived NO. For example, nNOS-derived NO regulates mean arterial blood pressure (MAP; 12, 16, 25) via central modulation of sympathetic outflow (1) and basal (5, 20) and contracting skeletal muscle (4, 22) vascular control.

Although a variety of nNOS inhibitors are available (15), S-methyl-L-thiocitrulline (SMTC) is a particularly potent and selective nNOS inhibitor *in vitro* and *in vivo* (8, 16, 25). nNOS inhibition via systemically-administered SMTC in rats evokes global hemodynamic effects including elevations in MAP and reductions in heart rate (HR; 4, 5, 25) consequent, at least in part, to peripheral vasoconstriction as evidenced by reductions in hindlimb skeletal muscle and renal blood flow and vascular conductance (VC; 3, 5, 12, 25). It is unknown, however, whether the SMTC-induced hindlimb skeletal muscle and renal vasoconstriction are mediated via alterations in regional sympathetic outflow and increases in lumbar and renal sympathetic nerve discharge (SND), respectively, or, alternatively, reflect peripheral nNOS-derived NO modulation of vascular tone. Moreover, SMTC-induced MAP elevations and concurrent reductions in HR (4, 5, 25) suggest that the baroreflex may mask full expression of the nNOS-derived NO arterial blood pressure and vascular control signals. These are crucial issues to address in order to enhance our understanding of the specific contribution of nNOS-derived NO to cardiovascular control and peripheral vascular regulation.

The purpose of the present investigation was to examine whether selective nNOS inhibition with systemic SMTC administration impacts regional SND. We tested the specific hypothesis that systemically-administered SMTC in baroreceptor-denervated rats would elevate MAP consequent, at least in part, to increased lumbar and renal SND.

Methods

Animal care and experimental approval

Nine young adult (4-5 months old, 412 ± 23 g) male Sprague-Dawley rats (Charles River Laboratories, Wilmington, MA, USA) were utilized in the present investigation. Rats were housed 2 per cage in accredited facilities on a 12:12 hour light/dark cycle with standard rat chow and water provided *ad libitum*. All experimental procedures were approved by the Institutional Animal Care and Use Committee of Kansas State University and conducted according to National Institute of Health guidelines.

Surgical preparation

Anesthesia was induced by isoflurane (3–5%) and maintained during surgical procedures using isoflurane (1.25–1.75%), α -chloralose (80 mg/kg i.p.), and urethane (800 mg/kg i.p.). Catheters (PE-50) were placed in the femoral vein and femoral artery. Maintenance doses of α -chloralose (35–45 mg/kg/hr) were administered intravenously, whereas maintenance doses of urethane (200 mg/kg every 4 h) were administered intraperitoneally. The trachea was cannulated and rats were artificially ventilated. Femoral arterial pressure was monitored using a pressure transducer connected to a blood pressure analyzer. HR was derived from the pulsatile arterial pressure output of the blood pressure analyzer. Core temperature was measured with a rectal thermistor probe and maintained at ~ 37 – 38°C during surgical interventions by a temperature-controlled table. Adequacy of anesthesia was indicated by an inability of mechanical stimulation of the hindlimb or tail to increase SND or MAP.

To eliminate baroreceptor-mediated afferent feedback that can alter central SND responses, experiments were conducted in baroreceptor (sino-aortic)-denervated (SAD) rats. Bilateral denervation of the aortic arch was completed by cutting the superior laryngeal nerve near its junction with the vagus nerve and removal of the superior cervical ganglion. Bilateral carotid sinus denervation was completed by removal of the adventitia from the area of the carotid sinus bifurcation. SADs were completed 3–4 hours before initiation of experimental protocols. The coherence function relating arterial pressure to SND was used to demonstrate the efficacy of the denervation procedure (11). Coherence analysis provides a measure of the strength of linear

correlation of two signals as a function of frequency. The lack of coherence between arterial pressure and SND at the frequency of the HR demonstrated a complete SAD (11).

The left renal nerve was isolated retroperitoneally whereas the left lumbar nerve was isolated from a midline approach. Nerve-electrode preparations were covered with silicone gel to prevent exposure to room air. SND was measured and recorded biphasically with a platinum bipolar electrode after capacity-coupled preamplification (bandpass 30-3,000 Hz) from the central end of cut or distally crushed lumbar or renal nerves. Filtered neurograms were routed to an oscilloscope and a nerve traffic analyzer, where sympathetic nerve potentials were full-wave rectified and integrated (10-ms time constant). Total power in lumbar and renal SND was quantified as microvolts \times seconds ($\mu\text{V}\cdot\text{s}$) and SND recordings were corrected for background noise after administration of the ganglionic blocker chlorisondamine (5 mg/kg iv). Technical complications precluded renal SND recordings in 2 rats (final sample size for lumbar SND: $n=9$, renal SND: $n=7$). *A priori* power analysis based on previously published data reporting the effects of non-selective NOS inhibition on lumbar and renal SND (10) indicated that a sample size of 6 was required for a statistical power >0.8 .

Experimental protocol

Anesthetized rats were allowed to stabilize for 60 minutes before initiation of the experimental protocol. Following stabilization, MAP, HR, and lumbar and renal SND were measured and recorded for an ~10-15 minute period where baseline values were determined from the average of the final ~60 seconds (baseline values are represented as time “zero” in Figures 5.2 and 5.3). Rats were then administered, in random order, SMTC (0.56 mg/kg dissolved in 0.5 ml heparanized saline; Sigma-Aldrich, St. Louis, MO, USA) or saline (0.5 ml) into the femoral vein catheter and MAP, HR and lumbar and renal SND were measured and recorded continuously for 20 minutes following each infusion. Following the initial infusion and 20 minute measurement period baseline values were determined as described above following a second ~5 minute stabilization period. SMTC is a highly selective inhibitor of nNOS versus eNOS both *in vitro* and *in vivo* (8, 16, 25) and this SMTC dose has been utilized recently in our laboratory to assess nNOS-mediated cardiovascular and skeletal muscle function in healthy (4, 5), heart failure (3), and senescent (9) rats (see *Experimental considerations* for further details regarding efficacy and selectivity of nNOS inhibition with SMTC). In one rat, a short bout of

combined hypoxia and hypercapnia (i.e., shutting off the mechanical ventilator for ~20 seconds) was implemented as a positive control following saline and SMTC in which it was confirmed that a physiological increase in SND could be detected following completion of the experimental protocol (Figure 6.1 inset). There were no qualitative or quantitative differences in MAP, HR, or lumbar and renal SND depending on the order of experimental conditions. For each rat the entire experiment (including surgery, stabilization, and experimental protocol) lasted ~6-8 hours. Following the experimental protocol rats were euthanized by an overdose of methohexital sodium (150 mg/kg i.v.).

Statistical analysis

Data are expressed as mean \pm SEM. MAP, HR, and lumbar and renal SND were compared between saline and SMTC conditions via paired Student's t-test (uncorrected for multiple comparisons). The differences between saline and SMTC conditions (i.e., SMTC-saline) were compared to "zero" via z-tests (2). This multi-statistical approach was utilized in order to improve the ability to detect a difference between saline and SMTC conditions should one exist (see *Experimental considerations* for more details). Significance was accepted at $p < 0.05$.

Results

Effects of nNOS inhibition with SMTC on lumbar and renal SND

Original tracings of lumbar and renal SND recordings for the different experimental conditions from a representative rat are shown in Figure 5.1. Note the similarity among baseline, saline, and SMTC conditions whereas subsequent combined hypoxia and hypercapnia markedly augmented SND (Figure 5.1 inset) which serves as a positive physiological control and establishes that increased SND, should it occur, can be detected. Specifically, there were no differences between saline and SMTC conditions for lumbar or renal SND at any time (Figure 5.2, top panels). The Δ SND between saline and SMTC conditions (SMTC-saline) for the lumbar and renal nerve were not different from zero at any time (Figure 5.2, bottom panels).

Effects of nNOS inhibition with SMTC on MAP and HR

SMTC administration increased MAP significantly compared to saline (Figure 5.3). Specifically, significant MAP elevations compared to saline were evident within 1 minute following SMTC infusion and this significant elevation persisted for 10 minutes. MAP was not different between saline and SMTC conditions at 15 and 20 minutes following infusion. HR was not different between saline and SMTC conditions at any time (Figure 5.3).

Discussion

The principal novel finding of the present investigation is that selective nNOS inhibition with systemic SMTC administration evoked marked increases in MAP but, contrary to our hypothesis, did not impact lumbar or renal SND in SAD rats. This finding suggests an important role for peripheral nNOS-derived NO in the regulation of MAP and vascular control. Specifically, these data support that systemic SMTC-induced reductions in rat hindlimb skeletal muscle and renal blood flow and VC observed previously by our laboratory (3, 5) and others (12, 25) reflected substantial peripheral nNOS-derived NO vascular control in those tissues. The present investigation contributes significantly to our understanding of cardiovascular regulation via peripheral nNOS-derived NO and has broad implications for chronic disease conditions associated with altered nNOS localization and/or function (24).

Effects of SMTC on MAP

Systemic SMTC administration in SAD rats induced increases in MAP ($\uparrow\sim 41\%$) which were markedly greater than reported previously in conscious and anesthetized baroreceptor-intact rats from our laboratory ($\uparrow\sim 10\text{-}12\%$; 4, 5) and others (12, 25). The significant reductions in HR in those previous reports (4, 5, 12, 25) and the greater MAP increases in SAD rats herein reveal that peripheral nNOS-derived NO pressure regulation is partially masked following systemic SMTC administration in baroreceptor-intact rats. In addition, the lack of any increase in lumbar and renal SND identifies that SMTC-induced peripherally-mediated vasoconstriction underlies a substantial portion of the MAP increase.

The rapid (i.e., within 1 minute) SMTC-induced MAP elevations reported herein peaked after 2 minutes and then returned to values not different from saline within 15 minutes. This is consistent with transient SMTC-induced MAP elevations reported previously (12, 25). Importantly, in recent investigations from our laboratory MAP, HR, and skeletal muscle and kidney blood flow were measured $\sim 4\text{-}5$ minutes following SMTC administration (3, 4, 5, 9). Thus, the present data support that those measurements occurred when the cardiovascular effects of SMTC were peaking.

Effects of systemic SMTC on lumbar and renal SND

Systemic SMTC administration in SAD rats did not alter lumbar or renal SND compared to saline. This suggests that systemically-administered SMTC-induced reductions in hindlimb skeletal muscle ($\downarrow\sim 33\%$; 5) and renal ($\downarrow\sim 37-40\%$; 3, 5) blood flow and VC reflect important peripheral nNOS-derived NO vascular control. Furthermore, given the use of rats with intact baroreceptors in those previous investigations, the reductions in blood flow and VC were, if anything, an underestimation of the peripheral nNOS-derived NO vascular control signal.

The present data should not be interpreted to reflect the lack of a role for nNOS-derived NO in the regulation of sympathetic outflow. It has been demonstrated clearly that direct intracerebroventricular SMTC administration elevates MAP and enhances renal SND (21) which is consistent with an overall sympathoinhibitory role of central nNOS-derived NO (1, 18). The present protocol cannot specifically delineate central versus peripheral effects of SMTC on MAP. However, in conjunction with previous reports (5, 25), the lack of any differences between lumbar and renal SND in the present investigation support that peripheral nNOS derived-NO constitutes an important controller of hindlimb skeletal muscle and renal vascular tone at rest and, therefore, serves as a critical modulator of basal blood pressure. Interestingly, the obligatory peripheral nNOS-derived NO vascular signal is lost in the active hindlimb skeletal muscle vasculature during low-speed treadmill running (5) where eNOS-derived NO presumably becomes the predominant NO signal in response to endothelial shear stress. In contrast, obligatory peripheral nNOS-derived NO vascular control is preserved in the renal vasculature during treadmill running (5) and in the anesthetized rat spinotrapezius muscle during electrically-induced contractions (4).

Experimental considerations

A crucial consideration of the current experimental approach is the efficacy of achieving nNOS inhibition without impacting eNOS-mediated function. Several key lines of evidence support this was achieved in the present investigation. First, SMTC is a potent nNOS inhibitor which possesses a 17-fold selectivity for nNOS over eNOS in rat tissue *in vivo* (8) and induced significant increases in MAP herein. Second, 0.56 mg/kg of SMTC (the identical dose utilized herein) does not attenuate the hypotensive response to rapid acetylcholine (ACh) infusion whereas it is blunted (smaller Δ MAP and faster recovery time) following non-selective NOS

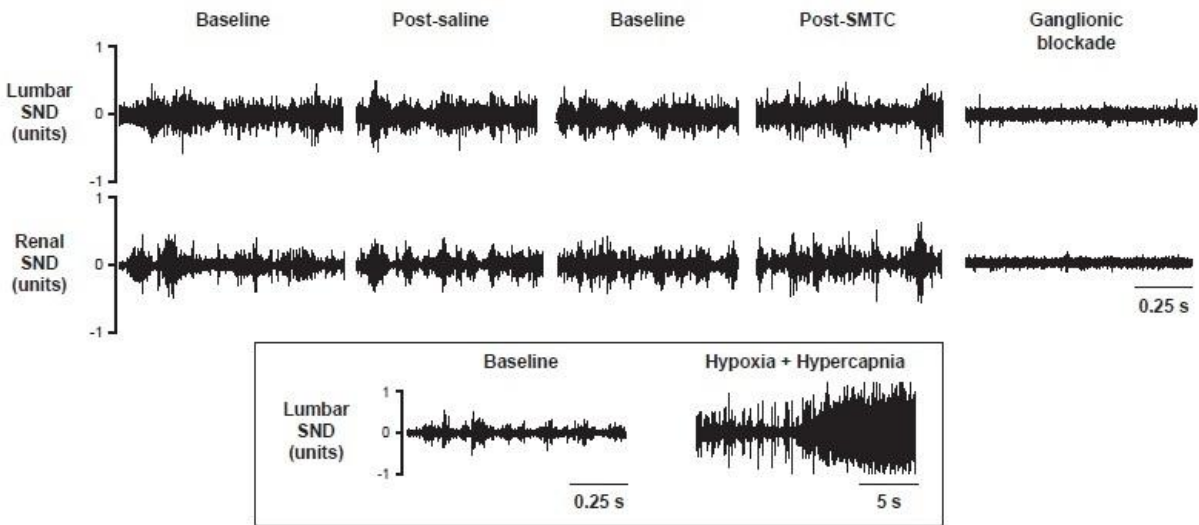
inhibition with L-NAME (3, 4, 5, 9). This is a crucial observation given that vasodilation in response to ACh is due, in large part, to eNOS-derived NO. Had the SMTC dose in those reports been so high that eNOS was inhibited it would have manifested as an attenuated hypotensive response similar to that seen following L-NAME. These important points suggest that efficacious nNOS inhibition occurred in the absence of any effects on eNOS-mediated function.

The less conservative statistical approach using t-tests uncorrected for multiple comparisons and z-tests increased our ability to detect a difference between saline and SMTC conditions should one have existed. However, by these analyses there was no effect of SMTC on SND. Applying the more conservative analyses via t-tests with Bonferroni correction and ANOVAs did not change this conclusion. *Post hoc* analyses revealed that 477 rats would be needed to detect statistically-significant SMTC-induced increases in both lumbar and renal SND. Even if this number of experiments were to be performed, the extremely small differences in SND would not be expected to contribute physiologically to the marked SMTC-induced reductions in hindlimb skeletal muscle ($\downarrow\sim 33\%$; 5) or renal ($\downarrow\sim 37-40\%$; 3, 5) blood flow and VC reported previously.

Perspectives and conclusions

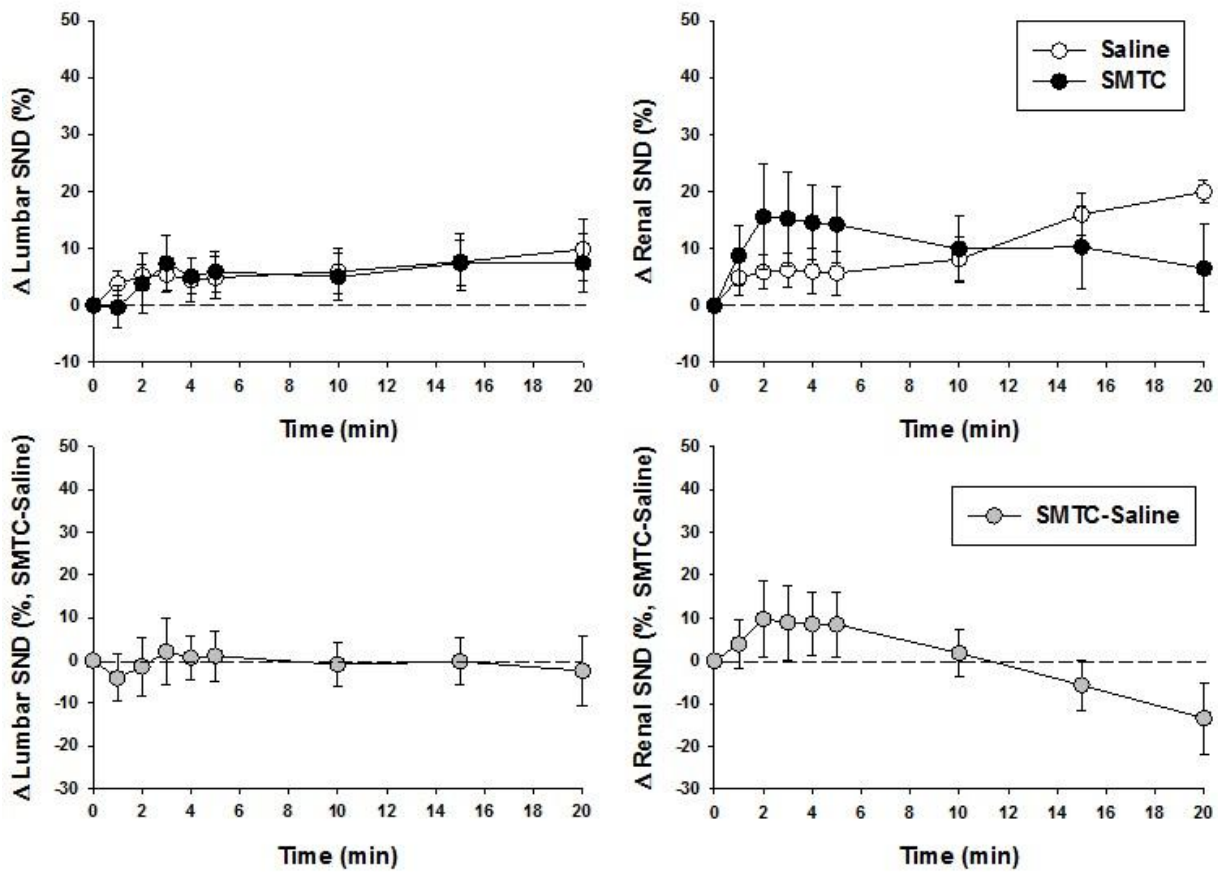
Selective nNOS inhibition with systemically-administered SMTC markedly elevated MAP without altering lumbar or renal SND. Previous investigations have demonstrated that SMTC-induced MAP elevations occur simultaneous with reductions in rat hindlimb skeletal muscle and renal blood flow and VC (3, 5, 25). Therefore, the present data reveal that those MAP elevations and peripheral vasoconstriction were likely not secondary to enhanced lumbar and renal SND but, rather, that they reflect important peripheral nNOS-derived NO vascular control. This contributes significantly to our current understanding of nNOS-derived NO cardiovascular modulation and challenges the conventional notion that eNOS-derived NO constitutes the principal basal NO cardiovascular control signal. This concept/regulation has important implications for chronic disease conditions associated with altered nNOS localization/function and/or impaired vascular control (24).

Figure 5.1. Original tracings of lumbar and renal SND from a representative rat



Original tracings of lumbar and renal sympathetic nerve discharge (SND) recordings for the baseline periods, saline and SMTC (0.56 mg/kg) conditions, as well as following ganglionic blockade via chlorisondamine from a representative rat. The inset shows an original lumbar nerve recording in which combined hypoxia and hypercapnia were implemented (following saline and SMTC) to provide a positive physiological control and establish that increased SND, should it occur, can be detected.

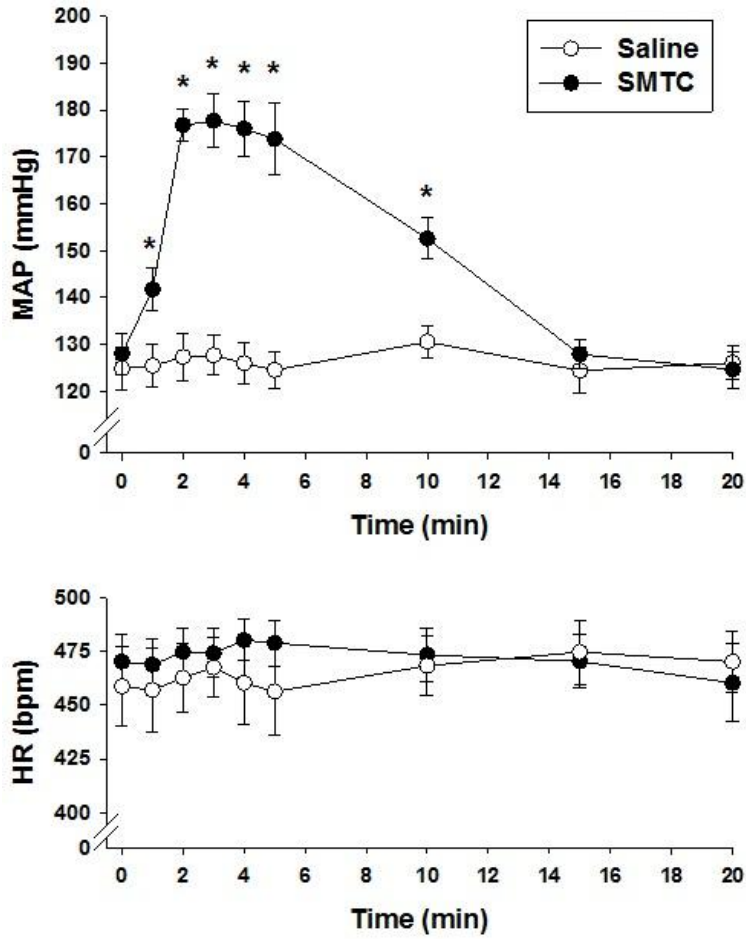
Figure 5.2. Effects of saline and SMTC infusions on lumbar and renal SND



Effects of saline and SMTC (0.56 mg/kg) infusions on lumbar (n=9) and renal (n=7) SND.

There were no differences between saline and SMTC at any time. Time “zero” represents pre-saline or SMTC infusion baseline values. Bottom panels depict the differences between saline and SMTC conditions (Δ SND, SMTC-saline). There were no differences from zero at any time. Data are expressed as mean \pm SEM.

Figure 5.3. Effects of saline and SMTC infusions on MAP and HR



Effects of saline and SMTC (0.56 mg/kg) infusions on MAP and HR (n=9). Time “zero” represents pre-saline or SMTC infusion baseline values. Data are expressed as mean±SEM. * $p < 0.05$ versus saline.

References

1. **Chowdhary S and Townend JN.** Role of nitric oxide in the regulation of cardiovascular autonomic control. *Clin Sci* 97: 5-17, 1999.
2. **Colton T.** *Statistics in Medicine.* Little, Brown and Company, Boston, MA, 1974.
3. **Copp SW, Hirai DM, Ferguson SK, Holdsworth CT, Musch TI, and Poole DC.** Effects of chronic heart failure on neuronal nitric oxide synthase-mediated control of microvascular O₂ pressure in contracting rat skeletal muscle. *J Physiol* 590: 3585-3596, 2012.
4. **Copp SW, Hirai DM, Ferguson SK, Musch TI, and Poole DC.** Role of neuronal nitric oxide synthase in modulating microvascular and contractile function in rat skeletal muscle. *Microcirculation* 18: 501-511, 2011.
5. **Copp SW, Hirai DM, Schwagerl PJ, Musch TI, and Poole DC.** Effects of neuronal nitric oxide synthase inhibition on resting and exercising hindlimb muscle blood flow in the rat. *J Physiol* 588: 1321-1331, 2010.
6. **Deanfield JE, Halcox JP, and Rabelink TJ.** Endothelial function and dysfunction: testing and clinical relevance. *Circulation* 115: 1285-1295, 2007.
7. **Fadel PJ, Zhao W, and Thomas GD.** Impaired vasomodulation is associated with reduced neuronal nitric oxide synthase in skeletal muscle of ovariectomized rats. *J Physiol* 549: 243-253, 2003.
8. **Furfine ES, Harmon MF, Paith JE, Knowles RG, Salter M, Kiff RJ, Duffy C, Hazelwood R, Oplinger JA, and Garvey EP.** Potent and selective inhibition of human nitric oxide synthases. Selective inhibition of neuronal nitric oxide synthase by S-methyl-L-thiocitrulline and S-ethyl-L-thiocitrulline. *J Biol Chem* 269: 26677-26683, 1994.
9. **Hirai DM, Copp SW, Holdsworth CT, Ferguson SK, Musch TI, and Poole DC.** Effects of neuronal nitric oxide synthase inhibition on microvascular and contractile function in skeletal muscle of aged rats. *Am J Physiol Heart Circ Physiol* 303; H1076-1084, 2012.

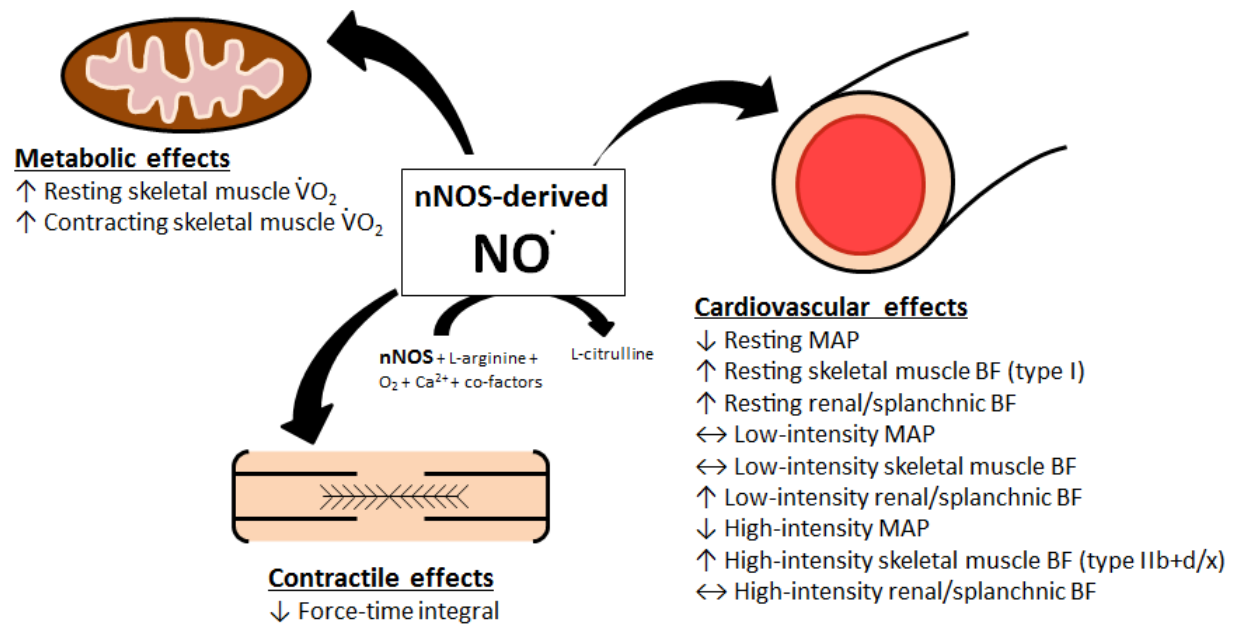
10. **Hirai T, Musch TI, Morgan DA, Kregal KC, Claassen DE, Pickar JG, Lewis SJ, and Kenney MJ.** Differential sympathetic nerve responses to nitric oxide synthase inhibition in anesthetized rats. *Am J Physiol Regul Integr Comp Physiol* 269: R807-R813, 1995.
11. **Kenney MJ.** Frequency characteristics of sympathetic nerve discharge in anesthetized rats. *Am J Physiol* 267: R830-840, 1994.
12. **Komers R, Oyama TT, Chapman JG, Allison KM, and Anderson S.** Effects of systemic inhibition of neuronal nitric oxide synthase in diabetic rats. *Hypertension* 35: 655-661, 2000.
13. **Melikian N, Seddon MD, Casadei B, Chowienczyk PJ, and Shah AM.** Neuronal nitric oxide synthase and human vascular regulation. *Trends Cardiovasc Med* 19: 256-262, 2009.
14. **Moncada S and Higgs EA.** The discovery of nitric oxide and its role in vascular biology. *Br J Pharmacol* 147: S193-201, 2006
15. **Moore PK and Handy RL.** Selective inhibitors of neuronal nitric oxide synthase-is no NOS really good NOS for the nervous system? *Trends Pharmacological Sci* 18: 204-211, 1997.
16. **Narayanan K and Griffith OW.** Synthesis of L-thiocitrulline, L-homothiocitrulline, and S-methyl-L-thiocitrulline: a new class of potent nitric oxide synthase inhibitors. *J Medicinal Chem* 37: 885-887, 1994.
17. **Narayanan K, Spack L, McMillan K, Kilbourn RG, Hayward MA, Masters BS, and Griffith OW.** S-alkyl-L-thiocitrullines. Potent stereoselective inhibitors of nitric oxide synthase with strong pressor activity in vivo. *J Biol Chem* 270: 11103-11110, 1995.
18. **Patel KP, Li YF, and Hirooka Y,** Role of nitric oxide in central sympathetic outflow. *Exp Biol Med* 226: 814-824, 2001.
19. **Rees DD, Palmer RM, and Moncada S.** Role of endothelium-derived nitric oxide in the regulation of blood pressure. *Proc Natl Acad Sci USA* 86: 3375-3378, 1989.
20. **Seddon MD, Chowienczyk PJ, Brett SE, Casadei B, Shah AM.** Neuronal nitric oxide synthase regulates basal microvascular tone in humans in vivo. *Circulation* 117: 1991-1996, 2008.

21. **Tandai-Hiruma M, Horiuchi J, Sakamoto H, Kemuriyama T, Hirakawa H, and Nishida Y.** Brain neuronal nitric oxide synthase neuron-mediated sympathoinhibition is enhanced in hypertensive Dahl rats. *J Hypertens* 23: 825-834, 2005.
22. **Thomas GD, Sander M, Lau KS, Huang PL, Stull JT, and Victor RG.** Impaired metabolic modulation of alpha-adrenergic vasoconstriction in dystrophin-deficient skeletal muscle. *Proc Natl Acad Sci* 95: 15090-15095, 1998.
23. **Thomas GD, Shaul PW, Yuhanna IS, Froehner SC, and Adams ME.** Vasomodulation by skeletal muscle-derived nitric oxide requires alpha-syntrophin-mediated sarcolemmal localization of neuronal Nitric oxide synthase. *Circ Res* 92: 554-560, 2003.
24. **Villanueva, C., and Giulivi, C.** Subcellular and cellular locations of nitric oxide synthase isoforms as determinants of health and disease. *Free Radic Biol Med* 49: 307-316, 2010.
25. **Wakefield ID, March JE, Kemp PA, Valentin JP, Bennett T, and Gardiner SM.** Comparative regional haemodynamic effects of the nitric oxide synthase inhibitors, S-methyl-L-thiocitrulline and L-NAME, in conscious rats. *Br J Pharmacol* 139: 1235-1243, 2003.

Chapter 6 - Conclusions

In conclusion, utilization of the selective nNOS inhibitor SMTC in established models of exercise performance has provided compelling evidence in healthy subjects that: 1) nNOS-derived NO plays an important role in modulating basal blood pressure and resting skeletal muscle perfusion, 2) nNOS-derived NO is an integral controller of skeletal muscle hyperemia during whole-body locomotor exercise with requisite exercise-intensity and muscle fiber-type dependency such that there were no effects of nNOS inhibition during low-speed running whereas during high-speed running nNOS inhibition reduced blood flow primarily within glycolytic fast-twitch muscle, 3) within skeletal muscle and associated vascular beds nNOS-derived NO evokes vasomotor (promotes contracting muscle hyperemia), metabolic (increases resting and contracting steady-state $\dot{V}O_2$), and contractile (depresses overall force output and muscle work) effects and, therefore, impacts skeletal muscle PO_{2mv} , and 4) that systemically-administered SMTC does not impact renal or lumbar SND therefore indicating that the vascular control effects of SMTC represent the actions of peripherally-located nNOS (Figure 6.1). The present data collectively supplant the conventional notions that eNOS is by far the most important peripheral NO source within the skeletal muscle vasculature during exercise and that cardiovascular disease associated impairments in vascular control and reductions in NO bioavailability reflect principally, and perhaps exclusively, eNOS-mediated dysfunction. Thus, the mandate has been established for future therapeutic treatments aimed at increasing NO bioavailability in cardiovascular disease patients to target improvements in peripheral nNOS- as well as eNOS-mediated function.

Figure 6.1. Summary of results



Schematic representation of the primary findings of this dissertation. BF, blood flow; MAP, mean arterial pressure; $\dot{V}O_2$, oxygen consumption.

Appendix A - Curriculum Vitae

Date of Birth: October 12, 1981

Place of Birth: Alexandria, VA, USA

Current Address: *Work*
122 Coles Hall
1600 Denison Avenue
Manhattan, KS, 66506
E-mail: scopp@vet.ksu.edu

Home
1521 Hillcrest
Manhattan, KS, 66502

Education

- 2008-present Doctoral Candidate (Anatomy and Physiology, Kansas State University)
Expected graduation: May 2013
Dissertation title: Enzymatic regulation of skeletal muscle oxygen transport: novel roles for neuronal nitric oxide synthase
Mentor: Dr. Timothy Musch
Co-mentor: Dr. David Poole
- May 2008 M.S. (Kinesiology, Kansas State University)
Mentor: Dr. Timothy Musch
- May 2006 B.S. (Kinesiology, Kansas State University)

Academic Appointments

- 2011-2013 Graduate Research Assistant – *Cardiorespiratory Exercise Physiology Laboratory, Department of Anatomy and Physiology, Kansas State University.*
- 2011-2013 Graduate Instructor – *Department of Kinesiology Kansas State University (Nutrition and Exercise KIN/HN 635 and Research Methods in Kinesiology KIN 815).* Sole instructor for the exercise section (16 lectures) of KIN/HN 635. Lectures focused on basic cardiopulmonary physiology, metabolic pathways, substrate utilization during exercise and implications of a healthy lifestyle vs. “ideal weight”. Sole instructor for KIN 815 graduate level research methodology course covering basics of experimental design, cause and effect relationships, and experimental validity.
- 2007-2013 Laboratory Teaching Assistant - *Department of Anatomy and Physiology, Kansas State University (Veterinary Physiology II, AP747).* Assist in instructing a laboratory experience for 1st year veterinary students focused on lung structure and function in health and disease. Demonstrations performed include maximal exercise tests and various pulmonary function tests.
- 2006-2011 Graduate Teaching Assistant - *Department of Kinesiology, Kansas State University (KIN161, KIN163, KIN 220, KIN 336).* Instruct both lifetime sport classes as well as exercise physiology laboratory experiences. Developed all course content for KIN 161 Fitness and Conditioning. Served as laboratory coordinator for KIN 336 Physiology of Exercise Laboratory and played an instrumental role in writing/updating the KIN 336 Physiology of Exercise Laboratory Manual and Manual Supplement.

Professional Memberships

2007-present The American College of Sports Medicine

2007-present The American Physiological Society, Environmental and Exercise
Physiology Section

2010-present The Microcirculatory Society

Peer-reviewed Manuscripts

1. Herspring KF, Ferreira LF, **Copp SW**, Snyder BS, Poole DC & Musch TI. (2008). Effects of antioxidants on contracting spinotrapezius muscle microvascular oxygenation and blood flow in aged rats. *J Appl Physiol* 105, 1889-1896.
2. **Copp SW**, Ferreira LF, Herspring KF, Musch TI & Poole DC. (2009). The effects of aging on capillary hemodynamics in contracting rat spinotrapezius muscle. *Microvasc Res* B77, 113-199.
3. **Copp SW**, Davis RT, Poole DC & Musch TI. (2009). Reproducibility of endurance capacity and VO_{2peak} in male Sprague-Dawley rats. *J Appl Physiol* 106, 1072-1078.
4. **Copp SW**, Ferreira LF, Herspring KF, Hirai DM, Snyder BS, Poole DC & Musch TI. (2009). The effects of antioxidants on microvascular oxygenation and blood flow in skeletal muscle of young rats. *Exp Physiol* 94, 961-971.

5. Hirai DM, **Copp SW**, Herspring KF, Ferreira LF, Poole DC & Musch TI. (2009). Aging impacts microvascular oxygen pressures during recovery from contractions in rat skeletal muscle. *Respir Physiol Neurobiol* 169, 315-322.
6. **Copp SW**, Hirai DM, Hageman KS, Poole DC & Musch TI. (2010) Nitric oxide synthase inhibition during treadmill exercise reveals fiber-type specific vascular control in the rat hindlimb. *Am J Physiol Regul Integr Comp Physiol* 298, R478-485.
7. **Copp SW**, Hirai DM, Schwagerl PJ, Musch TI & Poole DC. (2010). Effects of neuronal nitric oxide synthase inhibition on resting and exercising hindlimb muscle blood flow in the rat. *J Physiol* 588, 1321-1331.
8. Hirai DM, **Copp SW**, Ferreira LF, Musch TI & Poole DC. (2010). Nitric oxide bioavailability modulates the dynamics of microvascular oxygen exchange during recovery from contractions. *Acta Physiol* 200, 159-169.
9. **Copp SW**, Hageman KS, Behnke BJ, Poole DC & Musch TI. (2010). Effects of Type II diabetes on exercising skeletal muscle blood flow in the rat. *J Appl Physiol* 109, 1347-1353.
10. **Copp SW**, Hirai DM, Ferreira LF, Poole DC & Musch TI. (2010). Progressive chronic heart failure slows recovery of microvascular oxygen pressures following contractions in rat spinotrapezius muscle. *Am J Physiol Heart Circ Physiol* 299, H1755-H1761.
11. **Copp SW**, Hirai DM, Musch TI & Poole DC. (2010). Critical speed in the rat: implications for hindlimb muscle blood flow and fibre recruitment. *J Physiol* 588, 5077-5087.

12. Hirai DM, **Copp SW**, Schwagerl PJ, Haub MD, Poole DC & Musch TI. (2011) Acute antioxidant supplementation and skeletal muscle vascular conductance in aged rats: role of exercise and fiber type. *Am J Heart Circ Physiol* 300, H1536-H1544.
13. Hirai DM, **Copp SW**, Schwagerl PJ, Haub MD, Musch TI & Poole DC. (2011) Acute effects of hydrogen peroxide on skeletal muscle microvascular oxygenation from rest to contractions. *J Appl Physiol* 110, 1290-1298.
14. **Copp SW**, Hirai DM, Ferguson SK, Musch TI & Poole DC. (2011). Role of neuronal nitric oxide synthase in modulating microvascular and contractile function in rat skeletal muscle. *Microcirculation* 18, 501-511.
15. Hirai DM, **Copp SW**, Hageman KS, Poole DC & Musch TI. (2011). Aging alters the contribution of nitric oxide to regional muscle hemodynamic control at rest and during exercise in rats. *J Appl Physiol* 111, 989-998.
16. **Copp SW**, Hirai DM, Ferguson SK, Holdsworth CT, Musch TI & Poole DC. (2012). Chronic heart failure impairs nNOS-mediated control of microvascular O₂ pressure in contracting rat skeletal muscle. *J Physiol* 590(15): 3585-3596.
17. Hirai DM, **Copp SW**, Ferguson SK, Holdsworth CT, McCullough DJ, Behnke BJ, Musch TI & Poole DC. (2012). Exercise training and muscle microvascular oxygenation: functional role of nitric oxide bioavailability. *J Appl Physiol* 113(4): 557-565.
18. Hirai DM, **Copp SW**, Holdsworth CT, Ferguson SK, Musch TI & Poole DC. (2012). Effects of neuronal nitric oxide synthase inhibition on microvascular and contractile function in skeletal muscle of aged rats. *Am J Physiol Heart Circ Physiol* 303(8): H1076-1084.

19. **Copp SW**, Schwagerl PJ, Hirai DM, Poole DC & Musch TI. (2012). Acute ascorbic acid and hindlimb muscle blood flow distribution in old rats: rest and exercise. *Can J Physiol Pharmacol* 90(11): 1498-505.
20. Ferguson SK, Hirai DM, **Copp SW**, Holdsworth CT, Allen JD, Jones AM, Musch TI & Poole DC. (2013). Impact of dietary nitrate supplementation via beetroot juice on exercising muscle vascular control in rats. *J Physiol* 591:547-57.
21. **Copp SW**, Inagaki T, White MJ, Hirai DM, Ferguson SK, Holdsworth CT, Sims GE, Poole DC & Musch TI. (2013). (-)-Epicatechin administration and exercising skeletal muscle vascular control and microvascular oxygenation in healthy rats. *Am J Physiol Heart Circ Physiol* 304(2):H206-14.
22. Hirai DM, **Copp SW**, Ferguson SK, Holdsworth CT, Musch TI & Poole DC. (2013). Superfusion of the NO donor sodium nitroprusside: potential for skeletal muscle vascular and metabolic dysfunction. *Microvasc Res* 85: 104-11.
23. **Copp SW**, Hirai DM, Sims GE, Musch TI, Poole DC & Kenney MJ. (2013). Neuronal nitric oxide synthase inhibition and regional sympathetic nerve discharge: implications for peripheral vascular control. *Resp Phys Neurobiol* 186: 285-289.
24. **Copp SW**, Holdsworth CT, Ferguson SK, Hirai DM, Poole DC, & Musch TI. (2013). Muscle fibre-type dependence of neuronal nitric oxide synthase-mediated vascular control in the rat during high-speed treadmill running. *J Physiol* In press, doi:10.1113/jphysiol.2013.251082.
25. Ferguson SK, Hirai DM, **Copp SW**, Holdsworth CT, Allen JD, Jones AM, Musch TI, & Poole DC. (2013). Effects of nitrate supplementation via beetroot juice on contracting skeletal muscle microvascular oxygen pressure. *Resp Phys Neurobiol* In press, doi:10.1016/j.resp.2013.04.001.

26. Hirai DM, **Copp SW**, Holdsworth CT, Ferguson SK, McCullough DJ, Behnke BJ, Musch TI & Poole DC. (2013). Skeletal muscle microvascular oxygenation in heart failure: exercise training and nitric oxide-mediated function. (in preparation).
27. Sims GE, **Copp SW**, Hirai DM, Ferguson SK, Holdsworth CT, Poole DC, & Musch TI. (2013). Effects of pentoxifylline on exercising skeletal muscle vascular control in rats with chronic heart failure. (in preparation).

Peer-reviewed Review Articles

1. Poole DC, **Copp SW**, Hirai DM & Musch TI. (2011). Dynamics of muscle microcirculatory and blood-myocyte O₂ flux during contractions. *Acta Physiol* 202, 293-310.
2. Poole DC, Hirai DM, **Copp SW** & Musch TI. (2012). Muscle oxygen transport and utilization in heart failure: implications for exercise (in)tolerance. *Am J Heart Circ Physiol*. 302, H1050-H1063.

Published Letters

1. Poole DC, **Copp SW** & Hirai DM. (2009). Comments on point: counterpoint: the kinetics of oxygen uptake during muscular exercise do/do not manifest time-delayed phase. Experimental evidence does support a model of oxygen uptake kinetics with time-delayed phases. *J Appl Physiol* 107, 1670-1671.

2. **Copp SW**, Poole DC & Musch TI. (2010). Valid and reproducible endurance protocols underlie data interpretation, integration, and application. *J Appl Physiol* 108, 224-225.

Book Chapters

1. Poole DC, **Copp SW**, Hirai DM & Musch TI. Oxygen Partial Pressure (PO₂) in Heavy Exercise. Encyclopedia of Exercise Medicine in Health and Disease. Mooren FC (Ed.). Springer Reference. 2012.

Journals Reviewed

European Journal of Applied Physiology
Journal of Applied Physiology
Experimental Physiology
Journal of Visualized Experiments
Journal of Physiology
Applied Physiology, Nutrition, and Metabolism

National Presentations

Experimental Biology. San Diego, CA. April 2008.
Microcirculatory Society's Young Investigator Symposium.
"The effects of aging on microvascular O₂ delivery in contracting skeletal muscle"

ACSM National Meeting. Indianapolis, IN. May 2008
"The effects of aging on capillary hemodynamics in skeletal muscle"

ACSM National Meeting. Seattle, WA. May 2009

Featured Science Session. Fatigue Mechanism's Determining Exercise Performance.

"Microvascular oxygenation during contractions in aged muscle: implications for fatigue"

ACSM National Meeting. Baltimore, MD. June 2010

"Neuronal NOS inhibition modulates resting but not exercising blood flow in rat hindlimb muscles"

ACSM National Meeting. Denver, CO. June 2011

"Skeletal muscle vascular and contractile function: effects of nNOS inhibition"

Departmental Seminars

Kansas State University College of Veterinary Medicine. November 2008

Department of Anatomy and Physiology Seminar Series

"Skeletal muscle blood flow: upregulation and dysregulation"

Kansas State University College of Veterinary Medicine. September 2009

Department of Anatomy and Physiology Seminar Series

"Nitric oxide and vascular control: which part of NO don't you understand?"

Kansas State University College of Veterinary Medicine. October 2012

Department of Anatomy and Physiology Seminar Series

"Calming the perfect storm of O₂ transport deficits in heart failure"

Kansas State University College of Veterinary Medicine. April 2013

Dissertation Defense

"Enzymatic regulation of skeletal muscle oxygen transport: novel roles of neuronal nitric oxide synthase"

Awards and Honors

Microcirculatory Society Zweifach Graduate Student Award, 2009

Kansas State University Department of Anatomy and Physiology Clarenburg Research Fellow, 2009-2013

Graduate Award for Academics, Kansas State University Alumni Association, 2010

Microcirculatory Society August Krogh Young Investigator Award, 2011

American Heart Association Midwest Affiliate Predoctoral Fellowship, 2011-2013

Kansas State University Research Foundation Doctoral Student Fellowship, 2011-2012

Kansas State University College of Veterinary Medicine Graduate Executive Committee Travel Award, Spring 2012

Kansas State University Graduate Student Council Travel Award

Fall 2012

Spring 2013

Dr. Charles E. Cornelius Graduate Student Travel Award, Spring 2013

Department of Kinesiology Outstanding Graduate Student Award, Spring 2013

Grant Funding

American College of Sports Medicine Foundation Doctoral Student Research Grant.

Title: Vascular Dysfunction in Heart Failure: Effects of Fish Oil *Role:* PI, *Total costs:* \$5,000, *Status:* Awarded/Completed, *Effective dates:* 7/1/2011-6/31/2012

American Heart Association Midwest Affiliate Pre-doctoral Fellowship.

Title: Skeletal muscle vascular function in chronic heart failure: effects of fish oil *Role:* PI, *Total costs:* \$52,000, *Status:* Awarded/Active, *Effective dates:* 7/1/2011-6/30/2013

Abstracts

1. **Copp SW**, Ferreira LF, Herspring KF, Musch TI & Poole DC. (2008). The effects of aging on capillary hemodynamics in contracting rat spinotrapezius muscle. *Med. Sci. Sports Exerc* 40 (5), S70.
2. Herspring, KF, Ferreira LF, **Copp SW**, Poole DC & Musch TI. (2008). Effects of antioxidants on contracting spinotrapezius muscle force production and oxygen consumption in aged rats. *Med. Sci. Sports Exerc* 40 (5), S350.
3. **Copp SW**, Ferreira LF, Herspring KF, Musch TI & Poole DC. (2008). The effects of aging on microcirculatory oxygen delivery (QO₂) in contracting rat spinotrapezius muscle. *FASEB J* 22: 1141.2.
4. Herspring, KF, Ferreira LF, **Copp SW**, Poole DC & Musch TI. (2008). Effects of antioxidants on contracting spinotrapezius microvascular oxygen pressure and blood flow in aged rats. *FASEB J* 22: 1142.2.
5. **Copp SW**, Hirai DM, Schwagerl PJ, Herspring KF, Musch TI & Poole DC. (2009). Acute antioxidant (AOX) treatment increases muscle microvascular O₂ extraction in young rats. *FASEB J* 23: 948.3.

6. Hirai, DM, **Copp SW**, Ferreira LF, Musch TI & Poole DC. (2009). Nitric Oxide (NO) bioavailability underlies muscle microvascular O₂ delivery/utilization imbalance in chronic heart failure (CHF) rats. *FASEB J* 23: 948.12.
7. **Copp SW**, Davis RT, Poole DC & Musch TI. (2009). Measurement reproducibility of exercise tolerance and VO_{2peak} in male Sprague-Dawley rats. *Med. Sci. Sports Exerc* 41 (5), S258.
8. **Copp SW**, Hirai DM, Musch TI & Poole DC. (2009). Microvascular oxygenation during the on-transient and and recovery from contractions in aged muscle: implications for fatigue. *Med Sci. Sports Exerc* 45 (5), 8.
9. **Copp SW**, Hirai DM, Schwagerl PJ, Musch TI & Poole DC. (2010). Neuronal NOS inhibition modulates resting but not exercising blood flow in rat hindlimb muscles. *Med Sci Sports Exerc* 45 (5), S91.
10. Hirai DM, **Copp SW**, Schwagerl PJ, Musch TI & Poole DC. (2010). Hydrogen peroxide controls microvascular oxygenation in contracting skeletal muscle of healthy young rats. *Med Sci Sports Exerc* 45 (5), S90.
11. Schwagerl PJ, **Copp SW**, Hirai DM, Davis RT, Synder BS, Poole DC & Musch TI. (2010). The effects of ascorbic acid supplementation on muscle blood flow in aged rats. *Med Sci Sports Exerc* 45 (5), S91.
12. **Copp SW**, Hirai DM, Ferguson SK, Poole DC & Musch TI. (2011). Skeletal muscle vascular and contractile function: role of nNOS inhibition. *Med Sci. Sports Exerc* 43: S63
13. Hirai DM, **Copp SW**, Musch TI & Poole DC. (2011). Effects of nNOS inhibition on resting and contracting skeletal muscle microvascular oxygenation in aged rats. *Med Sci Sports Exerc* 43: S82.

14. **Copp SW**, Hirai DM, Ferguson SK, Poole DC & Musch TI. (2011). Effects of neuronal nitric oxide synthase (nNOS) inhibition on microvascular O₂ pressures during contractions in rat skeletal muscle. *FASEB J* 25:814.6.
15. Hirai DM, **Copp SW**, Poole DC & Musch TI. (2011). Novel skeletal muscle microvascular oxygenation indices as a function of chronic heart failure severity in rats. *FASEB J* 25:814.5.
16. Hirai DM, **Copp SW**, Ferguson SK, Holdsworth CT, Musch TI & Poole DC. (2012). Exercise training and muscle microvascular oxygenation: role of nitric oxide bioavailability. *FASEB J* 26:860.18.
17. Hirai DM, **Copp SW**, Ferguson SK, Holdsworth CT, Poole DC & Musch TI. (2012). Exercise training skeletal muscle blood flow: functional role of neuronal nitric oxide synthase (nNOS). *Med Sci Sports Exerc* 44: S583.
18. **Copp SW**, Hirai DM, Ferguson SK, Holdsworth CT, Poole DC & Musch TI. (2012). Chronic heart failure (CHF) alters nNOS-mediated control of skeletal muscle contractile function. *FASEB J* 26:860.19.
19. Holdsworth CT, **Copp SW**, Hirai DM, Ferguson SK, Hageman KS, Stebbins CL, Poole DC & Musch TI. (2012). Effects of dietary fish oil on exercising muscle blood flow in chronic heart failure rats. *Med Sci Sports Exerc* 44; S388.
20. **Copp SW**, Hirai DM, Ferguson SK, Holdsworth CT, Musch TI & Poole DC. (2012). Chronic heart failure alters nNOS-mediated control of skeletal muscle microvascular O₂ delivery and utilization. *Med Sci Sports Exerc* 44: S734.

21. Ferguson SK, Hirai DM, **Copp SW**, Holdsworth CT, Hageman KS, Jones AM, Musch TI & Poole DC. (2012). Acute dietary nitrate supplementation on resting and exercising hemodynamic control in the rat. *Med Sci Sports Exerc* 44: S879.
22. **Copp SW**, Hirai DM, Ferguson SK, Holdsworth CT, Poole DC & Musch TI. (2012). Efficacy of nitric oxide based treatments to improve peripheral vascular function: implications for chronic heart failure. *KSU Graduate Res Forum*.
23. Hirai DM, **Copp SW**, Ferguson SK, Holdsworth CT, Jones AM, Musch TI & Poole DC. (2012). Diet impacts blood flow control and matching muscle O₂ delivery-to-utilization. *Med Sci Sports Exerc* 44.
24. Kennedy AR, Pakdel A, Ryans J, Musch TI, Poole DC, Hageman KS, **Copp SW**, Malik F, Jasper J. (2012). The fast skeletal troponin activator, CK-2017357, improves resistance to fatigue in healthy, conscious rats. *FASEB J* 26:1121.7.
25. Hirai DM, **Copp SW**, Ferguson SK, Holdsworth CT, Sims GE, Musch TI, Poole DC. Chronic heart failure and muscle microvascular oxygenation: effects of exercise training. (2012 APS Intersociety Meeting: Integrative Biology of Exercise VI)
26. **Copp SW**, Hirai DM, Inagaki T, White MJ, Sims GE, Holdsworth CT, Ferguson SK, Poole DC, Musch TI. Chronic oral (-)-epicatechin does not affect rat hindlimb skeletal muscle vascular function during exercise. (2012 APS Intersociety Meeting: Integrative Biology of Exercise VI)
27. Holdsworth CT, **Copp SW**, Inagaki T, Hirai DM, Ferguson SK, Sims GE, White MJ, Poole DC, Musch TI. Chronic (-)-epicatechin administration does not affect contracting skeletal muscle microvascular oxygenation. (2012 APS Intersociety Meeting: Integrative Biology of Exercise VI)

28. Ferguson SK, Hirai DM, **Copp SW**, Holdsworth CT, Musch TI, Poole DC. The effects of acute dietary nitrate supplementation on muscle microvascular oxygenation in contracting rat skeletal muscle. *(2012 APS Intersociety Meeting: Integrative Biology of Exercise VI)*
29. Holdsworth, CT, Sims, GE, Ferguson SK, **Copp SW**, Hirai DM, White MJ, Hageman SK, Poole DC, Musch TI. Effects of pentoxifylline on contracting skeletal muscle microvascular oxygenation in chronic heart failure rats. *ACSM Annual Meeting, 2013 (submitted/accepted)*.
30. Sims GE, Hageman KS, **Copp SW**, Hirai DM, Ferguson SK, Holdsworth CT, Poole DC, Musch TI. Effects of pentoxifylline on skeletal muscle vascular control in rats with chronic heart failure. *ACSM Annual Meeting, 2013 (submitted/accepted)*.
31. Ferguson SK, Hirai DM, **Copp SW**, Holdsworth CT, Sims GE, Musch TI, Poole DC. Effects of low dose nitrate supplementation on contracting rat skeletal muscle microvascular oxygen pressure. *ACSM Annual Meeting, 2013 (submitted/accepted)*.
32. **Copp SW**, Hirai DM, Sims GE, Musch TI, Kenney MJ, Poole DC. (2013) Neuronal nitric oxide synthase (nNOS) and regional sympathetic nerve discharge: implications for peripheral vascular control. *FASEB J (submitted/accepted)*